Astronomy 702: (Fluid) Dynamics

Contents

1 Introducing Fluids

1.1 Properties of Fluids

1.1.1 What is a Fluid?

Examples from everyday experience:

- alcohol (low-viscosity liquid)
- water (medium-viscosity liquid)
- molasses (high-viscosity liquid)
- air (gas)

Unifying definition: fluids are *continuously deformable*, responding to applied forces by changing shape/state in a smooth, continuous manner.

1.1.2 Microscopic Description

We can characterize a fluid at some instant $t = t_0$ by specifying the

- mass
- position
- velocity
- ...

of every particle (atom, ion, molecule, electron, etc.) in the fluid. Then, the $t > t_0$ evolution of the fluid can be determined by integrating the equation of motion for each particle, accounting for the myriad interactions (electromagnetic, gravitational, etc.) between the particles.

Although for 'small' numbers of particles this *N-body dynamics* approach is effective, for fluids there are simply too many particles and interactions to keep track of. In the Sun, for instance, there are $\sim 10^{57}$ particles and thus $\sim 10^{114}$ two-particle interactions — more than the number of atoms in the Universe!

1.1.3 Macroscopic Description

An alternative approach is to characterize the fluid at some instant $t = t_0$ by specifying the

- velocity $\boldsymbol{v}$
- pressure P
- density ρ
- temperature T
- ...

as a function of position vector $\boldsymbol{r}$. Then, the $t > t_0$ evolution of the fluid can be determined by integrating a set of equations governing the macroscopic state variables $[\boldsymbol{v}, P, \rho, T, \ldots]$.

This *fluid dynamics* approach is effective when the state variables are well defined. Given that these variables represent macroscopic averages over the distributions of microscopic particle properties, we therefore require that the particle distributions themselves are well defined — for instance, particle velocities associated with random (thermal) motions that follow a Maxwell-Boltzmann distribution. If such requirements cannot be met, then fluid dynamics as a technique breaks down, and we have to resort to a more-basic (and typically, more computationally expensive) approach such as *kinetic theory*.

Sometimes, it is useful to consider how the fluid properties change in a frame of reference co-moving with the flow. A useful conceptual definition is then:

A *fluid element* (or *fluid parcel*) is a small amount of fluid made which retains its identity as it moves with the flow.

By 'retains its identity', we mean that if we could somehow tag the material comprising the element (e.g., by dyeing it), then the element will at all times contain the same tagged material — even if its volume or shape changes.

1.1.4 Ideal Gases

In astrophysical contexts, the most common fluids are ideal gases obeying the equation of state

$$P = \rho R_m T. \tag{1.1}$$

Here, R is the gas constant per unit mass, given in terms of Boltzmann's constant $k_{\rm B}$ and the mean particle mass $\bar{m}$ by

$$R_m \equiv \frac{k_{\rm B}}{\bar{m}}. \tag{1.2}$$

Given two of the *thermodynamic* state variables $[P, \rho, T]$ the equation of state (1.1) allows us to calculate the third.

The temperature T is a measure of the kinetic energy per particle due to random motions. In fluid dynamics, it's often more convenient to work with the internal energy, which combines both the kinetic energy due to random motions and the energy stored in internal degrees of freedom (e.g., ionization, molecular vibrations, etc.). The temperature and specific (per-unit-mass) internal energy u are related by

$$u = \frac{1}{\gamma - 1}\frac{k_\mathrm{B}T}{\bar{m}} = \frac{R_m T}{\gamma - 1}. \tag{1.3}$$

Here, γ is the ratio of specific heats of the gas; for a monatomic gas, $\gamma = 5/3$. With this energy relation, we can rewrite the equation of state as

$$P = (\gamma - 1)\rho u. \tag{1.4}$$

The internal energy is just one component of a fluid's total energy — the other being the kinetic energy associated with the bulk flow of the fluid at velocity $\boldsymbol{v}$. The relationship between the specific internal energy u and the specific total energy ε is thus

$$\varepsilon = u + \frac{v^2}{2}, \tag{1.5}$$

where $v \equiv |\boldsymbol{v}|$. This equation is universal, applying whether or not the fluid is an ideal gas.

1.2 Fluid Fluxes

The state of a fluid changes over time due to flows of conserved quantities — mass, momentum and energy — arising at both macroscopic and microscopic levels. These flows can be neatly characterized by specifying a flux for each conserved quantity.

The *flux* of a given quantity measures the amount of that quantity passing through a unit area in a unit time.

1.2.1 Mass Flux

The mass flux $\boldsymbol{F}_m$ is a vector defined such that the amount of mass Δm passing through the vector area element $\mathrm{d}\boldsymbol{A}$ in time Δt is

$$\Delta m = \boldsymbol{F}_m \cdot \mathrm{d}\boldsymbol{A}\, \Delta t. \tag{1.6}$$

In terms of the fluid state quantities, the mass flux is given by

$$\boldsymbol{F}_m = \rho\, \boldsymbol{v}. \tag{1.7}$$

Clearly, $\boldsymbol{F}_m$ is parallel to $\boldsymbol{v}$ and is therefore along the direction of the fluid flow.

1.2.2 Energy Flux

The total energy flux $\boldsymbol{F}_e$ is likewise a vector defined such that the amount of energy Δe passing through the vector area element $\mathrm{d}\boldsymbol{A}$ in time Δt is

$$\Delta e = \boldsymbol{F}_e \cdot \mathrm{d}\boldsymbol{A}\, \Delta t. \tag{1.8}$$

In terms of the fluid state quantities, the energy flux is given by

$$\boldsymbol{F}_e = \rho\varepsilon\boldsymbol{v} + P\boldsymbol{v}. \tag{1.9}$$

Again, $\boldsymbol{F}_e$ is parallel to $\boldsymbol{v}$ and is therefore along the direction of the fluid flow. The first term in this expression represents the bulk flow of internal energy, while the second term represents the work done by pressure forces.

1.2.3 Momentum Flux

The momentum flux $\boldsymbol{F_p}$ is a dyadic (see Appendix A) defined such that the amount of momentum $\Delta\boldsymbol{p}$ passing through the vector area element $\mathrm{d}\boldsymbol{A}$ in time Δt is

$$\Delta\boldsymbol{p} = \boldsymbol{F_p} \cdot \mathrm{d}\boldsymbol{A}\, \Delta t. \tag{1.10}$$

In terms of the fluid state quantities, and for the moment neglecting momentum transport by viscosity, the momentum flux is given by

$$\boldsymbol{F_p} = \rho\boldsymbol{v} \otimes \boldsymbol{v} + P\boldsymbol{I} \tag{1.11}$$

where $\otimes$ is the outer product and $\boldsymbol{I}$ the identity dyadic. The first term in this expression (which is a dyad) represents the bulk flow of momentum, while the second term represents the flux of momentum due to pressure[1].

1.3 The Fluid Equations

The fluid equations relate the fluxes given in the preceding section to the changes they cause; they are embodiments of standard conservation laws for fluids.

1.3.1 Mass Conservation

The fluid equation enforcing mass conservation is

$$\frac{\partial\rho}{\partial t} + \nabla \cdot \boldsymbol{F}_m = 0. \tag{1.12}$$

[1]Since force is rate of change of momentum, we can think of pressure as momentum per unit time per unit area — that is, a momentum flux

Substituting in the definition (1.7) of the mass flux vector $\boldsymbol{F}_m$, this becomes

$$\frac{\partial \rho}{\partial t} + \nabla \cdot (\rho \boldsymbol{v}) = 0. \tag{1.13}$$

This is sometimes known as the continuity equation. We can also express this as

$$\frac{\mathrm{D}\rho}{\mathrm{D}t} = -\rho \nabla \cdot \boldsymbol{v}, \tag{1.14}$$

where

$$\frac{\mathrm{D}}{\mathrm{D}t} \equiv \left(\frac{\partial}{\partial t} + \boldsymbol{v} \cdot \nabla \right) \tag{1.15}$$

is a differential operator which gives the rate of change of a quantity *as experienced by a fluid element as it moves with the flow*. This operator has a variety of names: the Stokes derivative, Lagrangian time derivative, advective time derivative, or material time derivative.

1.3.2 Momentum Conservation

The fluid equation enforcing momentum conservation, in the absence of viscosity and external forces, is

$$\frac{\partial \rho \boldsymbol{v}}{\partial t} + \nabla \cdot \boldsymbol{F_p} = 0. \tag{1.16}$$

Substituting in the definition (1.11) of the momentum flux dyadic $\boldsymbol{F_p}$, this becomes

$$\frac{\partial \rho \boldsymbol{v}}{\partial t} + \nabla \cdot (\rho \boldsymbol{v} \otimes \boldsymbol{v} + P \boldsymbol{I}) = 0. \tag{1.17}$$

Using eqn. (A.19), this can also be written in the form

$$\frac{\partial \rho \boldsymbol{v}}{\partial t} + \nabla \cdot (\rho \boldsymbol{v} \otimes \boldsymbol{v}) + \nabla P = 0, \tag{1.18}$$

explicitly revealing the role that pressure gradients play. Likewise, written in terms of the Stokes time derivative of the velocity, the conservation equation is

$$\rho \frac{\mathrm{D}\boldsymbol{v}}{\mathrm{D}t} = -\nabla P; \tag{1.19}$$

this is of course a fluid version of Newton's Second law, $ma = F$, with the pressure gradients providing the force F.

1.3.3 Energy Conservation

The fluid equation enforcing energy conservation, in the absence of viscosity, external forces and heat sources/sinks, is

$$\frac{\partial \rho\varepsilon}{\partial t} + \nabla \cdot \boldsymbol{F}_e = 0. \tag{1.20}$$

Substituting in the definition (1.9) of the total energy flux vector $\boldsymbol{F}_e$, this becomes

$$\frac{\partial \rho\varepsilon}{\partial t} + \nabla \cdot (\rho\varepsilon \boldsymbol{v} + P\boldsymbol{v}) = 0. \tag{1.21}$$

Written in terms of the Stokes time derivative of the specific total energy, the conservation equation is

$$\rho \frac{\mathrm{D}\varepsilon}{\mathrm{D}t} = -P\nabla \cdot \boldsymbol{v} - \boldsymbol{v} \cdot \nabla P. \tag{1.22}$$

Of the two terms on the right-hand side, the first represents internal energy changes due to compression/expansion of the fluid (i.e., microscopic work), and the second represents bulk kinetic energy changes due to acceleration of the fluid by pressure gradients (i.e., macroscopic work).

1.4 The Integral Fluid Equations

1.4.1 A Physical Basis for the Fluid Equations?

In the preceding sections we've written down a set of differential equations (1.13,1.17,1.21) describing conservation of mass, momentum and energy in a fluid. But we haven't yet explained *where* these equations come from — in particular, we haven't presented a physical basis for why the fluid equations appear as they do.

In fact, the differential fluid equations are special cases of more general *integral* fluid equations, which we'll now explore.

1.4.2 Mass Conservation

Consider an arbitrary volume element $\mathcal{V}$ which *doesn't* move with the fluid, but rather is fixed in space. Between any two instants in time, t and $t + \Delta t$, mass conservation requires that the net change in the fluid mass contained $\mathcal{V}$ exactly match the amount of mass flowing in or out of the volume via its boundaries. Written symbolically, this statement is

$$\int_{\mathcal{V}} [\rho(\boldsymbol{r}, t + \Delta t) - \rho(\boldsymbol{r}, t)] \, \mathrm{d}\tau = -\int_t^{t+\Delta t} \int_{\partial\mathcal{V}} \boldsymbol{F}_m(\boldsymbol{r}, t') \cdot \mathrm{d}\boldsymbol{A} \, \mathrm{d}t'. \tag{1.23}$$

The left hand side represents the change in the mass contained in $\mathcal{V}$, and the right hand side represents the time-integrated flow of mass out through the boundary $\partial\mathcal{V}$ of the volume, as described by the mass flux vector $\boldsymbol{F}_m$ (cf. eqn. 1.7).

To see how this integral fluid equation relates to the corresponding differential one (1.12) for mass conservation, let's take the limit of very small Δt. In this limit, the left-hand side of eqn. (1.23) becomes

$$\lim_{\Delta t\to 0}\left\{\int_{\mathcal{V}}\left[\rho(\boldsymbol{r},t+\Delta t)-\rho(\boldsymbol{r},t)\right]\,\mathrm{d}\tau\right\}=\left\{\int_{\mathcal{V}}\left[\frac{\partial\rho}{\partial t}\right]_{(\boldsymbol{r},t)}\mathrm{d}\tau\right\}\Delta t, \tag{1.24}$$

and the right hand side becomes

$$\lim_{\Delta t\to 0}\left\{\int_{t}^{t+\Delta t}\int_{\partial\mathcal{V}}\boldsymbol{F}_m(\boldsymbol{r},t')\cdot\mathrm{d}\boldsymbol{A}\,\mathrm{d}t'\right\}=\left\{\int_{\partial\mathcal{V}}\boldsymbol{F}_m(\boldsymbol{r},t)\cdot\mathrm{d}\boldsymbol{A}\right\}\Delta t. \tag{1.25}$$

Setting these two equal, and dividing through by Δt, we find that

$$\int_{\mathcal{V}}\frac{\partial\rho}{\partial t}\,\mathrm{d}\tau=\int_{\partial\mathcal{V}}\boldsymbol{F}_m\cdot\mathrm{d}\boldsymbol{A}. \tag{1.26}$$

Next, we apply the divergence theorem (A.22) to rewrite the surface integral on the right-hand side as a volume integral:

$$\int_{\mathcal{V}}\frac{\partial\rho}{\partial t}\,\mathrm{d}\tau=\int_{\mathcal{V}}\nabla\cdot\boldsymbol{F}_m\,\mathrm{d}\tau. \tag{1.27}$$

(An important note here: this step is only valid when $\boldsymbol{F}_m$ is a continuous function of position. More on this later). Because this equation holds for any choice of $\mathcal{V}$, the integrands must be equal and so

$$\frac{\partial\rho}{\partial t}=-\nabla\cdot\boldsymbol{F}_m. \tag{1.28}$$

With some trivial rearranging, we see that this is *identical* to the differential equation (1.12) governing mass conservation.

This is important result bears calling out:

In fluid flow with no discontinuities, the integral form of the (mass) conservation equation is identical to the differential form of the (mass) conservation equation.

The word 'mass' is in parentheses here to highlight the fact that the *same* statement also applies to the momentum and energy conservation equations, as we shall see below. The opening clause about 'no discontinuities' comes from the requirement that $\boldsymbol{F}_m$ — and hence the flow itself — be continuous. If this requirement is *not* met, then the integral form of the conservation equation remains valid even across discontinuities (a fact we'll exploit later when dealing with shocks), but the differential form blows up because derivatives become undefined there.

1.4.3 Momentum Conservation

Let's consider the same volume element $\mathcal{V}$ as before. Momentum conservation requires that the net change in the fluid momentum contained $\mathcal{V}$, between t and $t + \Delta t$, exactly match the amount of momentum flowing in or out of the volume via its boundaries. Written symbolically, this statement is

$$\int_{\mathcal{V}} [\rho(\boldsymbol{r}, t + \Delta t)\boldsymbol{v}(\boldsymbol{r}, t + \Delta t) - \rho(\boldsymbol{r}, t)\boldsymbol{v}(\boldsymbol{r}, t)] \, \mathrm{d}\tau = -\int_t^{t+\Delta t} \int_{\partial\mathcal{V}} \boldsymbol{F_p}(\boldsymbol{r}, t') \cdot \mathrm{d}\boldsymbol{A} \, \mathrm{d}t'. \quad (1.29)$$

The left hand side represents the change in the momentum contained in $\mathcal{V}$, and the right hand side represents the time-integrated flow of momentum out through the boundary, as described by the momentum flux dyadic $\boldsymbol{F_p}$ (cf. 1.11).

It's straightforward to apply the same analysis as in the preceding section[2] to convert this integral form for momentum conservation into the corresponding differential form

$$\frac{\partial \rho \boldsymbol{v}}{\partial t} = -\nabla \cdot \boldsymbol{F_p}. \quad (1.30)$$

With some rearranging we see that this is identical to eqn. (1.16). The same caveats as before apply: the integral form (1.29) is always valid, whereas the differential form is only valid for continuous flows.

1.4.4 Energy Conservation

Finishing off our discussion of the integral forms of the fluid equations, energy conservation requires that the net change in the fluid energy contained $\mathcal{V}$, between t and $t + \Delta t$, exactly match the amount of energy flowing in or out of the volume via its boundaries. Written symbolically, this statement is

$$\int_{\mathcal{V}} [\rho(\boldsymbol{r}, t + \Delta t)u(\boldsymbol{r}, t + \Delta t) - \rho(\boldsymbol{r}, t)u(\boldsymbol{r}, t)] \, \mathrm{d}\tau = -\int_t^{t+\Delta t} \int_{\partial\mathcal{V}} \boldsymbol{F}_e(\boldsymbol{r}, t') \cdot \mathrm{d}\boldsymbol{A} \, \mathrm{d}t'. \quad (1.31)$$

The left hand side represents the change in the energy contained in $\mathcal{V}$, and the right hand side represents the time-integrated flow of energy out through the boundary, as described by the energy flux vector $\boldsymbol{F}_e$ (cf. 1.9). As before, for continuous flows this reduces to the corresponding differential equation (1.20).

[2] The one wrinkle in the derivation is that we have to use the divergence theorem for dyadics, eqn. (A.23).

1.5 External Forces

So far we've considered fluid flows in the absence of external forces. These forces can be broadly divided into two categories:

A *body force* acts throughout the volume of a fluid, in contrast to a *surface force* (sometimes *contact force*) which acts through the boundaries of the fluid.

Examples of body forces are gravity, electromagnetic forces, and the inertial centrifugal and Coriolis forces; examples of surface forces are surface tension, and normal pressure forces exerted by rigid walls.

For the time being, let's concern ourselves only with body forces. For a fluid acted on by a force per unit mass $\boldsymbol{g}$ (which has units of acceleration), the momentum and energy conservation equations are modified to read

$$\frac{\partial \rho \boldsymbol{v}}{\partial t} + \nabla \cdot (\rho \boldsymbol{v} \otimes \boldsymbol{v} + P\boldsymbol{I}) = \rho \boldsymbol{g} \tag{1.32}$$

and

$$\frac{\partial \rho \varepsilon}{\partial t} + \nabla \cdot (\rho \varepsilon \boldsymbol{v} + P\boldsymbol{v}) = \rho \boldsymbol{g} \cdot \boldsymbol{v}, \tag{1.33}$$

respectively (the continuity equation is unaffected). Comparing these against eqns. (1.17) and (1.21), we see that the body force introduces new 'source' terms on the right-hand side, corresponding to the force per unit volume in the momentum equation and the rate of work per unit volume in the energy equation. The presence of these source terms means that momentum and energy are no longer conserved in the fluid — but, that's not surprising given that there are external forces at work.

The most common body force encountered in astrophysics is gravity. The gravitational acceleration is most easily obtained from the gradient of the scalar gravitational potential Φ_{grav},

$$\boldsymbol{g}_{\text{grav}} = -\nabla \Phi_{\text{grav}}, \tag{1.34}$$

and Φ_{grav} itself is calculated by solving Poisson's equation

$$\nabla^2 \Phi_{\text{grav}} = 4\pi G \rho. \tag{1.35}$$

For spherical mass distributions, things are simplified: the gravitational acceleration is given by

$$\boldsymbol{g}_{\text{grav}} = -\frac{GM_r}{r^2}\hat{\boldsymbol{r}}, \tag{1.36}$$

where M_r is the total mass contained inside the sphere with radius r, and $\hat{\boldsymbol{r}}$ is the unit vector in the radial direction. Note that it's generally *not* the case that

$$\Phi_{\text{grav}} = -\frac{GM_r}{r}, \tag{1.37}$$

unless there is no mass outside radius r.

For fluids acted on by body forces, there exists a special equilibrium configuration which is not just steady-state but also static:

Hydrostatic equilibrium is a static fluid state in which body forces exactly balance pressure gradients.

Mathematically, the condition of hydrostatic equilibrium (HSE) follows simply by setting the time derivatives and velocity to zero in the momentum equation (1.32), to obtain

$$\nabla P = \rho \boldsymbol{g}. \tag{1.38}$$

Most commonly, this equation is applied in situations where gravity comprises the body force; for spherical mass distributions, it becomes

$$\frac{\mathrm{d}P}{\mathrm{d}r} = -\frac{GM_r}{r^2}\rho. \tag{1.39}$$

2 Special Types of Fluid Flow

2.1 Rotational & Irrotational Flows

The *vorticity* of a fluid is the curl of its velocity, and represents the degree of fluid circulation about each point in the flow.

Symbolically, the vorticity $\boldsymbol{\omega}$ is

$$\boldsymbol{\omega} \equiv \nabla \times \boldsymbol{v}. \tag{2.40}$$

If $\boldsymbol{\omega}$ is zero we say the flow is *irrotational*; conversely, a non-zero vorticity indicates a *rotational* flow. Conceptually, rotational flows share the property that a miniature paddle wheel dropped into the fluid will start to turn around its center.

Parallel shear flow is a classic example of a rotational flow. Suppose the fluid velocity behaves as

$$\boldsymbol{v} = f(z)\,\hat{\boldsymbol{x}}, \tag{2.41}$$

where $f(z)$ is some function of the Cartesian z coordinate alone and $\hat{\boldsymbol{x}}$ is the unit vector in the Cartesian x direction. Taking the curl, we have

$$\boldsymbol{\omega} = \frac{\mathrm{d}f}{\mathrm{d}z}\,\hat{\boldsymbol{y}}, \tag{2.42}$$

and so we see that the flow is rotational everywhere except at extrema where $\mathrm{d}f/\mathrm{d}z = 0$.

Another example of rotational flow, with particular significance in astrophysical contexts, is circular motion around an axis (sometimes known as a *vortex*):

$$\boldsymbol{v} = \Omega(\varpi)\varpi\,\hat{\boldsymbol{\phi}}, \tag{2.43}$$

where ϖ is the distance from the axis (the 'radial' coordinate in the cylindrical coordinate system), Ω is the angular velocity (a function of ϖ), and $\hat{\boldsymbol{\phi}}$ the unit direction in the azimuthal (ϕ) direction. Taking the curl,

$$\boldsymbol{\omega} = \frac{\partial(\varpi^2\Omega)}{\partial\varpi}\,\hat{\boldsymbol{z}}. \tag{2.44}$$

From this we see that, for instance, uniform rotation ($\Omega = $ const.) is rotational flow, as is Keplerian rotation ($\Omega \propto \varpi^{-3/2}$). The former may come as a bit of a surprise; surely, a miniature paddle wheel won't turn if we drop it off-axis in a uniformly rotating fluid? In fact, it will — we're forgetting that as the paddle wheel completes one full orbit around the center of rotation, it also completes one full revolution about its own center. A direct analogy here is the way the stars in a tidally locked binary system complete a revolution at the same time as they complete an orbit.

An interesting special case arises with circular motion that's angular-momentum conserving; that is,

$$\varpi^2\Omega = j, \tag{2.45}$$

where j is the (constant) angular momentum per unit mass. Clearly, the vorticity vanishes everywhere and it appears we have an instance of an *irrotational vortex*! Physically, however, this isn't possible; if the above equation applies strictly, then both the angular velocity and the physical velocity become infinite as $\varpi \to 0$. Instead, there must be a small core region around the origin where the equation breaks down and the flow becomes rotational.

2.2 The Vorticity Equation

The vorticity of a fluid evolves via a well-defined equation, which we can derive from the fluid mass and momentum equations. Let's start by taking eqn. (1.19) and expanding out the Stokes derivative, to obtain

$$\frac{\partial\boldsymbol{v}}{\partial t} + (\boldsymbol{v}\cdot\nabla)\boldsymbol{v} = -\frac{1}{\rho}\nabla P. \tag{2.46}$$

Now we make use of the vector identity

$$(\boldsymbol{v}\cdot\nabla)\boldsymbol{v} = \frac{1}{2}\nabla(\boldsymbol{v}\cdot\boldsymbol{v}) - \boldsymbol{v}\times(\nabla\times\boldsymbol{v}) \tag{2.47}$$

(cf. eqn. A.21) to rewrite this as

$$\frac{\partial\boldsymbol{v}}{\partial t} + \frac{1}{2}\nabla(\boldsymbol{v}\cdot\boldsymbol{v}) - \boldsymbol{v}\times(\nabla\times\boldsymbol{v}) = -\frac{1}{\rho}\nabla P. \tag{2.48}$$

Taking the curl and rearranging, we arrive at the result

$$\frac{\partial\boldsymbol{\omega}}{\partial t} = \nabla\times(\boldsymbol{v}\times\boldsymbol{\omega}) + \frac{1}{\rho^2}\nabla\rho\times\nabla P. \tag{2.49}$$

2.3 Incompressible Flows

An *incompressible flow* is one in which the density of individual fluid elements does not vary with time.

The Stokes time derivative introduced in eqn. (1.15) gives the rate-of-change experienced by a fluid element, and so we see that an incompressible flow satisfies the relation

$$\frac{\mathrm{D}\rho}{\mathrm{D}t} \equiv \frac{\partial \rho}{\partial t} + \boldsymbol{v} \cdot \nabla \rho = 0. \tag{2.50}$$

Combining this with the continuity equation, it follows that

$$\nabla \cdot \boldsymbol{v} = 0, \tag{2.51}$$

which in turn tells us that the *volume* of a fluid element in an incompressible flow does not change (even though the element's shape may be distorted).

How realistic are incompressible flows? Some fluids (e.g., water) are intrinsically incompressible, and always exhibit incompressible flow — so, we often refer to them as *incompressible fluids*. In astrophysics, however, we deal with fluids (gas, plasma) which can most certainly be compressed. Nevertheless, in some situations even these fluids can flow in a manner satisfying the incompressibility condition (2.50). Typically, such situations are encountered when the flow velocity is much smaller than the propagation speed of acoustic (sound) waves; then, any pressure differences between a fluid elements and its neighbors are ironed over timescales much shorter than the typical fluid evolution timescale, and the flow behaves incompressibly.

For an incompressible flow with an initial density that's spatially uniform, the density remains uniform. Then, the vorticity equation (2.49) we derived above simplifies to

$$\frac{\partial \boldsymbol{\omega}}{\partial t} = \nabla \times (\boldsymbol{v} \times \omega). \tag{2.52}$$

Together with eqn. (2.40), this equation gives us all we need to know to calculate the evolution of the fluid.

2.4 Kelvin's Circulation Theorem

A simple result which follows directly from the incompressible vorticity equation (2.52) is that an initially irrotational flow will remain irrotational for all time.

In fact, this is a special case of a more general theorem:

Kelvin's circulation theorem states that in an inviscid, incompressible flow the circulation around a closed curve $\mathcal{C}$ (which encloses the same fluid elements) moving with the fluid remains constant with time.

The circulation is defined as the line integral of the velocity around the curve,

$$\Gamma = \oint_{\mathcal{C}} \boldsymbol{v} \cdot \mathrm{d}\boldsymbol{s}, \tag{2.53}$$

which by Stokes's theorem can be written as an integral of the vorticity over the surface $\partial\mathcal{V}$ bounded by $\mathcal{C}$,

$$\Gamma = \int_{\partial\mathcal{V}} (\nabla \times \boldsymbol{v}) \cdot \mathrm{d}\boldsymbol{A} = \int_{\partial\mathcal{V}} \boldsymbol{\omega} \cdot \mathrm{d}\boldsymbol{A}. \tag{2.54}$$

The circulation theorem then states that

$$\frac{\mathrm{D}\Gamma}{\mathrm{D}t} = 0 \tag{2.55}$$

for incompressible flow, and can be derived by combining eqn. (2.52) with Stokes' theorem and the Leibniz integral rule for line integrals (see Appendix C).

Although it may seem a little abstract, we've all seen Kelvin's circulation theorem in action. When water flows past an obstacle (e.g., a fallen tree), little whirlpools form and are subsequently carried downstream for some distance by the flow. These whirlpools are fluid elements having a large vorticity, and Kelvin's theorem tells us that these elements should retain this large vorticity as they move with the flow. Eventually, of course, the whirlpools dissipate; this is a consequence of viscosity, as we'll discuss in greater detail in §3.

2.5 Barotropic Flows

Consider a flow which isn't incompressible, but the pressure — for whatever reason — is everywhere a function of the density alone. It follows that ∇P and $\nabla\rho$ will be parallel, and the cross-product term in eqn. (2.49) vanishes, meaning that the fluid also satisfies the incompressible vorticity equation (2.52) and likewise Kelvin's circulation theorem. Such fluids are known as *barotropic*, and behave much like incompressible fluids even though $\nabla \cdot \boldsymbol{v}$ is not necessarily zero.

An example of a barotropic fluid is an isothermal gas (see, e.g., §B.3); because the temperature is fixed, the pressure and density are directly proportional and so the barotropic condition is met.

2.6 Potential Flows

For irrotational flows, the velocity can be written as the gradient of a scalar *velocity potential*:

$$\boldsymbol{v} = \nabla \Phi_v. \tag{2.56}$$

If the flow is also incompressible, then eqn. (2.51) indicates that

$$\nabla \cdot \nabla \Phi_v = \nabla^2 \Phi_v = 0; \tag{2.57}$$

hence, the velocity potential satisfies Laplace's equation. The solutions to this equation depend only on the boundary conditions — change these condtions, and the whole structure of the flow will change instantaneously. This highlights an artificial property of incompressible flows: signals propagate at infinite speed.

3 Viscosity

3.1 Introducing Viscosity

So far we've neglected the effects of viscosity on fluid motions. Viscosity is the resistance of a fluid to deformation by applied stresses. Everyday examples of viscous fluids include oil and honey. This resistance manifests itself as extra terms in the fluid momentum and energy equations, which we'll briefly review in the following subsections.

Let's start with a couple of definitions:

Stress is the force per unit area exerted on the boundary of a fluid element by a neighboring fluid element.

Rate of strain is the fractional change in the dimensions of a fluid element per unit time.

So, (rate of) strain represents the (rate of) deformation of the fluid, and stress represents the forces causing or resisting this deformation.

3.2 The Strain Rate Tensor

The rate of strain of a fluid is quantified by a *strain rate tensor* (or dyadic, if we're going to insist on consistent nomenclature). To derive an expression for this dyadic, let's consider the velocity field in the neighborhood of some point $\boldsymbol{r}_0$. Using a first-order Taylor-series expansion,

$$\boldsymbol{v}(\boldsymbol{r}, t) = \boldsymbol{v}(\boldsymbol{r}_0, t) + \boldsymbol{J}(\boldsymbol{r}_0, t) \cdot (\boldsymbol{r} - \boldsymbol{r}_0), \tag{3.58}$$

where the dyadic $\boldsymbol{J}$ — sometimes termed the *velocity gradient tensor*, and denoted $\nabla \boldsymbol{v}$ — has components

$$J^{ij} = \frac{\partial v^i}{\partial x^j}. \tag{3.59}$$

This $\boldsymbol{J}$ encapsulates all there is to know about the relative fluid motions around $\boldsymbol{r}$. It can always be decomposed into a dyadic describing rotational motions and a dyadic describing deformational motions — and the latter is the strain rate tensor.

To see this, let's write $\boldsymbol{J}$ in the form

$$\boldsymbol{J} = \boldsymbol{E} + \boldsymbol{R}, \tag{3.60}$$

where we define two additional dyadics

$$\boldsymbol{E} = \frac{1}{2}\left(\boldsymbol{J} + \boldsymbol{J}^{\mathrm{T}}\right), \qquad \boldsymbol{R} = \frac{1}{2}\left(\boldsymbol{J} - \boldsymbol{J}^{\mathrm{T}}\right). \tag{3.61}$$

The $^{\mathrm{T}}$ superscript indicates the transpose, so that for instance

$$(J^{\mathrm{T}})^{ij} = J^{ji}. \tag{3.62}$$

From the definition of $\boldsymbol{E}$ dyadic, we see that it is symmetric: $\boldsymbol{E} = \boldsymbol{E}^{\mathrm{T}}$. Likewise, we see that the $\boldsymbol{R}$ dyadic is anti-symmetric: $\boldsymbol{R} = -\boldsymbol{R}^{\mathrm{T}}$. (There's no magic here; any dyadic or rank-2 tensor can always be split into symmetric and anti-symmetric parts.)

The $\boldsymbol{R}$ dyadic represents the (locally uniform) rotation of the fluid about $\boldsymbol{r}_0$. To see this, we write it out in matrix form (and assuming Cartesian geometry) as

$$\boldsymbol{R} = \frac{1}{2}\begin{pmatrix} 0 & \frac{\partial v_x}{\partial y} - \frac{\partial v_y}{\partial x} & \frac{\partial v_x}{\partial z} - \frac{\partial v_z}{\partial x} \\ \frac{\partial v_y}{\partial x} - \frac{\partial v_x}{\partial y} & 0 & \frac{\partial v_y}{\partial z} - \frac{\partial v_z}{\partial y} \\ \frac{\partial v_z}{\partial x} - \frac{\partial v_x}{\partial z} & \frac{\partial v_z}{\partial y} - \frac{\partial v_y}{\partial z} & 0 \end{pmatrix} \tag{3.63}$$

We can recognize the non-zero entries in this matrix as the components of the vorticity vector $\boldsymbol{\omega}$ (cf. eqn. 2.40); hence, $\boldsymbol{R}$ can also be expressed

$$\boldsymbol{R} = \frac{1}{2}\begin{pmatrix} 0 & -\omega_z & -\omega_x \\ \omega_z & 0 & -\omega_y \\ \omega_x & \omega_y & 0 \end{pmatrix} \tag{3.64}$$

Clearly, $\boldsymbol{R}$ tells us about the rotation of the fluid around $\boldsymbol{r}_0$; if $\boldsymbol{R}$ vanishes, then the fluid must be (locally) irrotational, and vice versa.

The remaining symmetric part $\boldsymbol{E}$ of the velocity gradient tensor is the strain rate tensor, and describes the non-rotational changes to the fluid in the vicinity of $\boldsymbol{r}_0$ — whether due to compression/expansion or to shear deformation, or a combination thereof. The components of this tensor are

$$E^{ij} = \frac{1}{2}\left(\frac{\partial v^i}{\partial x^j} + \frac{\partial v^j}{\partial x^i}\right), \tag{3.65}$$

or in vector/dyadic notation

$$\boldsymbol{E} = \frac{1}{2}\left[\nabla\boldsymbol{v} + (\nabla\boldsymbol{v})^{\mathrm{T}}\right]. \tag{3.66}$$

Written out in matrix form (again assuming Cartesian geometry), we also have

$$\boldsymbol{E} = \frac{1}{2}\begin{pmatrix} 2\frac{\partial v_x}{\partial x} & \frac{\partial v_x}{\partial y} + \frac{\partial v_y}{\partial x} & \frac{\partial v_x}{\partial z} + \frac{\partial v_z}{\partial x} \\ \frac{\partial v_y}{\partial x} + \frac{\partial v_x}{\partial y} & 2\frac{\partial v_y}{\partial y} & \frac{\partial v_y}{\partial z} + \frac{\partial v_z}{\partial y} \\ \frac{\partial v_z}{\partial x} + \frac{\partial v_x}{\partial z} & \frac{\partial v_z}{\partial y} + \frac{\partial v_y}{\partial z} & 2\frac{\partial v_y}{\partial z} \end{pmatrix}. \tag{3.67}$$

To separate out the compression/expansion and shearing parts of $\boldsymbol{E}$, we can further decompose it as

$$\boldsymbol{E} = \frac{1}{2}\boldsymbol{D} + \frac{1}{3}(\nabla\cdot\boldsymbol{v})\boldsymbol{I}. \tag{3.68}$$

Here, the deformation rate tensor $\boldsymbol{D}$ is

$$\boldsymbol{D} \equiv \left[\nabla\boldsymbol{v} + (\nabla\boldsymbol{v})^{\mathrm{T}}\right] - \frac{2}{3}(\nabla\cdot\boldsymbol{v})\boldsymbol{I}, \tag{3.69}$$

or in component notation

$$D^{ij} = \left(\frac{\partial v^i}{\partial x^j} + \frac{\partial v^j}{\partial x^i}\right) - \frac{2}{3}(\nabla\cdot\boldsymbol{v})\delta_{ij}. \tag{3.70}$$

This tensor encapsulates the rate of shearing deformation of the fluid. It the traceless part of $\boldsymbol{E}$, meaning that

$$\mathrm{Tr}(\boldsymbol{D}) \equiv D^{ii} = 0. \tag{3.71}$$

3.3 The Viscous Stress Tensor

The stress of a fluid is quantified by a *viscous stress tensor* (or dyadic) $\boldsymbol{\sigma}$. This tensor gives the force exerted on a boundary area element $\mathrm{d}\boldsymbol{A}$ as

$$\boldsymbol{f} = \boldsymbol{\sigma}\cdot\mathrm{d}\boldsymbol{A}. \tag{3.72}$$

If we know the components of $\boldsymbol{\sigma}$ and $\mathrm{d}\boldsymbol{A}$, we can evaluate this force as

$$\boldsymbol{f} = \sigma^{ij}\mathrm{d}A^j\,\boldsymbol{e}_i \tag{3.73}$$

(cf. eqn. A.14).

When this stress is included in the fluid equations, the momentum equation (1.17) becomes

$$\frac{\partial\rho\boldsymbol{v}}{\partial t} + \nabla\cdot(\rho\boldsymbol{v}\otimes\boldsymbol{v} + P\boldsymbol{I} - \boldsymbol{\sigma}) = 0, \tag{3.74}$$

while the energy equation (1.21) becomes

$$\frac{\partial\rho\varepsilon}{\partial t} + \nabla\cdot(\rho\varepsilon\boldsymbol{v} + P\boldsymbol{v} - \boldsymbol{v}\cdot\boldsymbol{\sigma}) = 0. \tag{3.75}$$

The correctness of these expressions can be seen by including the viscous boundary force (3.72) in the integral forms of the conservation equations discussed in §1.4.

3.4 Newtonian Fluids

For general fluids, determining the nine components σ^{ij} of the viscous stress tensor is a pretty tough undertaking. However, there is a simple class of fluids for which things are significantly easier:

A *Newtonian fluid* is a viscous fluid in which the stress is linearly proportional to the rate of strain.

This linear proportionality can be a messy affair: each of the nine components of the stress tensor can be a linear combination of each of the nine strain rate tensor components, so we need $9^2 = 81$ constants of proportionality! But if the viscosity of the fluid is *isotropic* (the same in all directions), then it turns out there are only two independent constants. This leads to a viscous stress tensor with the general form

$$\boldsymbol{\sigma} = \mu \boldsymbol{D} + \beta(\nabla \cdot \boldsymbol{v})\boldsymbol{I}, \tag{3.76}$$

or in terms of components

$$\sigma^{ij} = \mu D^{ij} + \beta(\nabla \cdot \boldsymbol{v})\delta_{ij}, \tag{3.77}$$

where μ and β are respectively the *shear* and *bulk* coefficients of viscosity. The former corresponds to our day-to-day conception of viscosity as a resistance to shearing, while the latter amounts to a transient resistance to compression or expansion. A nice analogy to bulk viscosity is pushing down on a sealed piston with a 'sticky' plunger (one that experiences friction as it slides past the cylinder walls) — the resistance of the piston to being compressed only arises when the plunger is in motion. Bulk viscosity typically arises in fluids with internal degrees of freedom (e.g., molecular rotations and vibrations) or with inter-molecular forces. However, for an ideal monatomic gas (which has neither of these) it vanishes: $\beta = 0$. Also, for incompressible flows the $\nabla \cdot \boldsymbol{v}$ term is zero, and so bulk viscosity becomes irrelevant.

Sometimes it is useful to combine the viscous stress and pressure forces into a single dyadic, the total stress:

$$\boldsymbol{T} = \boldsymbol{\sigma} - P\boldsymbol{I} = \mu \boldsymbol{D} + [\beta(\nabla \cdot \boldsymbol{v}) - P]\,\boldsymbol{I}. \tag{3.78}$$

When we substitute eqn. (3.76) into the momentum equation (3.74), we end up with a version of the equation applicable to Newtonian fluids:

$$\frac{\partial \rho \boldsymbol{v}}{\partial t} + \nabla \cdot (\rho \boldsymbol{v} \otimes \boldsymbol{v}) + \nabla P = \mu \nabla \cdot \boldsymbol{D} + \beta \nabla(\nabla \cdot \boldsymbol{v}). \tag{3.79}$$

Here, we've assumed μ and β are independent of position, and taken the liberty of moving the viscosity-related terms to the right-hand side, to highlight the fact that they are additional terms which only arise when μ and/or β are non-zero. If we substitute in the definition (3.69) of the deformation rate tensor $\boldsymbol{D}$ this becomes

$$\frac{\partial \rho \boldsymbol{v}}{\partial t} + \nabla \cdot (\rho \boldsymbol{v} \otimes \boldsymbol{v}) + \nabla P = \mu \nabla \cdot \left[\nabla \boldsymbol{v} + (\nabla \boldsymbol{v})^{\mathrm{T}} - \frac{2}{3}(\nabla \cdot \boldsymbol{v})\boldsymbol{I}\right] + \beta \nabla(\nabla \cdot \boldsymbol{v}). \tag{3.80}$$

We can simplify this by noting that

$$\nabla \cdot [\nabla \boldsymbol{v}] = \nabla^2 \boldsymbol{v} \tag{3.81}$$

(this is the vector Laplacian operator), while

$$\nabla \cdot [(\nabla \boldsymbol{v})^{\mathrm{T}}] = \nabla(\nabla \cdot \boldsymbol{v}). \tag{3.82}$$

Hence,

$$\frac{\partial \rho \boldsymbol{v}}{\partial t} + \nabla \cdot (\rho \boldsymbol{v} \otimes \boldsymbol{v}) + \nabla P = \mu \nabla^2 \boldsymbol{v} + (\beta + \frac{1}{3}\mu)\nabla(\nabla \cdot \boldsymbol{v}). \tag{3.83}$$

If the bulk viscosity vanishes, then this further simplifies to

$$\frac{\partial \rho \boldsymbol{v}}{\partial t} + \nabla \cdot (\rho \boldsymbol{v} \otimes \boldsymbol{v}) + \nabla P = \mu \nabla^2 \boldsymbol{v} + \frac{1}{3}\mu\nabla(\nabla \cdot \boldsymbol{v}). \tag{3.84}$$

What about energy conservation for Newtonian fluids? Substituting eqn. (3.76) into the energy equation (3.74), we find after some (rather hairy) algebra that

$$\frac{\partial \rho \varepsilon}{\partial t} + \nabla \cdot (\rho \varepsilon \boldsymbol{v} + P \boldsymbol{v}) = \boldsymbol{v} \cdot (\nabla \cdot \boldsymbol{\sigma}) + \Phi, \tag{3.85}$$

where

$$\Phi \equiv 2\mu \sum_{i,j} \left(E^{ij}\right)^2 + \left(\beta - \frac{2}{3}\mu\right)(\nabla \cdot \boldsymbol{v})^2. \tag{3.86}$$

The first term on the right-hand side of eqn. (3.85) represents the rate at which work is done by viscous forces — i.e., the viscous contribution to the kinetic energy changes. The Φ term, which is always positive, likewise represents the rate of viscous heating — i.e., the viscous contribution to the internal energy changes. Its presence means that the flow is no longer adiabatic.

3.5 The Reynolds Number

To get a handle on how important viscous effects will be in any flow configuration, let's take the curl of the momentum equation (3.83) to arrive at the vorticity equation for Newtonian fluids:

$$\frac{\partial \boldsymbol{\omega}}{\partial t} = \nabla \times (\boldsymbol{v} \times \boldsymbol{\omega}) + \frac{1}{\rho^2}\nabla\rho \times \nabla P + \nu \nabla^2 \boldsymbol{\omega} \tag{3.87}$$

(as in §B.5, $\nu \equiv \mu/\rho$ is the kinematic viscosity). For barotropic flows, this simplifies to

$$\frac{\partial \boldsymbol{\omega}}{\partial t} = \nabla \times (\boldsymbol{v} \times \boldsymbol{\omega}) + \nu \nabla^2 \boldsymbol{\omega}. \tag{3.88}$$

If $\nu \to 0$ then we recover eqn. (2.52), and Kelvin's circulation theorem holds (cf. §2.4). For non-vanishing viscosity, however, the second term on the right-hand side corresponds to the diffusion of vorticity. It is this term which causes the gradually decay of eddies, as they share their vorticity with their surroundings (recall the discussion of whirlpools in water flow, in §2.4).

Suppose we now introduce a new set of 'primed' variables

$$\boldsymbol{r} = \boldsymbol{r}' L, \qquad \boldsymbol{v} = \boldsymbol{v}' V, \qquad t = t' \frac{L}{V}, \qquad \boldsymbol{\omega} = \boldsymbol{\omega}' \frac{V}{L}, \tag{3.89}$$

where L is the typical length scale of the system under consideration, and V is the typical flow velocity. Then, the vorticity equation becomes

$$\frac{\partial \boldsymbol{\omega}'}{\partial t'} = \nabla' \times (\boldsymbol{v}' \times \boldsymbol{\omega}') + \frac{1}{\mathcal{R}} \nabla'^2 \boldsymbol{\omega}', \tag{3.90}$$

where $\nabla' = L\nabla$ denotes spatial differential with respect to the scaled length. Here,

$$\mathcal{R} \equiv \frac{LV}{\nu} \tag{3.91}$$

is a dimensionless quantity known as the *Reynolds number*.

The significance of the Reynolds number is that flows involving geometrically similar configurations and similar Reynolds numbers will behave in the same manner. For instance, if we have a pair of systems involving incompressible flow around a fixed cylinder, the behavior of the systems will be the same if they have the same Reynolds number, regardless of the size of the systems, flow velocities, etc. This is known as the *law of similarity*. It means that to study, e.g., flow around cylinders in general, it is only necessary to consider systems spanning a range of $\mathcal{R}$; the actual dimensions, viscosities, etc. of the systems don't matter. A very good movie demonstrating these principles in action can be viewed at https://www.youtube.com/watch?v=0ThQ_nD97hY; this movie demonstrates that as $\mathcal{R}$ decreases, the flow around a cylinder becomes progressively more laminar.

Returning to the scaled vorticity eqn. (3.90), we can also say that

The Reynolds number characterizes the relative strength of inertial and viscous forces in a fluid.

(with the inertia force corresponding to the first term on the right-hand side, and the viscous force the second). For $\mathcal{R} \ll 1$ viscosity always dominates, whereas for $\mathcal{R} \gg 1$ inertia dominates — although viscous forces remain important near boundaries, as we shall now see.

3.6 Boundary Layers

For an inviscid flow, the boundary condition we must apply for flow adjacent to a fixed surface is the *no-penetration* condition: the component of the velocity perpendicular to the surface vanishes (cf. §B.4).

However, even for fluids having very large Reynolds numbers (and thus behaving almost inviscidly) this condition is rarely realized. Experiments instead show that a more realistic condition is the *no-slip* condition which we encounter in §B.5: the component of the velocity parallel to the surface also vanishes, in the frame where the surface is at rest. The reasons behind the no-slip condition are complicated, involving consideration of molecular forces between the fluid and the surface which lie outside the scope of hydrodynamics.

However, that doesn't stop us from discussing the consequences of the no-slip condition. Essentially, the condition means that in the vicinity of a boundary there is a region of strong shear, as the flow velocity drops from its 'free' (away-from-the-boundary) value down to zero. In this *boundary layer* the shear is sufficiently large that the viscous terms in the fluid equations become comparable to the other terms, even though viscosity itself may be very small. To get an order-of-magnitude estimate for the size of the boundary layer, lets consider a steady flow beside a straight boundary. The shear caused by the no-slip condition will produce viscous stresses which tend to decelerate the flow. Over a distance L parallel to the boundary, this deceleration scales as $\sim V^2/L$, where V is the flow velocity away from the boundary. Equating this to the viscous stresses, we thus have

$$\frac{V^2}{L} \sim \nu \frac{V}{\delta^2} \tag{3.92}$$

where δ is the thickness of the boundary layer. Solving,

$$\delta \sim \sqrt{\frac{\nu L}{V}}; \tag{3.93}$$

this indicates that the boundary layer gets thicker as L gets larger, and in this respect we can interpret L in this expression as the distance from the upstream beginning of the boundary layer.

4 Waves & Instabilities

4.1 What is a Wave?

Quoting from Wikipedia[3]:

> A wave is a disturbance or oscillation that travels through spacetime, accompanied by a transfer of energy.

The two important words in this definition are *disturbance* and *travels*; the former implies a perturbation to a background state, and the latter indicates that this perturbation does not remain fixed but moves around.

4.2 Perturbation Description

To model waves, we consider the time-dependent behavior of perturbations to some well-defined background fluid state. We can represent these perturbations by decomposing the density, pressure, velocity and specific total energy of the fluid as

$$\rho = \rho_0 + \rho', \tag{4.94}$$
$$P = P_0 + P', \tag{4.95}$$
$$\boldsymbol{v} = \boldsymbol{v}_0 + \boldsymbol{v}', \tag{4.96}$$
$$\varepsilon = \varepsilon_0 + \varepsilon'; \tag{4.97}$$

here, the subscript 0 denotes the background state, while the prime ($'$) indicates the fixed-position perturbation[4]. Note that these perturbations aren't completely independent; from the definition (1.5) of the total energy, we have

$$\varepsilon_0 + \varepsilon' = u_0 + u' + \frac{1}{2}|\boldsymbol{v}_0 + \boldsymbol{v}'|^2, \tag{4.98}$$

where u_0 and u' are the background specific internal energy and the perturbation thereof, respectively. If we assume that the perturbations are small, then we can expand the terms on the right-hand side neglecting terms of second- or higher-order in the perturbed (primed) quantities. After some algebra, we find

$$\varepsilon_0 + \varepsilon' = u_0 + u' + \frac{1}{2}|\boldsymbol{v}_0|^2 + \boldsymbol{v}_0 \cdot \boldsymbol{v}'. \tag{4.99}$$

(strictly speaking, we should use $\approx$ here rather than $=$; but the approximation is a very good one when the perturbation amplitudes are small). Since the background state independently

[3] Which is a useful resource, *if* you already know the answer — verify, then trust!

[4] Also known as the 'Eulerian' perturbation, to distinguish it from the 'Lagrangian' perturbation experienced by a given fluid element.

(and exactly) satisfies eqn. (1.5),

$$\varepsilon_0 = u_0 + \frac{1}{2}|\boldsymbol{v}_0|^2, \tag{4.100}$$

we can subtract it away to give

$$\varepsilon' = u' + \boldsymbol{v}_0 \cdot \boldsymbol{v}'. \tag{4.101}$$

For an ideal gas, perturbing the equation of state (1.4) gives

$$P' = (\gamma - 1)\left[\rho' u_0 + \rho_0 u'\right] \tag{4.102}$$

(where again we've neglected second-order terms, and substracted the background state). Combining this with eqn. (4.2), we arrive at the result

$$\varepsilon' = \frac{1}{\gamma - 1}\frac{P_0}{\rho_0}\left(\frac{P'}{P_0} - \frac{\rho'}{\rho_0}\right) + \boldsymbol{v}_0 \cdot \boldsymbol{v}'. \tag{4.103}$$

This supports our assertion above that the four perturbations ρ', P', $\boldsymbol{v}'$ and ε' are not completely independent.

4.3 Linearized Equations

Let's substitute the above expressions (4.94–4.97) into the fluid equations (1.13,1.17,1.21), with the inclusion of an external body force per unit mass $\boldsymbol{g}$ (cf. §1.5) to allow us to consider waves in hydrostatic stratifications. Applying the same *linearization* process of ignoring second- or higher-order terms and subtracting away the background state, the resulting equations are

$$\frac{\partial \rho'}{\partial t} + \nabla \cdot (\rho_0 \boldsymbol{v}') + \nabla \cdot (\rho' \boldsymbol{v}_0) = 0, \tag{4.104}$$

$$\frac{\partial \boldsymbol{v}'}{\partial t} + \boldsymbol{v}_0 \cdot \nabla \boldsymbol{v}' + \boldsymbol{v}' \cdot \nabla \boldsymbol{v}_0 + \frac{1}{\rho_0}\nabla P' - \frac{\rho'}{\rho_0^2}\nabla P_0 = \boldsymbol{g}' \tag{4.105}$$

$$\frac{\partial \varepsilon'}{\partial t} + \boldsymbol{v}' \cdot \nabla \varepsilon_0 + \boldsymbol{v}_0 \cdot \nabla \varepsilon' + \frac{1}{\rho_0}\nabla \cdot (P_0 \boldsymbol{v}' + P' \boldsymbol{v}_0) - \frac{\rho'}{\rho_0^2}\nabla \cdot (P_0 \boldsymbol{v}_0) = \boldsymbol{v}' \cdot \boldsymbol{g}_0 + \boldsymbol{v}_0 \cdot \boldsymbol{g}'. \tag{4.106}$$

In the majority of cases we'll encounter the background state is static, and the linearized equations then simplify to

$$\frac{\partial \rho'}{\partial t} + \nabla \cdot (\rho_0 \boldsymbol{v}') = 0, \tag{4.107}$$

$$\frac{\partial \boldsymbol{v}'}{\partial t} + \frac{1}{\rho_0}\nabla P' - \frac{\rho'}{\rho_0^2}\nabla P_0 = \boldsymbol{g}' \tag{4.108}$$

$$\frac{\partial \varepsilon'}{\partial t} + \boldsymbol{v}' \cdot \nabla \varepsilon_0 + \frac{1}{\rho_0}\nabla \cdot (P_0 \boldsymbol{v}') = \boldsymbol{v}' \cdot \boldsymbol{g}_0. \tag{4.109}$$

For an ideal gas, we can use eqn. (4.103) to re-cast the energy equation into one for the gas pressure perturbations,

$$\frac{\partial P'}{\partial t} + \gamma P_0 \nabla \cdot \boldsymbol{v}' + \boldsymbol{v}' \cdot \nabla P_0 = 0 \tag{4.110}$$

(the $\boldsymbol{g}_0$ term on the right-hand side has been eliminated using the equation hydrostatic equilibrium).

4.4 Acoustic Waves

4.4.1 Wave Equation

Let's now apply the linearized equations (4.107,4.108,4.110) to explore waves in a static, *uniform* ideal gas with no external forces. Setting all background-state gradients to zero, the equations become

$$\frac{\partial \rho'}{\partial t} + \rho_0 \nabla \cdot \boldsymbol{v}' = 0, \tag{4.111}$$

$$\frac{\partial \boldsymbol{v}'}{\partial t} + \frac{1}{\rho_0} \nabla P' = 0 \tag{4.112}$$

$$\frac{\partial P'}{\partial t} + \gamma P_0 \nabla \cdot \boldsymbol{v}' = 0. \tag{4.113}$$

Taking the divergence of the momentum equation, we find that

$$\frac{\partial}{\partial t} \nabla \cdot \boldsymbol{v}' = -\frac{1}{\rho_0} \nabla^2 P'. \tag{4.114}$$

Likewise, differentiating the pressure equation with respect to time,

$$\frac{\partial}{\partial t} \nabla \cdot \boldsymbol{v}' = -\frac{1}{\gamma P_0} \frac{\partial^2 P'}{\partial t^2}. \tag{4.115}$$

Combining these two expressions, we arrive at the result

$$\nabla^2 P' = \frac{\rho_0}{\gamma P_0} \frac{\partial^2 P'}{\partial t^2}. \tag{4.116}$$

This has the classic form of a *wave equation*, describing the propagation of pressure disturbances throughout the fluid — that is, acoustic (sound) waves. Its general solutions are plane waves of the form

$$\frac{P'(\boldsymbol{r}, t)}{P_0} = A \exp[\mathrm{i}(\boldsymbol{k} \cdot \boldsymbol{r} - \omega t)] \tag{4.117}$$

(we'll demonstrate this rigorously below). Here, A is a dimensionless constant giving the amplitude of the waves; $\boldsymbol{k}$ is the wavevector, which points in the direction of propagation and has magnitude $|\boldsymbol{k}| = 2\pi/\lambda$, where λ is the wavelength; and ω is the angular frequency of the waves.

4.4.2 Dispersion Relation

The wavevector and angular frequency of the acoustic waves in eqn. (4.117) are not independent quantities — they are tied together by a *dispersion relation*

$$\omega(\boldsymbol{k}) = \pm a_{\rm ad}|\boldsymbol{k}|, \tag{4.118}$$

where

$$a_{\rm ad} \equiv \sqrt{\frac{\gamma P_0}{\rho_0}}. \tag{4.119}$$

Every type of wave — not just the acoustic waves considered here — has an associated dispersion relation, which neatly encapsulates many aspects of the waves' behavior. The phase velocity can be obtained from the dispersion relation via

$$\boldsymbol{c}_{\rm ph} = \omega \frac{\boldsymbol{k}}{|\boldsymbol{k}|^2}, \tag{4.120}$$

and likewise the group velocity by

$$\boldsymbol{c}_{\rm gr} = \nabla_{\boldsymbol{k}} \omega, \tag{4.121}$$

where $\nabla_{\boldsymbol{k}}$ is the gradient operator in wavevector space. Applied to the acoustic-wave dispersion relation (4.118), we find that both group and phase velocities are parallel to $\boldsymbol{k}$, and have magnitude equal to $a_{\rm ad}$. Hence, $a_{\rm ad}$ is appropriately referred to as the sound speed — or more explicitly, the *adiabatic* sound speed, to distinguish it from the *isothermal* sound speed

$$a_{\rm iso} \equiv \sqrt{\frac{P_0}{\rho_0}}. \tag{4.122}$$

We encounter the isothermal sound speed in a number of the worked examples in Appendix B; in the present context, it would arise if we solved the linearized equations with the pressure equation (4.113) replaced by the isothermal relation

$$\frac{P'}{P_0} = \frac{\rho'}{\rho_0}. \tag{4.123}$$

4.4.3 Matrix Formulation

The plane-wave solutions (4.117) to the acoustic wave equation (4.116) can be derived using a matrix formulation, which we discuss in some detail here to lay the groundwork for considering more-complex wave systems later on. Let's start by noting that the linearized

equations (4.111–4.113) are homogeneous and have constant coefficients. This motivates us to search for solutions of the form

$$\boldsymbol{Y}(\boldsymbol{r}, t) = \boldsymbol{y} \exp[\mathrm{i}(\boldsymbol{k} \cdot \boldsymbol{r} - \omega t)] \tag{4.124}$$

where

$$\boldsymbol{Y} \equiv \begin{pmatrix} \rho'/\rho_0 \\ v_x'/a_\mathrm{ad} \\ v_y'/a_\mathrm{ad} \\ v_z'/a_\mathrm{ad} \\ P'/P_0 \end{pmatrix} \tag{4.125}$$

is the vector of unknowns (scaled by the background values), and $\boldsymbol{y}$ is a constant vector to be determined. Substituting this expression for $\boldsymbol{Y}$ into the linearized equations leads to a set of *algebraic* equations for $\boldsymbol{y}$,

$$\boldsymbol{M}\boldsymbol{y} = \omega \boldsymbol{y} \tag{4.126}$$

where the 5×5 matrix $\boldsymbol{M}$ is

$$\boldsymbol{M} = \begin{pmatrix} 0 & a_\mathrm{ad}k_x & a_\mathrm{ad}k_y & a_\mathrm{ad}k_z & 0 \\ 0 & 0 & 0 & 0 & a_\mathrm{ad}k_x/\gamma \\ 0 & 0 & 0 & 0 & a_\mathrm{ad}k_y/\gamma \\ 0 & 0 & 0 & 0 & a_\mathrm{ad}k_z/\gamma \\ 0 & a_\mathrm{ad}k_x\gamma & a_\mathrm{ad}k_y\gamma & a_\mathrm{ad}k_z\gamma & 0 \end{pmatrix}, \tag{4.127}$$

with (k_x, k_y, k_z) the Cartesian components of $\boldsymbol{k}$.

Equation (4.126) has the classic form of a *matrix eigenvalue problem*: non-trivial solutions only exist for specific combinations of ω and $\boldsymbol{y}$, which are known as the *eigenvalues* and *eigenvectors*, respectively, of the matrix $\boldsymbol{M}$. The eigenvalues are found by solving the *characteristic equation*

$$\det(\boldsymbol{M} - \omega \boldsymbol{I}) = 0, \tag{4.128}$$

where det() denotes the matrix determinant and $\boldsymbol{I}$ is the identity matrix. Using *Mathematica* to calculate this determinant, we find a characteristic equation

$$(a_\mathrm{ad}^2 |\boldsymbol{k}|^2 - \omega^2)\omega^3 = 0 \tag{4.129}$$

where a_ad is the adiabatic sound speed introduced in eqn. (4.119). This is a fifth-order polynomial in ω, and therefore has five solutions — three trivial, with $\omega = 0$, and two non-trivial, with

$$\omega = \pm a_\mathrm{ad} |\boldsymbol{k}| \tag{4.130}$$

But these latter solutions are the same as eqn. (4.118), and so we see that the characteristic equation (or the solutions thereof) *is* the dispersion relation!

The eigenvectors corresponding to the non-trivial eigenvalues $\omega = \pm a_{\rm ad}|\boldsymbol{k}|$ are found[5] as

$$\boldsymbol{y} = A \begin{pmatrix} 1 \\ \pm\gamma k_x/|\boldsymbol{k}| \\ \pm\gamma k_y/|\boldsymbol{k}| \\ \pm\gamma k_z/|\boldsymbol{k}| \\ \gamma \end{pmatrix}, \tag{4.131}$$

where A is an arbitrary dimensionless constant[6]. Combining this with eqn. (4.124), we obtain the solutions to the acoustic wave equation as

$$\begin{pmatrix} P'/P_0 \\ v'_x/a_{\rm ad} \\ v'_y/a_{\rm ad} \\ v'_z/a_{\rm ad} \\ \rho'/\rho_0 \end{pmatrix} = A \begin{pmatrix} 1 \\ \pm\gamma k_x/|\boldsymbol{k}| \\ \pm\gamma k_y/|\boldsymbol{k}| \\ \pm\gamma k_z/|\boldsymbol{k}| \\ \gamma \end{pmatrix} \exp[{\rm i}(\boldsymbol{k}\cdot\boldsymbol{r} - \omega t)]. \tag{4.132}$$

These are the same plane-wave solutions as obtained before (cf. eqn. 4.117), but now we can see, for instance, that fluid motions are parallel to the direction of propagation, and therefore that acoustic waves are longitudinal.

What about the three trivial $\omega = 0$ solutions to the characteristic equation (4.129)? These represent to time-independent perturbations to the fluid. One has an eigenvector

$$\boldsymbol{y} = A \begin{pmatrix} 1 \\ 0 \\ 0 \\ 0 \\ 0 \end{pmatrix}, \tag{4.133}$$

corresponding to a static, spatially-periodic perturbation to the fluid density. The other two have eigenvectors

$$\boldsymbol{y} = A \begin{pmatrix} 0 \\ -k_z/k_x \\ 0 \\ 1 \\ 0 \end{pmatrix} \tag{4.134}$$

and

$$\boldsymbol{y} = A \begin{pmatrix} 0 \\ -k_y/k_x \\ 1 \\ 0 \\ 0 \end{pmatrix}. \tag{4.135}$$

These both describe steady-state fluid flows in a direction perpendicular to $\boldsymbol{k}$. It's straightforward to confirm that these flows are incompressible, with $\nabla\cdot\boldsymbol{v}' = 0$ (this could also be surmised from the fact that the density perturbation ρ' is zero).

[5] Using, for instance, *Mathematica's* `Eigenvectors[]` routine.

[6] The overall normalization of eigenvectors is always arbitrary.

4.5 Gravito-Acoustic Waves

4.5.1 Wave Equation

We're now going to examine waves in a gravitationally stratified medium — specifically, one in which the gravity acts downward in the Cartesian z direction (which we'll term the 'vertical' direction) with an acceleration g. The background state for this medium satisfies the equation of hydrostatic equilibrium,

$$\nabla P_0 = -\rho_0 g \hat{\boldsymbol{z}}. \tag{4.136}$$

For simplicity let's assume that this state is isothermal, so that $P_0 = a_{\rm iso}^2 \rho_0$ everywhere; then, the vertical variation of both P_0 and ρ_0 is exponential:

$$P_0 = P_{0,0} \left(-\frac{z}{H}\right), \tag{4.137}$$

$$\rho_0 = \rho_{0,0} \left(-\frac{z}{H}\right), \tag{4.138}$$

where $P_{0,0}$ and $\rho_{0,0}$ are the pressure and density at $z = 0$, respectively, and

$$H \equiv \frac{a_{\rm iso}^2}{g}. \tag{4.139}$$

is the pressure/density scale height.

The linearized equations governing perturbations to this background state are found as

$$\frac{\partial \rho'}{\partial t} + \rho_0 \nabla \cdot \boldsymbol{v}' - \frac{\rho_0}{H} v_z' = 0, \tag{4.140}$$

$$\frac{\partial \boldsymbol{v}'}{\partial t} + \frac{1}{\rho_0} \nabla P' + \frac{\rho'}{\rho_0^2} \frac{P_0}{H} \hat{\boldsymbol{z}} = 0, \tag{4.141}$$

$$\frac{\partial P'}{\partial t} + \gamma P_0 \nabla \cdot \boldsymbol{v}' - v_z' \frac{P_0}{H} = 0. \tag{4.142}$$

Here, we've neglected perturbations to the gravitational acceleration — the so-called *Cowling approximation*, which amounts to assuming that the gravitational field is unaffected by small perturbations to the mass distribution in the medium.

We could in principle combine these equations to derive a monstrous (fifth-order!) ordinary differential equation for one of the perturbed variables. However, there's little insight to be gained from such mathematical pain.

4.5.2 Matrix Formulation

Instead, let's assume trial solutions

$$\boldsymbol{Y}(\boldsymbol{r}, t) = \boldsymbol{y} \exp[\mathrm{i}(\boldsymbol{k} \cdot \boldsymbol{r} - \omega t) + z/2H] \tag{4.143}$$

where $\boldsymbol{Y}$ is the same as in eqn. (4.125). The additional scaling by $\exp(z/2H)$ in eqn. (4.143) is not strictly necessary, but it simplifies the following analysis considerably and is therefore advantageous. Substituting these trial solutions into the linearized equations results in an eigenvalue problem (cf. eqn. 4.126), with a matrix

$$\boldsymbol{M} = \begin{pmatrix} 0 & a_{\rm ad}k_x & a_{\rm ad}k_y & a_{\rm ad}k_z + {\rm i}a_{\rm ad}/2H & 0 \\ 0 & 0 & 0 & 0 & a_{\rm ad}k_x/\gamma \\ 0 & 0 & 0 & 0 & a_{\rm ad}k_y/\gamma \\ -{\rm i}a_{\rm ad}/\gamma H & 0 & 0 & 0 & a_{\rm ad}k_z/\gamma + {\rm i}a_{\rm ad}/2\gamma H \\ 0 & \gamma a_{\rm ad}k_x & \gamma a_{\rm ad}k_y & \gamma a_{\rm ad}k_z - {\rm i}a_{\rm ad}(\gamma-2)/2H & 0 \end{pmatrix}. \tag{4.144}$$

Comparing this against eqn. (4.127), we see that the two matrices are the same in the limit $H \to \infty$, corresponding to $g \to 0$.

The characteristic equation for this eigenvalue problem is found (again, using *Mathematica*) as

$$\left\{\omega^4 - \left[\omega_{\rm ac}^2 + a_{\rm ad}^2|\boldsymbol{k}|^2\right]\omega^2 + a_{\rm ad}^2 N^2(k_x^2 + k_y^2)\right\}\omega = 0, \tag{4.145}$$

where $k_{\rm h}$ is the horizontal wavenumber defined via

$$k_{\rm h}^2 \equiv k_x^2 + k_y^2, \tag{4.146}$$

and

$$\omega_{\rm ac} \equiv \frac{a_{\rm ad}}{2H} = \frac{\gamma g}{2a_{\rm ad}} \tag{4.147}$$

and

$$N \equiv \frac{a_{\rm ad}}{\gamma H}\sqrt{\gamma - 1} = \frac{g}{a_{\rm ad}}\sqrt{\gamma - 1} \tag{4.148}$$

serve to introduce the acoustic cutoff frequency $\omega_{\rm ac}$ and the Brunt-Väisälä frequency N, respectively. These are key characteristic frequencies of a stably stratified medium — more of this later.

The characteristic equation above has a single $\omega = 0$ trivial solution. The remaining non-trivial solutions satisfy

$$\omega^4 - \left[\omega_{\rm ac}^2 + a_{\rm ad}^2|\boldsymbol{k}|^2\right]\omega^2 + a_{\rm ad}^2 N^2 k_{\rm h}^2 = 0. \tag{4.149}$$

This is quadratic in ω^2, and hence can be solved using the standard formula:

$$\omega^2 = \frac{\omega_{\rm ac}^2 + a_{\rm ad}^2|\boldsymbol{k}|^2 \pm \sqrt{\left(\omega_{\rm ac}^2 + a_{\rm ad}^2|\boldsymbol{k}|^2\right)^2 - 4a_{\rm ad}^2 N^2 k_{\rm h}^2}}{2} \tag{4.150}$$

4.5.3 Vertical Propagation

If we focus on vertically propagating waves, with $k_\mathrm{h} = 0$, then then the solutions above simplify to

$$\omega^2 = \omega_\mathrm{ac}^2 + a_\mathrm{ad}^2 k_z^2 \tag{4.151}$$

and

$$\omega^2 = 0. \tag{4.152}$$

We'll discuss the latter, zero-frequency solutions later on. In the limit $a_\mathrm{ad}^2 k_z^2 \gg \omega_\mathrm{ac}$, the former solutions are well approximated by

$$\omega \approx \pm a_\mathrm{ad} k_z, \tag{4.153}$$

which resembles the acoustic-wave dispersion relation (4.118) for a uniform medium. This is no coincidence: these solutions to the dispersion relation correspond to acoustic waves!

Although largely unaffected at high wavenumbers, vertically propagating acoustic waves become increasingly influenced by the stratification of the medium as k_z approaches and then drops below $\omega_\mathrm{ac}/a_\mathrm{ad}$ (this threshold corresponding, approximately, to $\lambda \sim H$). Specifically, rather than varying proportionally to k_z, the frequency approaches a constant value equal to the acoustic cutoff frequency ω_ac. So, ω_ac represents the smallest frequency an acoustic wave can have if it is to propagate upward or downward in the stratified medium.

What then happens if we try to drive oscillations with ω below this cutoff? Since eqn. (4.151) must still be satisfied, k_z^2 must be negative and hence k_z is imaginary. These solutions are known as *evanescent* waves — their spatial dependence is exponentially growing/decaying, rather than being oscillatory. Evanescent solutions are usually associated with quantum mechanical systems (e.g., the Schrödinger equation), representing the behavior of wavefunctions as they tunnel into 'forbidden' regions — but here we see a classical manifestation of this phenomenon.

Propagating ($k_z^2 > 0$) and evanescent ($k_z^2 < 0$) waves show a fundamental difference in the spatial variation of their energy density. To explore this, let's introduce the time-averaged kinetic energy density of waves as

$$\mathcal{E} = \frac{1}{2}\langle \rho_0 |\boldsymbol{v}'|^2 \rangle; \tag{4.154}$$

here, the angle brackets $\langle\rangle$ denote the average over one wave cycle, with period $P = 2\pi/\omega$. With

$$\boldsymbol{v}' = \begin{pmatrix} v_x'/a_\mathrm{ad} \\ v_y'/a_\mathrm{ad} \\ v_z'/a_\mathrm{ad} \end{pmatrix} \exp[\mathrm{i}(k_z z - \omega t) + z/2H] \tag{4.155}$$

(cf. eqn 4.143, with $\boldsymbol{k} = k_z \hat{\boldsymbol{z}}$), it follows that

$$\mathcal{E} = \frac{1}{2}\rho_{0,0}(v_z'^2 + v_y'^2 + v_z'^2)\langle \exp(-z/H) |\exp[\mathrm{i}(k_z z - \omega t) + z/2H]|^2 \rangle. \tag{4.156}$$

If $k_z^2 > 0$, corresponding to propagating waves with real k_z, then we find

$$\mathcal{E} = \frac{1}{2}\rho_{0,0}(v_z'^2 + v_y'^2 + v_z'^2), \tag{4.157}$$

which is independent of z. This is unsurprising — as waves propagate up through the medium, they're not being dissipated and hence their kinetic energy density should remain the same. Conversely, if $k_z^2 < 0$, corresponding to evanescent waves with pure-imaginary k_z, then

$$\mathcal{E} = \frac{1}{2}\rho_{0,0}(v_z'^2 + v_y'^2 + v_z'^2)\exp(\pm|k_z|z), \tag{4.158}$$

which grows or decays exponentially with z, depending on the sign chosen for k_z. The reason for this exponential variation is that as a wave travels through an evanescent region ($\omega < \omega_{\rm ac}$), it is progressively reflected back toward the boundary of the region.

4.5.4 Horizontal Propagation

Now let's consider horizontally propagating waves, with $k_z = 0$. The solutions (4.150) become

$$\omega^2 = \frac{\omega_{\rm ac}^2 + a_{\rm ad}^2 k_{\rm h}^2 \pm \sqrt{\left(\omega_{\rm ac}^2 + a_{\rm ad}^2 k_{\rm h}^2\right)^2 - 4a_{\rm ad}^2 N^2 k_{\rm h}^2}}{2} \tag{4.159}$$

In the limiting case $a_{\rm ad}^2 k_{\rm h}^2 \gg \omega_{\rm ac}^2, N^2$, these simplify to

$$\omega = \pm a_{\rm ad} k_{\rm h} \tag{4.160}$$

(corresponding to horizontal propagating acoustic waves), and

$$\omega = \pm N, \tag{4.161}$$

corresponding to a new type of wave we've not encountered yet: *internal gravity waves*. The frequency of these gravity waves does not depend on the wavenumber, but is instead fixed to the Brunt-Väisälä frequency.

In the opposite limit $a_{\rm ad}^2 k_{\rm h}^2 \to 0$, the solutions likewise simplify to

$$\omega = \pm\omega_{\rm ac} \tag{4.162}$$

and

$$\omega = 0, \tag{4.163}$$

which is the same result we found for vertical propagation.

Between these limiting cases, the two pairs of solutions (one acoustic, one gravity) vary smoothly as a function of horizontal wavenumber. We can see this variation in Fig. 4.1,

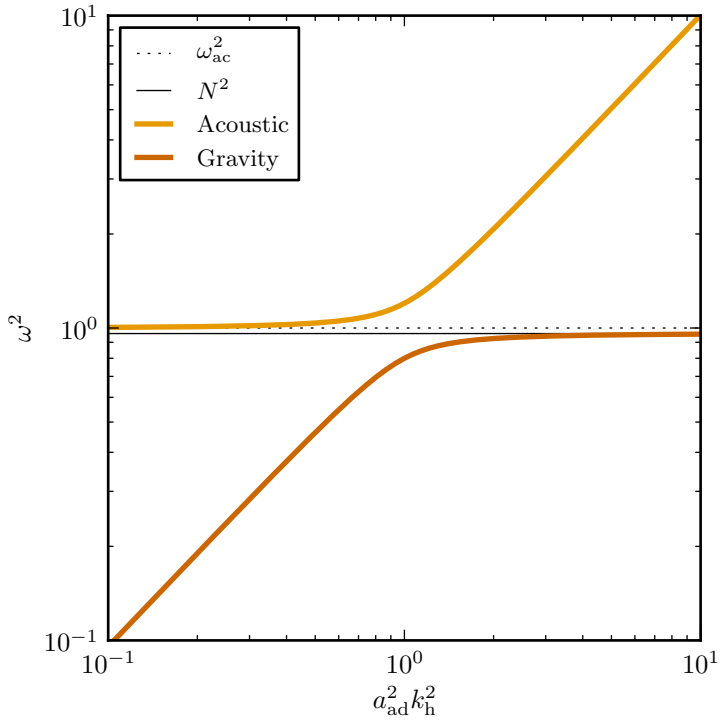

Figure 4.1: Squared frequencies ω^2 of horizontally propagating waves in an isothermal stratified medium, plotted as a function of squared horizontal wavenumber k_{h}^2. Also shown are the acoustic cutoff frequency ω_{ac} and the Brunt-Väisälä frequency N.

which plots ω^2 as a function of k_{h}^2 for horizontally propagating waves. The figure highlights the role played by the two characteristic frequencies: in the limit of small wavenumber (long wavelength) the acoustic-wave frequency approaches the acoustic cutoff frequency ω_{ac}, while the gravity-wave frequency approaches zero. Whereas, in the limit of large wavenumber (short wavelength) the acoustic-wave frequency behaves as it would in a uniform medium, while the gravity-wave frequency approaches the Brunt-Väisälä frequency.

4.5.5 General Cases

In general cases where propagation is neither exactly vertical or exactly horizontal, there are two independent wavenumbers appearing in the dispersion relation, k_{h} and k_z. To visualize the dispersion relation (4.149), we can use a generalization of Fig. 4.1 known as a *propagation diagram*. Fig. 4.2 shows the propagation diagram for our isothermal stratified medium, plotting ω^2 as a function of $a_{\mathrm{ad}}^2 k_{\mathrm{h}}^2$ for various fixed values of k_z^2 (positive, negative and zero). The zero-k_{h} curves correspond to horizontally propagating acoustic and gravity waves, and are the same as plotted in Fig. 4.1. The dotted lines have $k_z^2 > 0$, and therefore correspond to obliquely propagating acoustic and gravity waves. The dashed lines have $k_z^2 < 0$, and therefore grow/decay exponentially in the vertical direction — these are horizontally

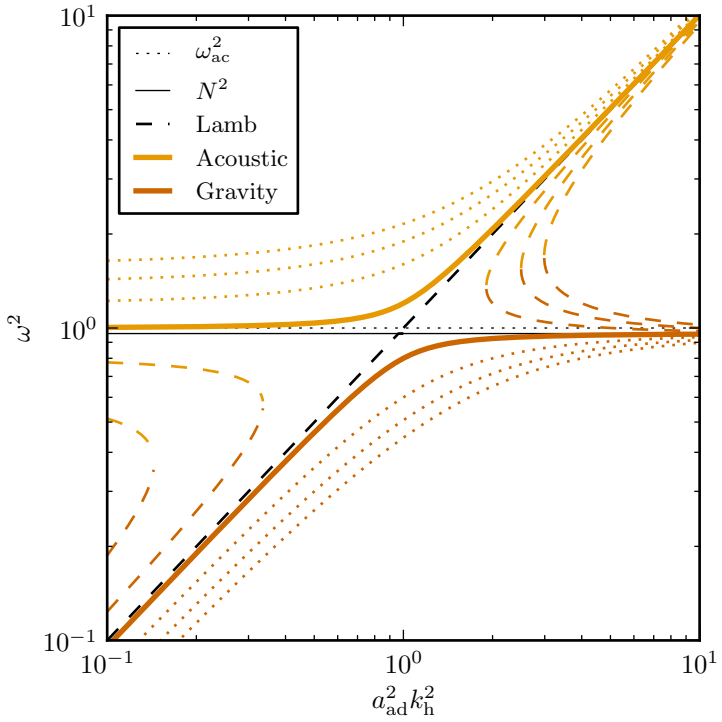

Figure 4.2: The propagation diagram for waves in an isothermal stratified medium. Each of the colored curves corresponds to waves with a fixed k_z^2; the $k_z^2 = 0$ cases are shown by solid lines, $k_z^2 > 0$ by dotted lines and $k_z^2 < 0$ by dashed lines.

propagating but vertically evanescent waves.

Two of the vertically evanescent curves stand out as straight lines in the propagation diagram. If $k_z^2 = N^2 - \omega_{\rm ac}^2 < 0$, then the full dispersion relation (4.149) has the simple solutions

$$\omega^2 = N^2 \tag{4.164}$$

(corresponding to the horizontal black line in Fig. 4.2), and

$$\omega^2 = a_{\rm ad}^2 k_{\rm h}^2. \tag{4.165}$$

(corresponding to the diagonal dashed line in the figure). These solutions look identical to the ones we found previously for horizontal propagation ($k_z = 0$) — but an important difference here is that these expressions are valid for any $k_{\rm h}$, not just when $a_{\rm ad}^2 k_{\rm h}^2 \gg \omega_{\rm ac}, N^2$. Equation (4.165) was first derived by Horace Lamb, and in honor these waves — which propagate horizontally like pure acoustic waves, at any frequency — are known as Lamb waves.

4.5.6 Filtering Approximations

The two special cases discussed above, comprising the Lamb wave and the $\omega = N^2$ wave, exhibit what one might term 'pure' behavior — they extend the large-k_h behavior of acoustic and gravity waves, respectively, all the way down to $k_\mathrm{h} = 0$. This property is not shared by the other solutions shown in Fig. 4.2; for instance, horizontally propagating acoustic waves behave more like gravity waves ($\omega^2 = \omega_\mathrm{ac}^2 \approx N^2$) in the $k_\mathrm{h} \to 0$ limit, and conversely horizontally propagating gravity waves behave more like acoustic waves ($\omega^2 \approx a_\mathrm{ad}^2 k_\mathrm{h}^2$). In a sense, the acoustic-like and gravity-like properties found in the large-k_h limit get mixed up when $a_\mathrm{ad}^2 k_\mathrm{h}^2 \lesssim \omega_\mathrm{ac}^2, N^2$.

Filtering approximations are a way of untangling this mixing, so that we can study the two different wave types in isolation. We've already kind of encountered one filtering approximation: in the limit $H \to \infty$, the linearized equations (4.140–4.142) reduce to the uniform-medium equations (4.111–4.113), whose non-trivial solutions are pure acoustic waves. In effect, taking $H \to \infty$ stops the gravity waves from mixing with the acoustic waves, by forcing the frequencies of the former to zero.

There's another useful filtering approximation which moves the acoustic waves out of the way, allowing us to examine pure gravity waves. This approximation involves taking the limit $a_\mathrm{ad} \to \infty$ in the dispersion relation (4.149), which then reduces to

$$|\boldsymbol{k}|^2 \omega^2 + N^2 k_\mathrm{h}^2 = 0. \tag{4.166}$$

Solving for the frequency,

$$\omega = \pm \frac{k_\mathrm{h}}{|\boldsymbol{k}|} N = \pm \sin\theta N, \tag{4.167}$$

where in the second equality we introduce θ as the angle the wavevector makes with the vertical direction. From this expression, we see a curious result: the frequencies of these pure gravity waves depend only on the *direction* they are propagating in, and are independent of the wavenumber. Contrast this with pure acoustic waves, whose frequencies depend only on the wavenumber and are independent of their direction.

Equation (4.167) helps us to understand a number of results we've encountered previously. For horizontally propagating waves $\omega = \pm N$, reproducing the large-a_ad k_h limit seen in Fig. 4.2 for the gravity waves. Likewise, for vertically propagating waves $\omega = 0$, explaining why we failed to find any non-trivial gravity-wave solutions in §4.5.3.

What does the $a_\mathrm{ad} \to \infty$ limit mean, physically? As the adiabatic sound speed gets larger and larger, any acoustic waves generated by disturbances to the fluid propagate out of the fluid more rapidly, and the fluid behaves as if it were closer and closer to being incompressible. So, this limit corresponds to enforcing a form of incompressibility on the fluid.

4.6 Interface Waves & Instabilities

We're now going to look at waves and instabilities which arise at the interface between two fluids. The background state consists of one fluid lying atop the other, in hydrostatic equilibrium subject to a downward gravitational acceleration g and separated by an interface $z = 0$, with a steady and uniform horizontal flow in each fluid. For simplicity we'll assume that the fluids are incompressible and inviscid, and are subject to a uniform gravity downward in the z direction.

Let's denote the densities in these fluids as ρ_ℓ and ρ_u (using the subscript l to label the lower fluid with $z < 0$, and u to label the upper fluid with $z > 0$), and their velocities as $\boldsymbol{v}_\ell$ and $\boldsymbol{v}_\mathrm{u}$. In the steady background state, these velocities are uniform and purely in the horizontal direction

The linearized equations describing perturbations to the background state are

$$\nabla \cdot \boldsymbol{v}'_\ell = 0,$$
$$\nabla \cdot \boldsymbol{v}'_\mathrm{u} = 0,$$

(this is just the incompressibility condition), and

$$\frac{\partial \boldsymbol{v}'_\ell}{\partial t} + \boldsymbol{v}_{\ell,0} \cdot \nabla \boldsymbol{v}'_\ell + \frac{1}{\rho_{\ell,0}} \nabla P'_\ell = -g\rho'_\ell \, \hat{\boldsymbol{z}}, \tag{4.168}$$

$$\frac{\partial \boldsymbol{v}'_\mathrm{u}}{\partial t} + \boldsymbol{v}_{\mathrm{u},0} \cdot \nabla \boldsymbol{v}'_\mathrm{u} + \frac{1}{\rho_{\mathrm{u},0}} \nabla P'_\mathrm{u} = -g\rho'_\mathrm{u} \, \hat{\boldsymbol{z}}. \tag{4.169}$$

These equations are augmented by the requirement that the perturbation to the vorticity in each fluid vanishes,

$$\boldsymbol{\omega}'_\mathrm{l} = \nabla \times \boldsymbol{v}'_\ell = 0,$$
$$\boldsymbol{\omega}'_\mathrm{u} = \nabla \times \boldsymbol{v}'_\mathrm{u} = 0.$$

The justification for this requirement can be found back in §2.3, where we showed that a fluid which is initially irrotational must remain irrotational for all time[7].

To determine the evolution of the fluid perturbations, we need to augment the above equations with a prescription for what happens at the boundary between the two fluids. Let's describe the shape of this boundary via a function $\zeta(x, y, t)$, which gives the vertical coordinate of the interface at horizontal coordinates (x, y) and time t:

$$z_\mathrm{interface} = \zeta(x, y, t). \tag{4.170}$$

Continuity requires that fluid elements initially at the interface remain at the interface (otherwise a gap could open up between the two fluids). To express this constraint mathematically, let's introduce the function

$$F(\boldsymbol{r}, t) \equiv z - \zeta(x, y, t). \tag{4.171}$$

[7] In fact, our background state is not completely irrotational; the shear at the boundary between the fluids ($z = 0$) has a non-vanishing vorticity, but this vorticity remains locked in the boundary due to Kelvin's circulation theorem, and does not affect either fluid.

A fluid element which is at the interface at some initial time clearly has $F = 0$. For this element to *remain* at the interface for all subsequent times, we require that

$$\frac{\mathrm{d}F}{\mathrm{d}t} = 0, \tag{4.172}$$

or — combining the above expressions, and expanding the Stokes derivative —

$$-\frac{\partial \zeta}{\partial t} - \boldsymbol{v} \cdot \nabla \zeta + \boldsymbol{v} \cdot \hat{\boldsymbol{z}} = 0. \tag{4.173}$$

We linearize this to obtain

$$-\frac{\partial \zeta'}{\partial t} - \boldsymbol{v}_0 \cdot \nabla \zeta' + \boldsymbol{v}' \cdot \hat{\boldsymbol{z}} = 0,$$

where we've taken advantage of the fact that $\zeta_0 = 0$ for fluid elements which are at the interface in the unperturbed background state. This expression applies on either side of the interface, and so we finally arrive at the boundary conditions

$$-\frac{\partial \zeta'}{\partial t} - \boldsymbol{v}_{\ell,0} \cdot \nabla \zeta' + \boldsymbol{v}'_\ell \cdot \hat{\boldsymbol{z}} = 0, \tag{4.174}$$

$$-\frac{\partial \zeta'}{\partial t} - \boldsymbol{v}_{\mathrm{u},0} \cdot \nabla \zeta' + \boldsymbol{v}'_\mathrm{u} \cdot \hat{\boldsymbol{z}} = 0. \tag{4.175}$$

These strictly apply at $z = \zeta$ but to first order we can also apply them at $z = 0$.

One additional boundary condition arises from requiring continuity of the pressure across the interface. Without going into details, this condition is that

$$P'_\ell - \rho_{\ell,0}\, g\, \zeta' = P'_\mathrm{u} - \rho_{\mathrm{u},0}\, g\, \zeta', \tag{4.176}$$

which also strictly applies at $z = \zeta$ but to first order can be applied at $z = 0$.

4.6.1 Static Background State: Surface Gravity Waves & Rayleigh-Taylor Instability

Let's now consider a simple situation where the background state is static — that is, $\boldsymbol{v}_{\ell,0}$ and $\boldsymbol{v}_{\mathrm{u},0}$ in the above equations vanish. We consider trial solutions of the form

$$\boldsymbol{Y}_\ell(\boldsymbol{r}, t) = \boldsymbol{y}_\ell \exp[kz] \exp[\mathrm{i}(k\boldsymbol{n}_\perp \cdot \boldsymbol{r} - \omega t)], \tag{4.177}$$

$$\boldsymbol{Y}_\mathrm{u}(\boldsymbol{r}, t) = \boldsymbol{y}_\mathrm{u} \exp[-kz] \exp[\mathrm{i}(k\boldsymbol{n}_\perp \cdot \boldsymbol{r} - \omega t)], \tag{4.178}$$

$$\zeta(\boldsymbol{r}, t) = Z \exp[\mathrm{i}(k\boldsymbol{n}_\perp \cdot \boldsymbol{r} - \omega t)] \tag{4.179}$$

where

$$\boldsymbol{Y}_\ell \equiv \begin{pmatrix} v'_{x,\ell} \\ v'_{y,\ell} \\ v'_{z,\ell} \\ P'_\ell \end{pmatrix}, \qquad \boldsymbol{Y}_\mathrm{u} \equiv \begin{pmatrix} v'_{x,\mathrm{u}} \\ v'_{y,\mathrm{u}} \\ v'_{z,\mathrm{u}} \\ P'_\mathrm{u} \end{pmatrix}, \tag{4.180}$$

are the vector of unknowns in the lower and upper fluids, respectively; $\boldsymbol{y}_\ell$ and $\boldsymbol{y}_\mathrm{u}$ are constant vectors to be determined; k is a scalar; and $\boldsymbol{n}_\perp$ is a unit vector in the $x-y$ plane which gives the horizontal propagation direction of the perturbations. The z dependence in eqns. (4.177) and (4.178) is chosen to ensure that far away from the interface the disturbances tend to zero. Likewise, the appearance of the same constant k in the vertical and horizontal dependencies of the solutions comes from the requirement that the solutions satisfy the incompressible and irrotational conditions.

Substituting these trial solutions into the linearized equations, and setting the determinant of the resulting matrix to zero, ultimately leads to the characteristic equation

$$(\rho_{\ell,0} + \rho_{\mathrm{u},0})\omega^2 + hk(\rho_{\ell,0} - \rho_{\mathrm{u},0}) = 0. \tag{4.181}$$

Assuming for the moment that $\rho_{\ell,0} > \rho_{\mathrm{u},0}$, this is trivially solved to find the dispersion relation

$$\omega = \pm\sqrt{gk\frac{\rho_{\ell,0} - \rho_{\mathrm{u},0}}{\rho_{\ell,0} + \rho_{\mathrm{u},0}}} \tag{4.182}$$

This real frequency means that the solutions have a wave-like nature, propagating horizontally in a direction given by the vector $\boldsymbol{n}_\perp$. In the limit where the upper fluid density is negligible compared to the lower fluid density[8], the dispersion relation reduces further to

$$\omega = \pm\sqrt{gk},$$

independent of the density of the lower fluid. These waves are related to the internal gravity waves considered in §4.5, in that both rely on gravity as the restoring force for displaced fluid elements; however, they have a quite different dispersion relation (compare the above expression with eqn. 4.167), and are referred to as *surface* gravity waves to highlight this difference.

What happens when $\rho_\ell < \rho_\mathrm{u}$ — that is, the upper fluid is more dense than the lower fluid? The dispersion relation can now be written

$$\omega = \pm\mathrm{i}\sqrt{gk\frac{\rho_{\mathrm{u},0} - \rho_{\ell,0}}{\rho_{\ell,0} + \rho_{\mathrm{u},0}}}. \tag{4.183}$$

The complex frequencies mean that the solutions have an exponentially growing or decaying nature — that is, we have an instability. Any infinitesimal perturbation will be amplified by this instability, and grow until the assumptions of linearity are violated. This instability is known as the *Rayleigh-Taylor* (R-T) instability, and develops at the boundary of two fluids when the more-dense one overlays the less-dense one. See Fig. 4.3 for an example of the R-T instability.

[8] Air and water are one example of such a configuration.

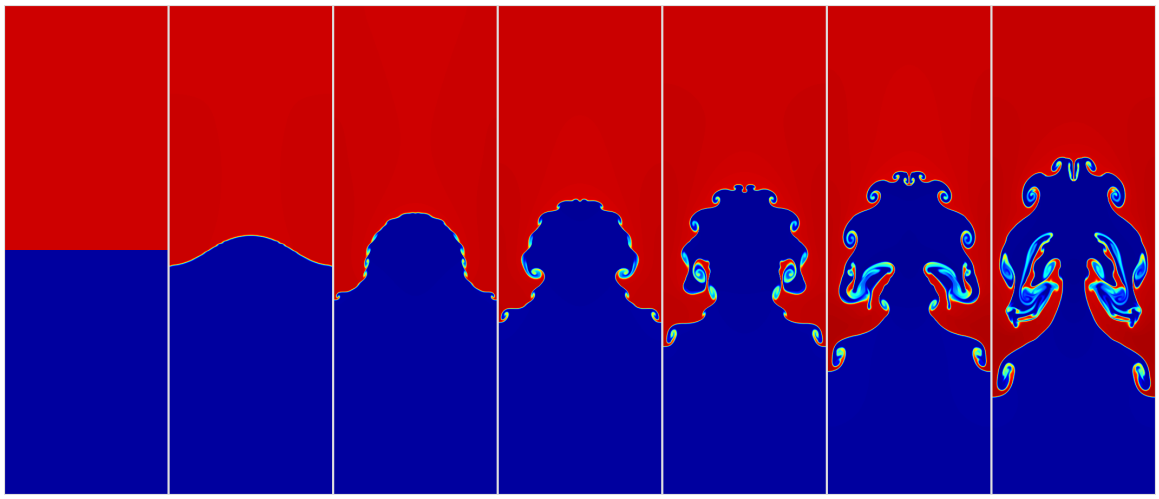

Figure 4.3: 2-D numerical simulation (using the freely available Athena3D code) of instabilities at the interface between two fluids. The red fluid is more dense than the blue one, and so (with a downward gravitational force) the equilibrium state is Rayleigh-Taylor unstable. As the R-T instability develops, the shear established due to different vertical velocities at the interface causes secondary Kelvin-Helmholtz instabilities, with their characteristic roll structure.

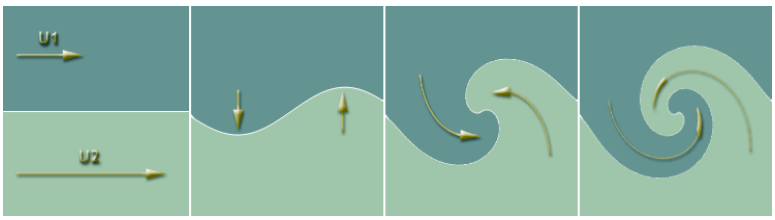

Figure 4.4: Schematics of the development of the Kelvin-Helmholtz instability.

4.6.2 Shear Background State: Kelvin-Helmholtz Instability

We now turn to another simple case, where the background state is Rayleigh-Taylor stable ($\rho_{\ell,0} > \rho_{\mathrm{u},0}$) but the two layers are not at rest relative to one another. For simplicity, we'll take the background flow velocities to be equal and opposite in the x-direction: $\boldsymbol{v}_{\mathrm{u},0} = v_{\mathrm{f}}\,\hat{\boldsymbol{x}}$ and $\boldsymbol{v}_{\ell,0} = -v_{\mathrm{f}}\,\hat{\boldsymbol{x}}$.

The trial solutions take the same form as before (cf. eqns. 4.177–4.179), and we follow through the usual procedure to arrive at a dispersion relation

$$\omega = \frac{-kv_{\mathrm{f}}(\rho_{\ell,0} - \rho_{\mathrm{u},0}) \pm \sqrt{D}}{\rho_{\ell,0} + \rho_{\mathrm{u},0}} \tag{4.184}$$

where the discriminant D is defined as

$$D \equiv gk(\rho_{\ell,0} - \rho_{\mathrm{u},0})(\rho_{\ell,0} + \rho_{\mathrm{u},0}) - 4k^2 v_{\mathrm{f}}^2 \rho_{\ell,0}\rho_{\mathrm{u},0}.$$

The nature of the solutions will clearly depend on the sign of D. If the shear flow is small enough that $D > 0$, then ω remains real and we have wave-like solutions with phase velocities

$$c = \frac{\omega}{k} = \frac{-v_{\rm f}(\rho_{\ell,0} - \rho_{{\rm u},0}) \pm \sqrt{D/k}}{\rho_{\ell,0} + \rho_{{\rm u},0}}. \tag{4.185}$$

These are the same interface gravity waves we encountered previously, but modified by the shear flow of the background state: the phase velocity is reduced and biased toward the negative direction. In fact, the bias is exactly equal to the velocity

$$v_{\rm com} \equiv -v_{\rm f}\frac{\rho_{\ell,0} - \rho_{{\rm u},0}}{\rho_{\ell,0} + \rho_{\ell,0}} \tag{4.186}$$

of the center-of-momentum frame of the background state. If we transform to this frame, then the bias will vanish.

If the shear is sufficiently large that D becomes negative, then the nature of solutions change: ω acquires an imaginary part meaning that perturbations will grow or decay exponentially with time. This is known as the *Kelvin-Helmholtz* (K-H) instability, and arises whenever we have an interface two incompressible fluids with a shear

$$|v_{\rm f}| > \frac{1}{2}\sqrt{\frac{g(\rho_{\ell,0} - \rho_{{\rm u},0})(\rho_{\ell,0} + \rho_{{\rm u},0})}{k\rho_{\ell,0}\rho_{{\rm u},0}}} \tag{4.187}$$

(note that the velocity of the fluids relative to each other is actually $2\,v_{\rm f}$). Due to the appearance of k in the denominator, we see that we can make this threshold as small as we like by considering shorter- and shorter-wavelength perturbations — *all* shear flows are in principle susceptible to the K-H instability. In practice, however, surface tension at the interface tends to suppress the instability for short-wavelength perturbations.

When D is negative, ω still has a non-zero real part, and so the instability still has a wave-like nature. Thus, the K-H instability takes the form of wave-like perturbations to the interface which grow with time and moreover propagate along the interface with a phase velocity $v_{\rm com}$. Fig. 4.4 shows idealized schematics of the development of the instability, highlighting the formation of the roll-like structures which are the characteristic fingerprint of the instability.

Its worth noting that the K-H instability exists even in situations where there is no gravitational stratification between the fluids ($g = 0$), or where the fluids have identical densities. The former situation typically arises when the shear flow is parallel to the gravity, and is especially important as a secondary instability which develops on top of the R-T instability. This is illustrated in Fig. 4.3.

5 Non-linear Fluid Dynamics

In the previous sections we've focused exclusively on solutions to the *linearized* fluid equations, which govern the time evolution of small perturbations to some equilibrium background state. This approach allows us to model wave propagation, but excludes many interesting — and astrophysically important — phenomena, such as shocks and rarefactions. Let's now focus on these phenomena.

Solution of the full fluid equations is tricky, as they comprise a non-linear, coupled set of partial differential equations. Usually, therefore, we use numerical approaches — which themselves can be quite complex. However, there is a very powerful approach, the *method of characteristics*, which can offer deep insights into the general nature of solutions to the equations.

5.1 The Method of Characteristics

The basic idea of the method of characteristics is to reduce a set of *partial* differential equations (PDEs) to a set of *ordinary* differential equations (ODEs). To illustrate how this is done, consider the following 'scalar[9] conservation' PDE governing the space-time evolution of some unknown $u(x,t)$:

$$\frac{\partial u}{\partial t} + a(x,t)\frac{\partial u}{\partial x} = 0. \tag{5.188}$$

Here, $a(x,t)$ is some abitrary function of x and t. If this equation is to be reduced to an ODE, then we must find a way of making the solution u depend on just a single variable, which we'll call s. This can be done by considering solutions along the family of space-time curves described by the differential equations

$$\frac{\mathrm{d}x}{\mathrm{d}s} = a, \qquad \frac{\mathrm{d}t}{\mathrm{d}s} = 1. \tag{5.189}$$

These curves — known as the *characteristic curves* of the PDE — all share the property that their speed (the reciprocal of their slope) in the space-time (x-t) plane is given by

$$\frac{\mathrm{d}x}{\mathrm{d}t} = \frac{\mathrm{d}x}{\mathrm{d}s}\frac{\mathrm{d}s}{\mathrm{d}t} = a. \tag{5.190}$$

Along a characteristic curve, the PDE can then be written as the ODE

$$\frac{\partial u}{\mathrm{d}t}\frac{\mathrm{d}t}{\mathrm{d}s} + \frac{\partial u}{\mathrm{d}x}\frac{\mathrm{d}x}{\mathrm{d}s} \equiv \frac{\mathrm{d}u}{\mathrm{d}s} = 0. \tag{5.191}$$

This indicates that u does not change along characteristic curves — meaning that if we know the initial state $u(x, t = 0)$ of the PDE, it is possible to determine u at any space-time point (x_1, t_1) using the following simple steps:

[9] Used in this context to indicate that there's only one unknown variable.

1. Construct the characteristic curve passing through (x_1, t_1); at each x and t along this curve, the tangent should be $\mathrm{d}t/\mathrm{d}x = a^{-1}$.

2. Determine the point $(x_0, 0)$ where this curve intersects the $t = 0$ line;

3. Read off the initial value $u(x_0, 0)$ at this point; because u does not change along the characteristic curve, this is also the value of $u(x_1, t_1)$.

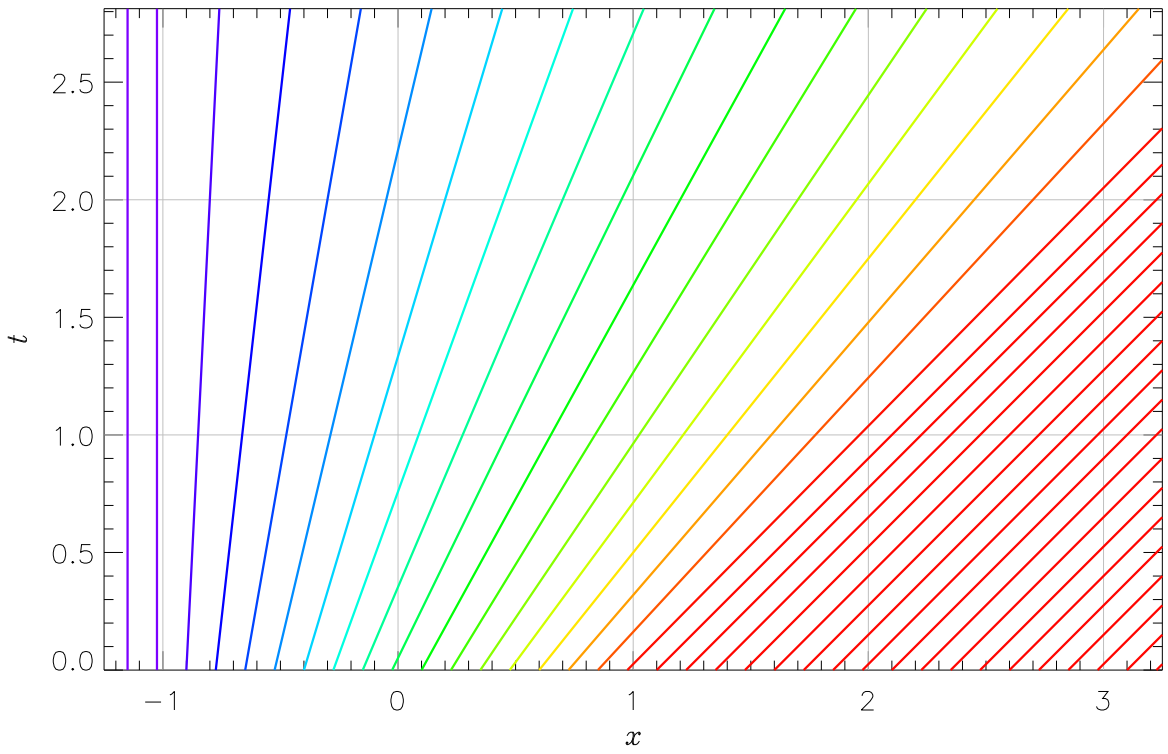

Figure 5.5: Characteristic curves in the x-t plane for the inviscid Burgers' equation, with initial conditions given in eqn. (5.194). The curves are colored by their u-value, with purple corresponding to $u = 0$ and red corresponding to $u = 1$.

5.2 The Inviscid Burgers' Equation

As a specific example of the method of characteristics in action, let's now consider a scalar non-linear PDE known as the inviscid Burgers'[10] equation:

$$\frac{\partial u}{\partial t} + u\frac{\partial u}{\partial x} = 0. \tag{5.192}$$

Although somewhat artificial, this equation is often used as a model for how non-linearity affects the solutions to the full fluid equations. Note that here the speed $a(x, t)$ is just the dependent variable u — which, although not known explicitly, is still a function of x and

[10] Named after J. M. Burgers, who first proposed the equation.

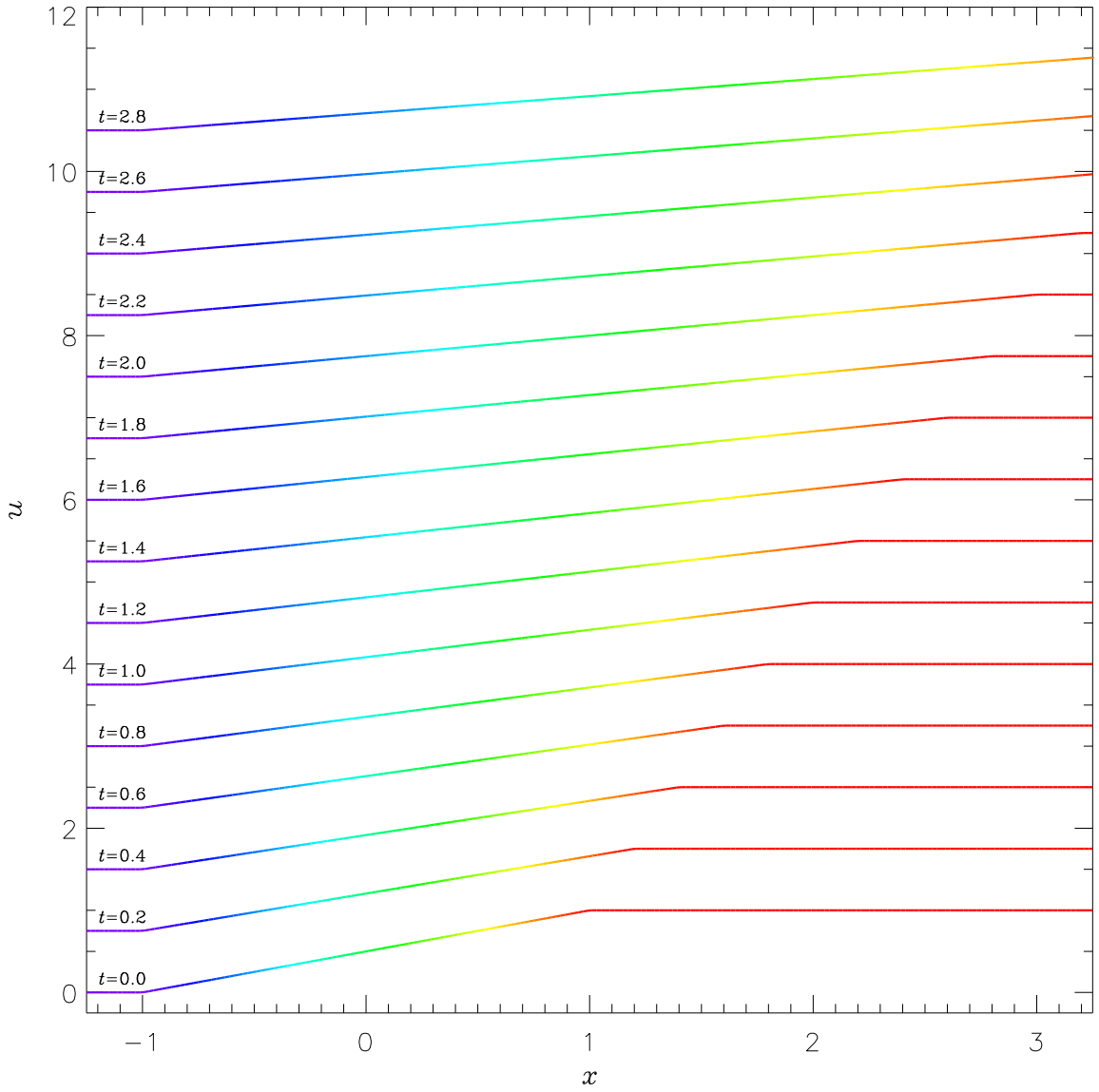

Figure 5.6: Solutions to the inviscid Burgers' equation, based on the characteristic curves plotted in Fig. 5.5. For clarity, profiles for successive time values are shifted vertically by 0.25. The profiles are colored using the same u-dependent scheme as before.

t. Applying the method of characteristics, the characteristic curves are described by the equations

$$\frac{\mathrm{d}x}{\mathrm{d}s} = u, \qquad \frac{\mathrm{d}t}{\mathrm{d}s} = 1.$$

Recall that u is constant along a characteristic curve, and hence constant in these equations; the curves are therefore trivially found as

$$x = x_0 + u(x_0, 0)s, \qquad t = s,$$

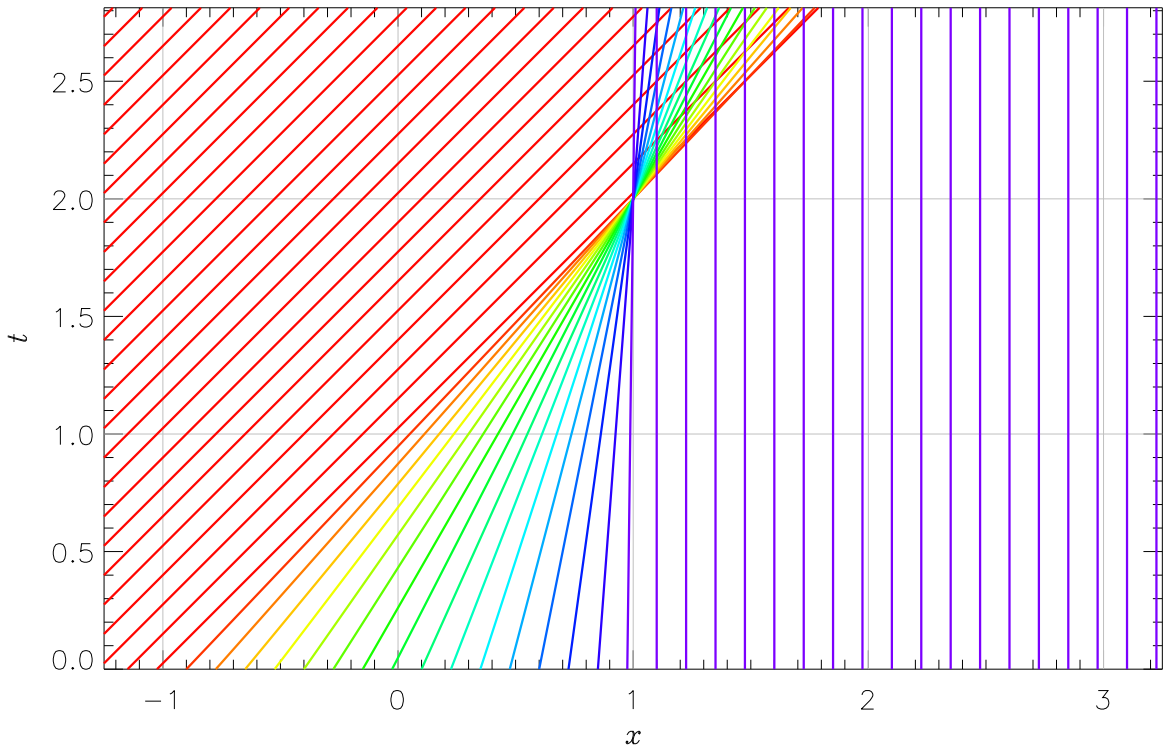

Figure 5.7: *Incorrect* characteristic curves in the x-t plane for the inviscid Burgers' equation, with initial conditions given in eqn. (5.195). The curves are colored by their u-value, with purple corresponding to $u = 0$ and red corresponding to $u = 1$. Note the unphysical crossing of characteristic curves, beginning at $t = 2$.

where x_0 is as before the x coordinate of the curve when $t = 0$. Combining these, we can also write

$$x = x_0 + u(x_0, 0)t. \tag{5.193}$$

Thus, we have a situation where the characteristic curves are straight lines, with a speed depending on the initial state. The corresponding solution to the PDE is tricky to write down in closed form, but can be found using a simple graphical approach.

Let's do this first by considering the initial state

$$u(x,0) = \begin{cases} 0 & x < -1 \\ \frac{x+1}{2} & -1 \le x < 1 \\ 1 & x \ge 1 \end{cases}. \tag{5.194}$$

Fig. 5.5 plots selected characteristic curves in the x-t plane for this configuration, with each curve colored by the corresponding value of u set by the initial state (recall that u is unchanging along characteristic curves). The dependence of the speed $\mathrm{d}x/\mathrm{d}t$ of the characteristics on the initial state can clearly be seen. The solution to Burgers' equation for any $t > 0$ can be read off from this plot by taking slices at constant t. In Fig. 5.6 we see that the initial

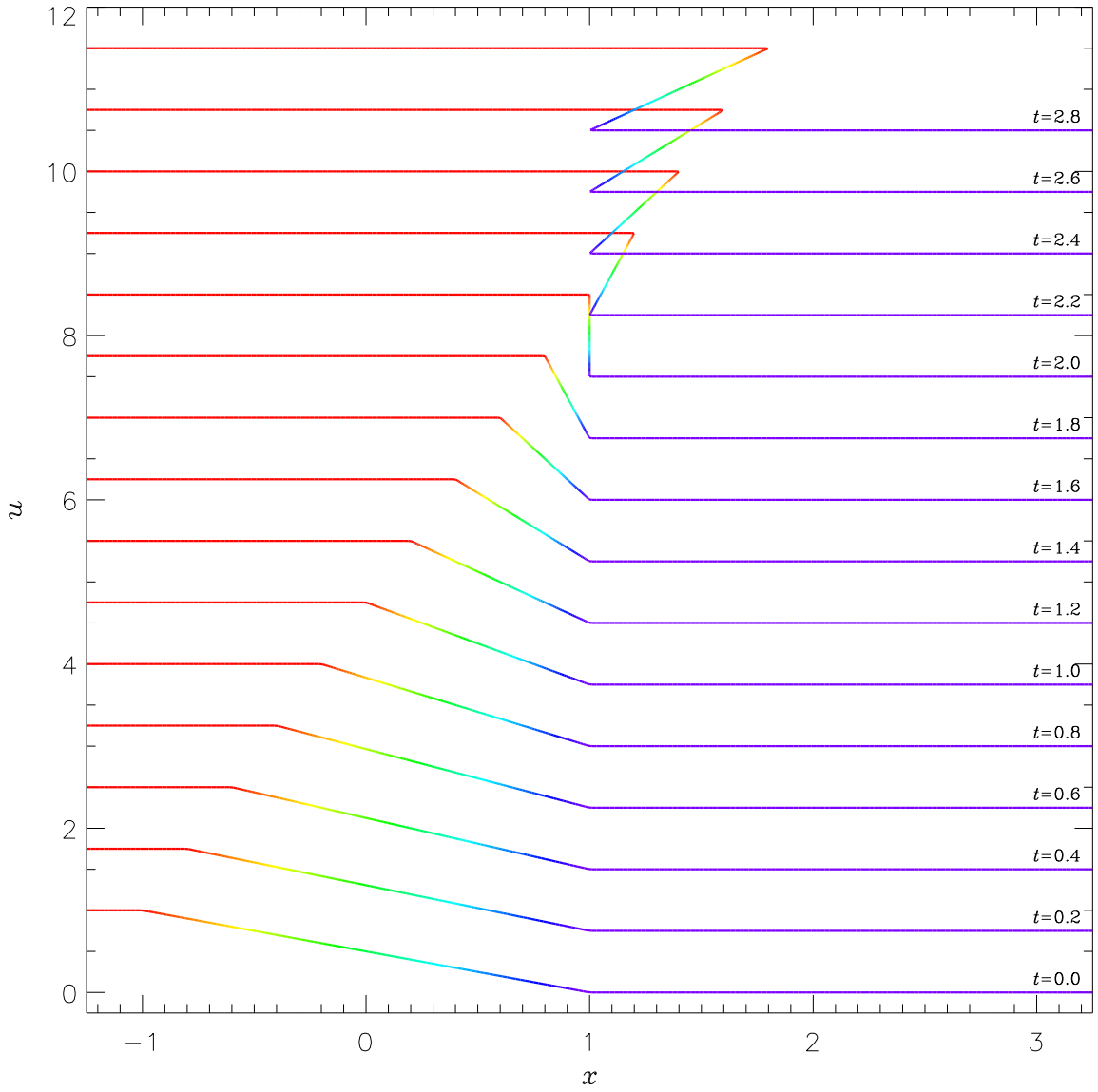

Figure 5.8: *Incorrect* solutions to the inviscid Burgers' equation, based on the characteristic curves plotted in Fig. 5.7. For clarity, profiles for successive time values are shifted vertically by 0.25. The profiles are colored using the same u-dependent scheme as before. Note the unphysical multiple-valued solutions which appear for $t \geq 2$.

profile evolves in two ways: it is advected to the right, and it is stretched out. The stretching is a direct consequence of the non-linearity of Burgers' equation; if instead we considered a linear equation with a constant speed a, then the advection to the right would remain, but the stretching would vanish.

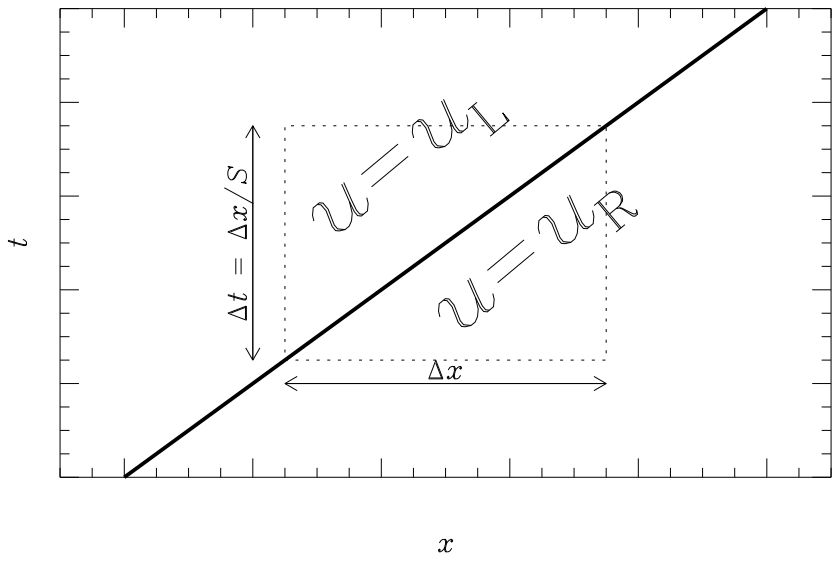

Figure 5.9: Control region of spatial extent Δx and temporal extent $\Delta t = \Delta x/S$, across a shock (thick line) having speed $\mathrm{d}x/\mathrm{d}t = S$ and separating uniform states $u = u_\mathrm{L}$ to the left and $u = u_\mathrm{R}$ to the right.

Now let's consider an initial state which is a mirror image of the one above; specifically,

$$u(x,0) = \begin{cases} 1 & x < -1, \\ 1 - \frac{x+1}{2} & -1 \le x < 1, \\ 0 & x \ge 1 \end{cases}. \tag{5.195}$$

Fig. 5.7 shows what happens when we naively plot the characteristic curves: at $(x,t) = (1,2)$, the curves originating from $-1 < x_0 < 1$ intersect with one another. Since each curve is associated with a different value of u, this suggests u becomes multi-valued at the intersection. Fig. 5.8 reveals what is happening in this case; it is evident that a discontinuity in u forms when, at $t = 2$, the characteristics first cross. For $t > 2$, u becomes double valued as the high-u part of the profile 'overshoots' the low-u part (because it is moving to the right at a greater speed).

The formation of the discontinuity means that Burgers' equation becomes invalid, at least in the form given by eqn. (5.192. To see this, let's first note that the equation can be written in the 'conservation' form

$$\frac{\partial u}{\partial t} + \frac{\partial f}{\partial x} = 0, \tag{5.196}$$

where $f(u)$, the flux of u, is given by

$$f(u) = \frac{u^2}{2}. \tag{5.197}$$

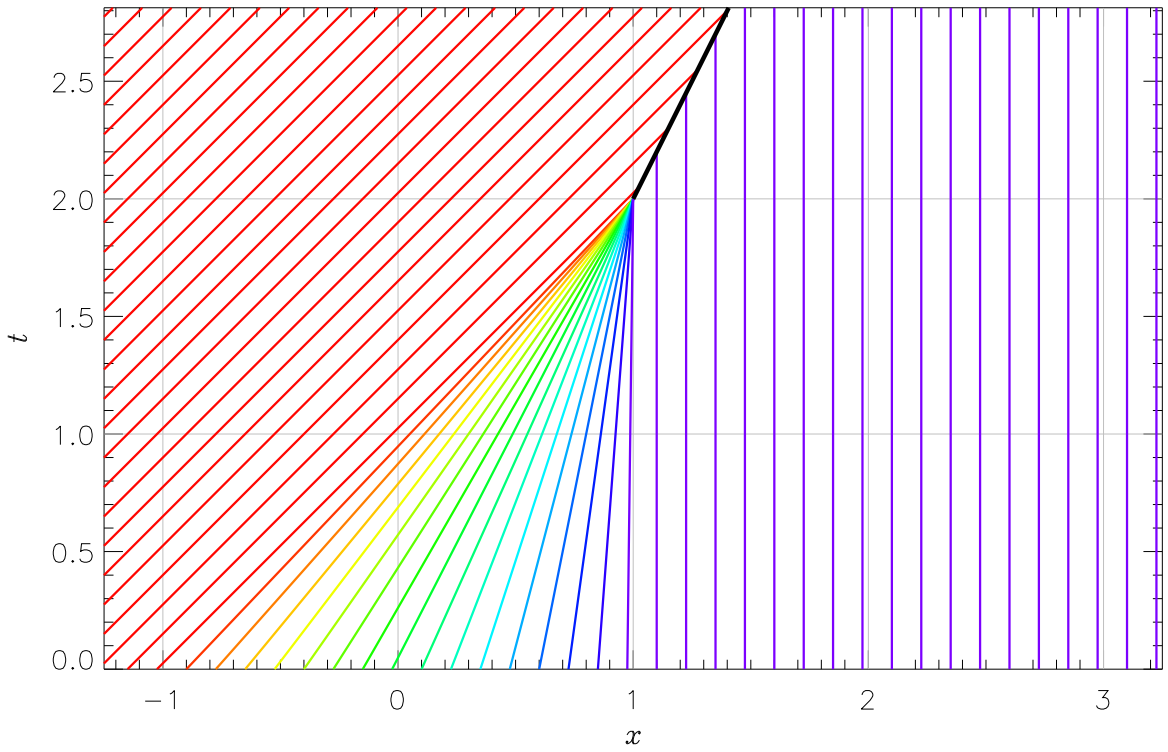

Figure 5.10: *Correct* characteristic curves in the x-t plane for the inviscid Burgers' equation, with initial conditions given in eqn. (5.195). The curves are colored by their u-value, with purple corresponding to $u = 0$ and red corresponding to $u = 1$. The thick solid black line beginning at $t = 2$ is the shock, which propagates with a speed $S = 1/2$ given by the jump condition (5.202).

(Observe how eqn. 5.196 is very reminiscent of the fluid conservation equations 1.12,1.16,1.20). Now consider the integral conservation law for u,

$$\int_{x_\mathrm{a}}^{x_\mathrm{b}} u(x,t_\mathrm{b}) - u(x,t_\mathrm{a})\,\mathrm{d}x + \int_{t_\mathrm{a}}^{t_\mathrm{b}} f[u(x_\mathrm{b},t)] - f[u(x_\mathrm{a},t)]\,\mathrm{d}t = 0 \tag{5.198}$$

where $x_\mathrm{a}, x_\mathrm{b}$ are arbitrary locations and $t_\mathrm{a}, t_\mathrm{b}$ arbitrary times. Let's divide this latter equation by both $x_\mathrm{b} - x_\mathrm{a}$ and $t_\mathrm{b} - t_\mathrm{a}$:

$$\frac{1}{x_\mathrm{b}-x_\mathrm{a}}\int_{x_\mathrm{a}}^{x_\mathrm{b}} \frac{u(x,t_\mathrm{b}) - u(x,t_\mathrm{a})}{t_\mathrm{b}-t_\mathrm{a}}\,\mathrm{d}x + \frac{1}{t_\mathrm{b}-t_\mathrm{a}}\int_{t_\mathrm{a}}^{t_\mathrm{b}} \frac{f[u(x_\mathrm{b},t)] - f[u(x_\mathrm{a},t)]}{x_\mathrm{b}-x_\mathrm{a}}\,\mathrm{d}t. \tag{5.199}$$

As $t_\mathrm{b} - t_\mathrm{a} \to 0$, the integrand in the first expression will approach $\partial u/\partial t$, *if* u remains continuous with respect to t. Likewise, as $x_\mathrm{b} - x_\mathrm{a} \to 0$, the integrand in the second expression will approach $\partial f/\partial x$, *if* u remains continuous with respect to x. Assuming that these continuity requirements are met, then taking both limits simultaneously gives the result

$$\frac{\partial u}{\partial t} + \frac{\partial f}{\partial x} = 0, \tag{5.200}$$

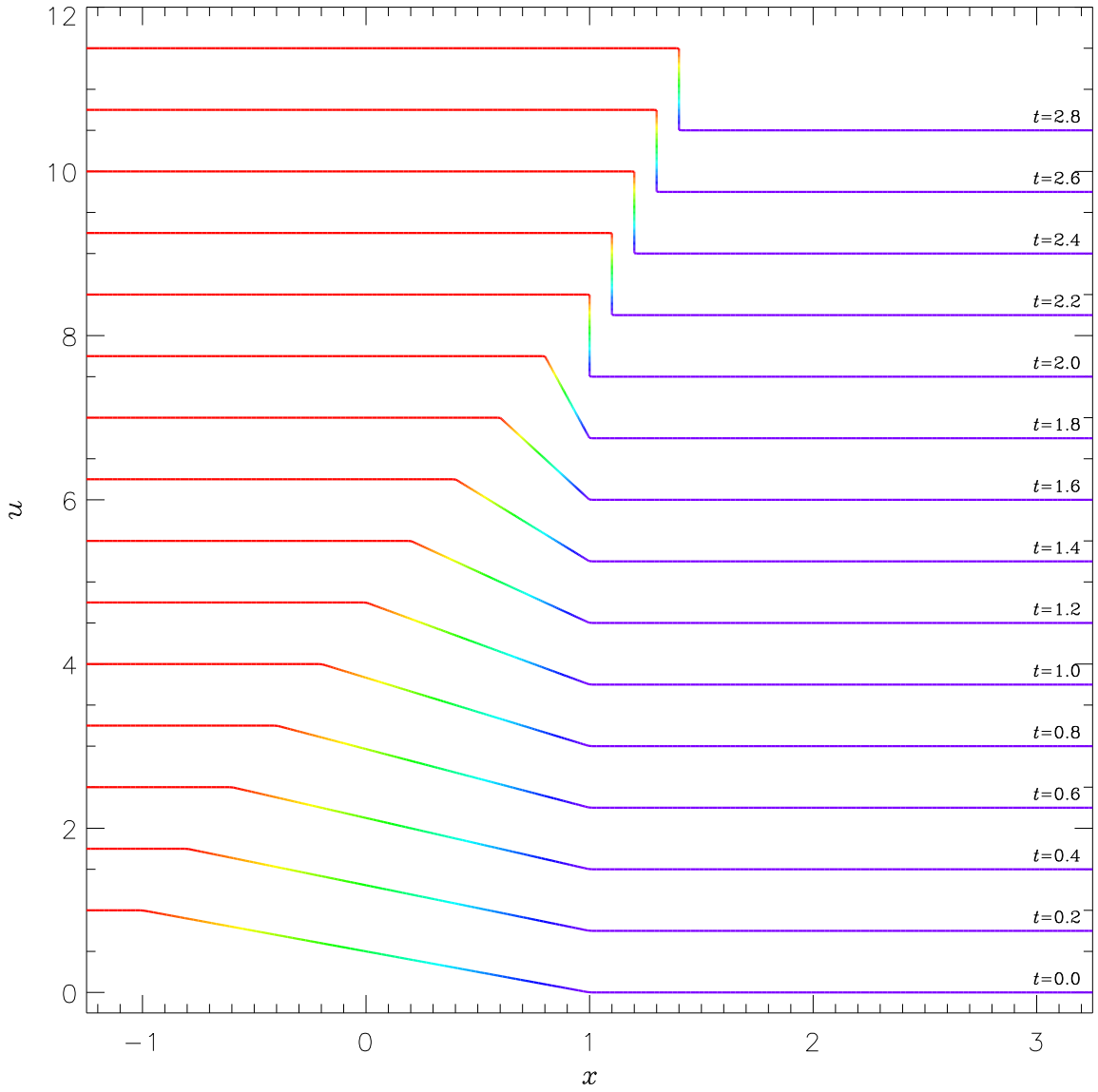

Figure 5.11: *Correct* solutions to the inviscid Burgers' equation, based on the characteristic curves plotted in Fig. 5.10. For clarity, profiles for successive time values are shifted vertically by 0.25. The profiles are colored using the same u-dependent scheme as before. Note the formation and subsequent rightward propagation of the shock for $t \geq 2$.

which is identical to eqn. (5.196). So, the integral and differential forms, eqns. (5.198) and (5.200) are completely equivalent *if u is a continuous function of both x and t.*

What happens when the continuity requirements are not met? At discontinuities in u, the equivalence between the two forms is broken. In fact, the differential form becomes invalid, because the derivative of u is undefined at discontinuities. In such cases, we must switch to the integral form to figure out how the system behaves. Let's now do that.

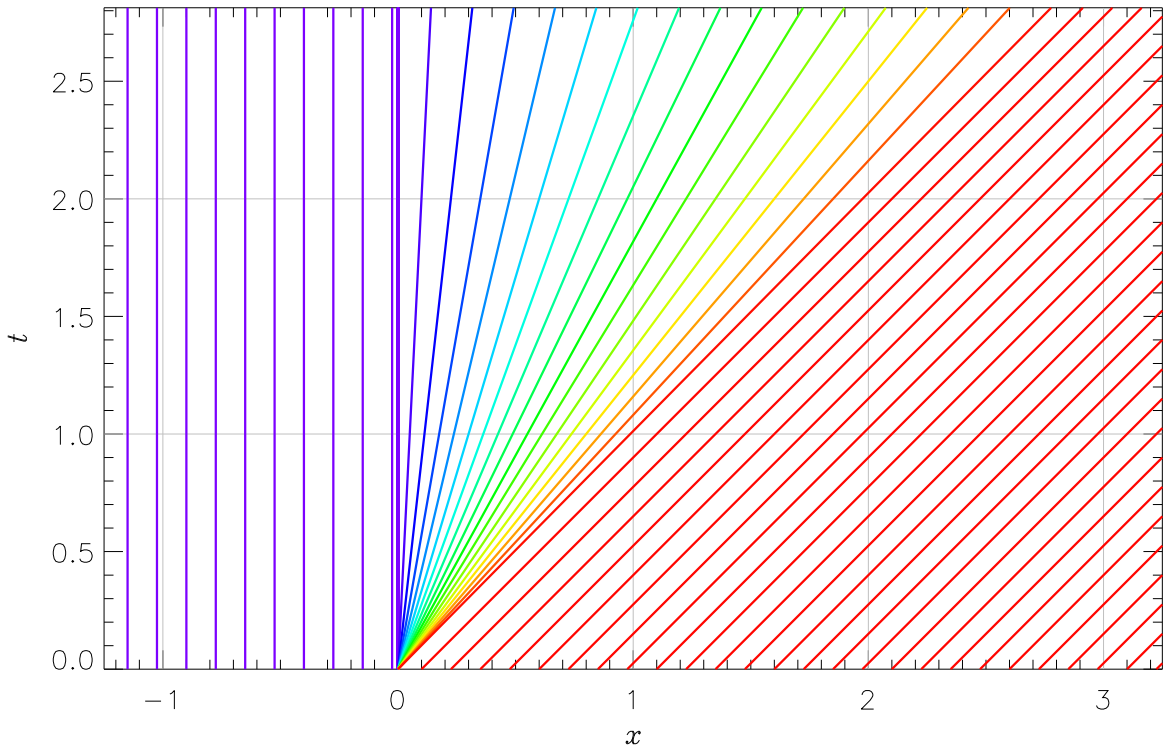

Figure 5.12: Characteristic curves in the x-t plane for the inviscid Burgers' equation, with initial conditions given in eqn. (5.204). The curves are colored by their u-value, with purple corresponding to $u = 0$ and red corresponding to $u = 1$. Note how the initial discontinuity evolves as an expansion fan.

Suppose we have a discontinuity in u which is moving with a speed $\mathrm{d}x/\mathrm{d}t = S$ in the x-t plane, and separates uniform states $u = u_\mathrm{L}$ to its left and $u = u_\mathrm{R}$ to its right. Let's evaluate the integrals in eqn. (5.198) over a control region with space interval $x_\mathrm{b} - x_\mathrm{a} \equiv \Delta x$ and time interval $t_\mathrm{b} - t_\mathrm{a} \equiv \Delta t = \Delta x/S$. Fig. 5.9 sketches this configuration in the x-t plane. We find that

$$(u_\mathrm{L} - u_\mathrm{R})\Delta x + (f[u_\mathrm{R}] - f[u_\mathrm{L}])\Delta t = 0, \tag{5.201}$$

which can be rearranged and simplified to

$$S(u_\mathrm{R} - u_\mathrm{L}) = f[u_\mathrm{R}] - f[u_\mathrm{L}]. \tag{5.202}$$

This 'jump relation' enforces the conservation of u across shocks, by linking the jump in u, the jump in the fluxes, and the speed of propagation of the discontinuity.

For the shock which forms at $(x, t) = (1, 2)$ in Figs. (5.7 and (5.8), we have $u_\mathrm{L} = 1$, $u_\mathrm{R} = 0$, $f_\mathrm{L} = 1/2$ and $f_\mathrm{R} = 0$. Applying the above jump relation gives the propagation speed of the shock as $S = 1/2$, and the shock therefore follows the curve

$$x = St = \frac{1}{2}t \qquad t \geq 2. \tag{5.203}$$

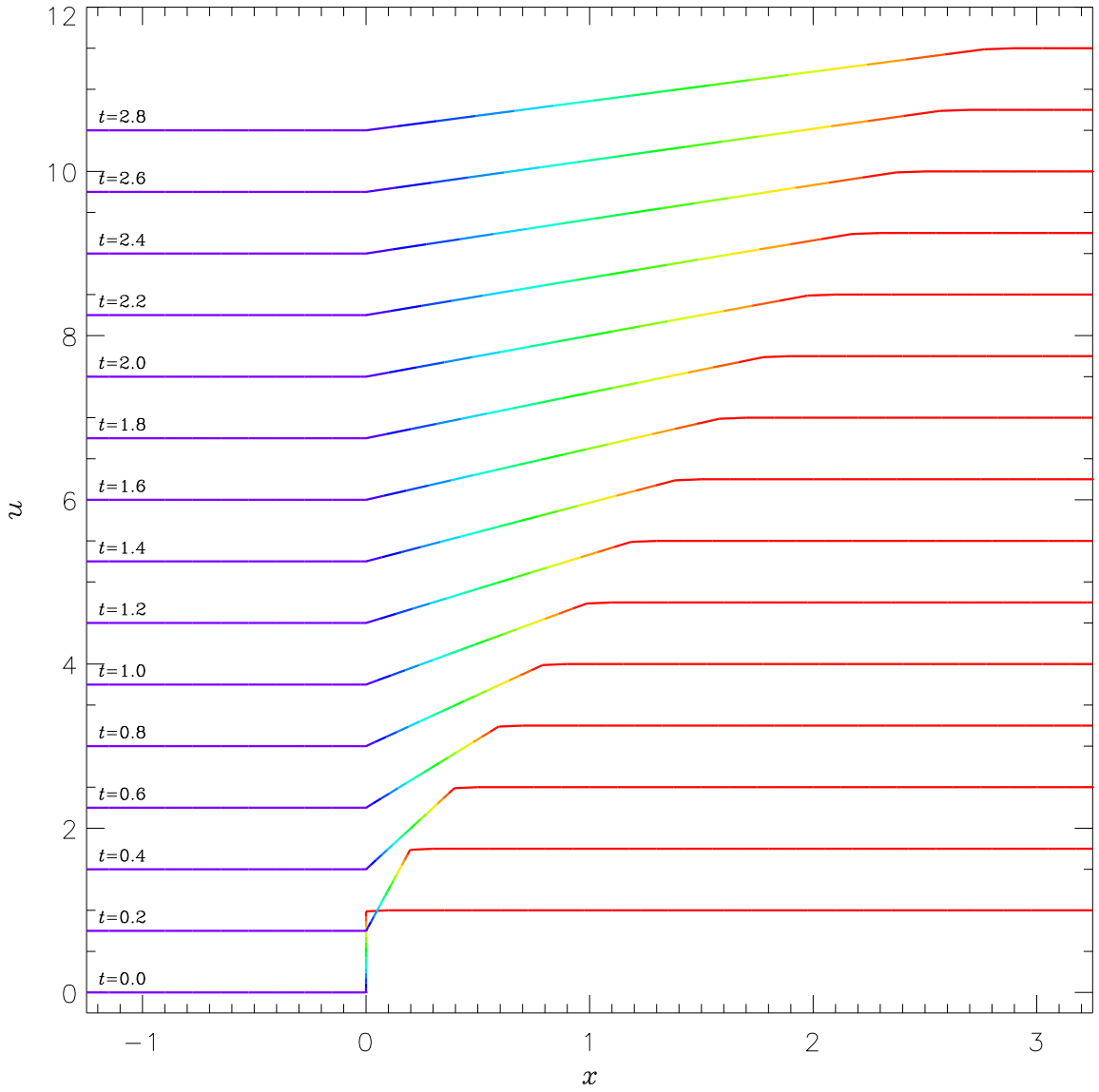

Figure 5.13: Solutions to the inviscid Burgers' equation, based on the characteristic curves plotted in Fig. 5.12. For clarity, profiles for successive time values are shifted vertically by 0.25. The profiles are colored using the same u-dependent scheme as before.

Characteristic curves which impinge on the shock for $t > 2$ get 'eaten' — they do not pass though it, because the differential form (5.192) of Burgers' equation no longer applies. This is illustrated in Fig. 5.10, which plots the characteristic curves in the x-t plane along with the shock curve. Fig. 5.11 shows the corresponding solutions. Note how the u profile progressively steepens until the shock forms at $t = 2$; the shock then propagates to the right with a speed between the speeds of the left and right states: $u_{\mathrm{L}} > S > u_{\mathrm{R}}$.

To close off our discussion of Burgers' equation, let's have a look at situations where the

initial condition is two uniform states separated by a jump at $x = 0$. There are two possible options, (a):

$$u(x,0) = \begin{cases} 0 & x < 0, \\ 1 & x > 0, \end{cases} \tag{5.204}$$

and (b):

$$u(x,0) = \begin{cases} 1 & x < 0, \\ 0 & x > 0. \end{cases} \tag{5.205}$$

In fact, we've already considered case (b) — it's what we see in Fig. 5.11 for $t \geq 2$, with a shock propagating to the right.

Case (a) requires a little more thought, however. One way of approaching it is to consider the ramp initial state

$$u(x,0) = \begin{cases} 0 & x < -\alpha \\ \frac{x+\alpha}{2\alpha} & -\alpha \leq x < \alpha \\ 1 & x \geq \alpha \end{cases}, \tag{5.206}$$

where $\alpha \geq 0$ is a tuneable parameter. Figs. 5.5 and 5.6 show the situation for $\alpha = 1$. If we reduce α, then the initial transition region connecting $u = 0$ on the left and $u = 1$ on the right gets spatially smaller and smaller. In the limit where α reaches zero, we recover case (a) above. Therefore, the characteristic curves for (a) will take the form of a fan originating from $x = 0$, $t = 0$, as seen in Figs. 5.12 and 5.13 — a so-called *expansion fan*.

This highlights the fact that when we have discontinuities in the initial state, we cannot blindly assume that they will continue to exist in the flow as propagating shocks. Sometimes an initial discontinuity will instead morph into a region of smooth flow, like the expansion fan in the figure.

5.3 Non-linearity in the Fluid Equations

Let's now look at the non-linear behavior of the fluid equations, to determine what the characteristic curves look like, and to see how discontinuities behave. This task is complicated by the fact that they involve more than a single variable. For simplicity, let's restrict ourselves to one spatial dimension and Cartesian geometry, with an independent spatial variable x. Then, the fluid equations are

$$\begin{aligned} \frac{\partial \rho}{\partial t} + \frac{\partial}{\partial x}(\rho v) &= 0, \\ \frac{\partial \rho v}{\partial t} + \frac{\partial}{\partial x}\left(\rho v^2 + p\right) &= 0, \\ \frac{\partial \rho \varepsilon}{\partial t} + \frac{\partial}{\partial x}(\rho \varepsilon v + P v) &= 0, \end{aligned}$$

with v being used as a shorthand for v_x. These can be written in a compact vector notation as

$$\frac{\partial \boldsymbol{u}}{\partial t} + \frac{\partial \boldsymbol{F}}{\partial x} = 0, \tag{5.207}$$

where the state vector $\boldsymbol{u}$ is

$$\boldsymbol{u} = \begin{pmatrix} \rho \\ \rho v \\ \rho \varepsilon \end{pmatrix} \tag{5.208}$$

and the flux vector $\boldsymbol{F}$ is

$$\boldsymbol{F} = \begin{pmatrix} \rho v \\ \rho v^2 + P \\ \rho \varepsilon v + P v \end{pmatrix}. \tag{5.209}$$

Eqn. (5.207) can also be written in the form

$$\frac{\partial \boldsymbol{u}}{\partial t} + \boldsymbol{A}\frac{\partial \boldsymbol{u}}{\partial x} = 0, \tag{5.210}$$

where the *Jacobian matrix* $\boldsymbol{A}$ has components

$$A^{ij} = \frac{\partial F^i}{\partial u^j} \tag{5.211}$$

Equation (5.210) is very similar to the scalar conservation PDE (5.188) considered previously, except that now we have the vector $\boldsymbol{u}$ in the place of the scalar u, and the matrix $\boldsymbol{A}$ in the place of the scalar a. These differences mean that we can't apply the method of characteristics, as it stands, to eqn. (5.210); instead, we must transform to another set of variables

To perform this transformation, we first note that the Jacobian matrix can be decomposed as

$$\boldsymbol{A} = \boldsymbol{Q}\boldsymbol{\Lambda}\boldsymbol{Q}^{-1}, \tag{5.212}$$

where the elements of the diagonal matrix $\boldsymbol{\Lambda}$ are the eigenvalues of $\boldsymbol{A}$, and the columns of the matrix $\boldsymbol{Q}$ are the corresponding eigenvectors. Now we introduce a new vector of unknowns $\boldsymbol{w}$, known as the *characteristic variables* and defined so that

$$\frac{\partial \boldsymbol{u}}{\partial t} = \boldsymbol{Q}\frac{\partial \boldsymbol{w}}{\partial t}, \tag{5.213}$$

$$\frac{\partial \boldsymbol{u}}{\partial x} = \boldsymbol{Q}\frac{\partial \boldsymbol{w}}{\partial x}. \tag{5.214}$$

$$\tag{5.215}$$

The fluid equations then become

$$\boldsymbol{Q}\frac{\partial \boldsymbol{w}}{\partial t} + \boldsymbol{A}\boldsymbol{Q}\frac{\partial \boldsymbol{w}}{\partial x} = 0. \tag{5.216}$$

Multiplying through by $\boldsymbol{Q}^{-1}$, this simplifies to

$$\frac{\partial \boldsymbol{w}}{\partial t} + \boldsymbol{\Lambda}\frac{\partial \boldsymbol{w}}{\partial x} = 0. \tag{5.217}$$

Because $\boldsymbol{\Lambda}$ is a diagonal matrix, this can be decomposed into three *decoupled* equations

$$\frac{\partial w_i}{\partial t} + \Lambda_{ii}\frac{\partial w_i}{\partial x} = 0 \qquad i = 1, 2, 3. \tag{5.218}$$

We can now apply the method of characteristics to these decoupled equations: the characteristic curves are described by

$$\frac{\mathrm{d}x}{\mathrm{d}t} = \Lambda_{ii} \tag{5.219}$$

and along each of these curve the corresponding characteristic variable w_i will be constant. Every point in space and time has three of these curves passing through it, one for each characteristic variable; if we trace these curves back to $t = 0$, then we can determine the values of the characteristic variables from the initial state, as we did in previous sections.

The foregoing discussion has been relatively generic, since we haven't explicitly written down $\boldsymbol{A}$, $\boldsymbol{Q}$ or $\boldsymbol{\Lambda}$. Let's now look at our specific case of the fluid equations for an ideal gas. It can be shown[11] that the characteristic speeds are given by

$$\Lambda_{11} = v - a_{\mathrm{ad}}, \qquad \Lambda_{22} = v, \qquad \Lambda_{33} = v + a_{\mathrm{ad}}, \tag{5.220}$$

where a_{ad} is the usual adiabatic sound speed. These in some sense represent the information propagation speeds through the fluid, as they link the flow state at each point back to the initial state. The first and third correspond to information propagating in the form of sound waves, Doppler-shifted by the flow velocity v. The second speed (which is always between the first and third) represents the bulk advection of material in the flow. Along the corresponding characteristic curves, the variable

$$w_2 = \frac{P}{\rho^\gamma} + \text{const.} \tag{5.221}$$

is constant. Recall that for adiabatic (isentropic) changes an ideal gas follows the law

$$P \propto \rho^\gamma. \tag{5.222}$$

Therefore, the constancy of w_2 along the Λ_{22} characteristic curves corresponds to the entropy not changing — i.e., adiabatic motion.

[11] By forming the Jacobian matrix $\boldsymbol{A}$ and calculating its eigenvalues and eigenvectors.

5.4 The Rankine-Hugoniot Jump Relations

As was the case with Burgers' equation, two curves associated with the same characteristic variable of the fluid equations can sometimes come together and intersect. When this occurs, a discontinuity in characteristic variable arises — and this produces a matching discontinuity in one or more components of $\boldsymbol{u}$. In such cases, we have to switch to the integral form of the fluid equations. Using the same approach applied to Burgers' equation (see, e.g., Fig. 5.9) we then find that, across the discontinuity,

$$S(\boldsymbol{u}_\mathrm{R} - \boldsymbol{u}_\mathrm{L}) = \boldsymbol{F}_\mathrm{R} - \boldsymbol{F}_\mathrm{L}. \tag{5.223}$$

Writing this out in full using the definitions of $\boldsymbol{u}$ and $\boldsymbol{F}$,

$$S(\rho_\mathrm{R} - \rho_\mathrm{L}) = \rho_\mathrm{R} v_\mathrm{R} - \rho_\mathrm{L} v_\mathrm{L} \tag{5.224}$$

$$S(\rho_\mathrm{R} v_\mathrm{R} - \rho_\mathrm{L} v_\mathrm{L}) = (\rho_\mathrm{R} v_\mathrm{R}^2 + P_\mathrm{R}) - (\rho_\mathrm{L} v_\mathrm{L}^2 + P_\mathrm{L}) \tag{5.225}$$

$$S(\rho_\mathrm{R}\varepsilon_\mathrm{R} - \rho_\mathrm{L}\varepsilon_\mathrm{L}) = (\rho_\mathrm{R}\varepsilon_\mathrm{R} v_\mathrm{R} + P_\mathrm{R} v_\mathrm{R}) - (\rho_\mathrm{L}\varepsilon_\mathrm{L} v_\mathrm{L} + P_\mathrm{L} v_\mathrm{L}). \tag{5.226}$$

These are the famous *Rankine-Hugoniot jump relations*, which determine how states on either side of a fluid discontinuity are interconnected. In a frame of reference in which the shock is at rest ($S = 0$), they simplify to

$$\rho_\mathrm{L} v_\mathrm{L} = \rho_\mathrm{R} v_\mathrm{R}, \tag{5.227}$$

$$\rho_\mathrm{L} v_\mathrm{L}^2 + P_\mathrm{L} = \rho_\mathrm{R} v_\mathrm{R}^2 + P_\mathrm{R}, \tag{5.228}$$

$$\rho_\mathrm{L}\varepsilon_\mathrm{L} v_\mathrm{L} + P_\mathrm{L} v_\mathrm{L} = \rho_\mathrm{R}\varepsilon_\mathrm{R} v_\mathrm{R} + P_\mathrm{R} v_\mathrm{R}. \tag{5.229}$$

It's important to realize that the RH relations describe flow discontinuities across which only a single characteristic variable (w_1, w_2 or w_3) is discontinuous. It's possible to construct left and right states across which two or three of the w_i's are simultaneously discontinuous. In such cases we have to insert intermediate states, and apply the RH relations multiple times. The supersonic colliding flows example in §B.7 illustrates how this is done.

Let's now look at the RH relations in a couple of important limiting cases. First, suppose that the fluid in the left and right states is at rest, in the $S = 0$ frame of reference. Then, the RH relations reduce to

$$P_\mathrm{L} = P_\mathrm{R} \tag{5.230}$$

This configuration is known as a *contact discontinuity* — the left and right states have different densities[12], but they are at rest relative to each other and in pressure balance. From eqn. (5.221), we see that it's the w_2 characteristic variable that jumps across a contact discontinuity.

Now suppose that, again in the $S = 0$ frame, the fluid in the left-hand state has a large mach number[13]:

$$M_\mathrm{L} = \frac{v_\mathrm{L}}{a_\mathrm{ad,L}} \gg 1. \tag{5.231}$$

[12] If they had the same density, there would be no discontinuity at all!

[13] The mach number is the ratio of the flow speed to the sound speed.

This large mach number means that the internal energy of the fluid is negligible compared to its kinetic energy, allowing us to neglect the $P_{\rm L}$ terms in eqns. (5.228) and (5.229) and approximate $\varepsilon_{\rm L}$ as $v_{\rm L}^2/2$:

$$\rho_{\rm L} v_{\rm L}^2 = \rho_{\rm R} v_{\rm R}^2 + P_{\rm R}, \tag{5.232}$$

$$\frac{1}{2}\rho_{\rm L} v_{\rm L}^3 = \rho_{\rm R}\varepsilon_{\rm R} v_{\rm R} + P_{\rm R} v_{\rm R}. \tag{5.233}$$

This set of simultaneous equations can be solved, to find the right-hand states in terms of the left-hand ones:

$$\rho_{\rm R} = \frac{\gamma+1}{\gamma-1}\rho_{\rm L}, \tag{5.234}$$

$$v_{\rm R} = \frac{\gamma-1}{\gamma+1} v_{\rm L}, \tag{5.235}$$

$$P_{\rm R} = \frac{2}{\gamma+1}\rho_{\rm L} v_{\rm L}^2, \tag{5.236}$$

$$\varepsilon_{\rm R} = \frac{5+\gamma(\gamma-2)}{2(1+\gamma)^2} v_{\rm R}^2. \tag{5.237}$$

For a monatomic gas with $\gamma = 5/3$, these simplify to

$$\rho_{\rm R} = 4\rho_{\rm L}, \tag{5.238}$$

$$v_{\rm R} = \frac{v_{\rm L}}{4}, \tag{5.239}$$

$$P_{\rm R} = \frac{3}{4}\rho_{\rm L} v_{\rm L}^2, \tag{5.240}$$

$$\varepsilon_{\rm R} = \frac{5}{16} v_{\rm L}^2. \tag{5.241}$$

This configuration is known as a *shock* — the left-hand state is a supersonic flow ($M_{\rm L} > 1$) toward the discontinuity, and the right-hand state is a subsonic flow ($M_{\rm R} < 1$) away from the discontinuity. A key feature of a shock is the conversion of a fraction of the flow kinetic energy into thermal (internal) energy. In the present case, the $M_{\rm L} \gg 1$ presumption is a special limiting case known as a *strong shock*, characterized by a density jump of a factor four, and a post-shock kinetic-to-internal energy ratio of

$$\frac{\frac{1}{2}v_{\rm R}^2}{u_{\rm R}} = \frac{1}{9}. \tag{5.242}$$

Shocks correspond to jumps in the w_1 or w_3 characteristic variables (the case considered here has a discontinuous w_1). In astrophysical settings they are an important heating mechanism. For a flows of solar-composition gas, the temperature downstream of a strong shock is readily found as

$$T_{\rm R} = \frac{P_{\rm R}\bar{m}}{\rho_{\rm R} k_{\rm B}} \approx 14 \times 10^6 \left(\frac{v_{\rm L}}{1000\,{\rm km\,s^{-1}}}\right)^2 \tag{5.243}$$

(the mean particle mass $\bar{m}$ is ≈ 0.61 atomic mass units, for solar composition). Thus, we see that a $1,000\,{\rm km\,s^{-1}}$ flow speed is sufficient to shock-heat the gas to over 10 million kelvin, in turn producing copious X-ray emission.

6 Magnetohydrodynamics

6.1 Introducing Plasmas

Astrophysical fluids often take the form of the so-called fourth state of matter — plasmas. A plasma is a gas containing a non-negligible fraction of charge carriers, typically electrons and ions. The presence of these charge carriers make plasmas electrically conductive, meaning that they interact strongly with magnetic fields. To account for this interaction, we need to modify the fluid equations and introduce additional equations governing the field evolution.

6.2 Review of Electromagnetism

We'll start by briefly reviewing the parts of electromagnetism needed for the subsequent analysis. These primarily consist of the vacuum[14] Maxwell's equations, which in cgs (Gaussian) units are

$$\nabla \cdot \boldsymbol{E} = 4\pi\rho_{\rm c}, \tag{6.244}$$

$$\nabla \cdot \boldsymbol{B} = 0, \tag{6.245}$$

$$\nabla \times \boldsymbol{E} = -\frac{1}{c}\frac{\partial \boldsymbol{B}}{\partial t}, \tag{6.246}$$

$$\nabla \times \boldsymbol{B} = \frac{1}{c}\frac{\partial \boldsymbol{E}}{\partial t} + 4\pi\frac{\boldsymbol{J}}{c}. \tag{6.247}$$

Typically, a plasma is neutral over macroscopic-sized regions, because any charge build-up is rapidly short-circuited by currents. Hence, we shall set the charge density $\rho_{\rm c}$ in Gauss' law (6.244) to zero. We'll also assume that the time evolution of the electric field is slow (compared to the light crossing time of the system) so we can neglect the displacement current term ($c^{-1}\partial\boldsymbol{E}/\partial t$) in Ampère's law (6.247).

The coupling between the electromagnetic field and the fluid comes via the charge carriers. As they move relative to the fluid's bulk velocity $\boldsymbol{v}$, these charge carriers on the one hand yield a current $\boldsymbol{J}$[15], and on the other are acted on electric and magnetic fields, with a force per unit volume of

$$\boldsymbol{f} = \rho_{\rm c}\boldsymbol{E} + \frac{\boldsymbol{J}\times\boldsymbol{B}}{c} = \frac{\boldsymbol{J}\times\boldsymbol{B}}{c}. \tag{6.248}$$

[14] I.e., without any dielectric or magnetic materials, so there's no need to worry about $\boldsymbol{D}$, $\boldsymbol{H}$, polarizations etc.

[15] $\boldsymbol{J}$ is the *current density*.

The second equality follows from our stipulation that the plasma is electrically neutral.

The currents themselves are driven by electromagnetic induction: as indicated by Faraday's law (6.246), a varying magnetic flux through any closed loop C will generate a current around that loop. The magnitude of the current is limited by the electrical resistance of the plasma. Let's assume that the plasma follows Ohms law, so that

$$\widetilde{\boldsymbol{J}} = \sigma \widetilde{\boldsymbol{E}}. \tag{6.249}$$

Here, σ is the conductivity of the plasma, and the tildes $\tilde{()}$ indicate that the equation applies *in the frame co-moving with the fluid*. The latter stipulation arises because it is the charge carriers colliding with other particles in the plasma, which are (on average) at rest in the co-moving frame, which ultimately limits the current $\boldsymbol{J}$. To transform back to the usual inertial frame in which the fluid moves with velocity $\boldsymbol{v}$, we apply a Lorentz transformation to the electromagnetic tensor and the current four-vector. Assuming $|\boldsymbol{v}| \ll c$, the appropriate transformations are[16]

$$\widetilde{\boldsymbol{J}} = \boldsymbol{J}, \qquad \widetilde{\boldsymbol{E}} = \boldsymbol{E} + \frac{\boldsymbol{v} \times \boldsymbol{B}}{c}, \tag{6.250}$$

and so Ohm's law becomes

$$\boldsymbol{J} = \sigma \left(\boldsymbol{E} + \frac{\boldsymbol{v} \times \boldsymbol{B}}{c} \right). \tag{6.251}$$

This gives the current flowing in the inertial frame of reference in which the plasma is moving with velocity $\boldsymbol{v}$.

6.3 The Magnetohydrodynamical Equations

It's relatively straightforward to derive the equations governing a magnetized plasma, under the various conditions outlined in the previous section: we just modify the fluid equations to include the effects of the Lorentz force $\boldsymbol{f}$ (cf. eqns. 6.248). The resulting equations are

$$\frac{\partial \rho}{\partial t} + \nabla \cdot (\rho \boldsymbol{v}) = 0, \tag{6.252}$$

$$\frac{\partial \rho \boldsymbol{v}}{\partial t} + \nabla \cdot (\rho \boldsymbol{v} \otimes \boldsymbol{v}) + \nabla P = \frac{1}{c} \boldsymbol{J} \times \boldsymbol{B}, \tag{6.253}$$

$$\frac{\partial \rho \varepsilon}{\partial t} + \nabla \cdot (\rho \varepsilon \boldsymbol{v} + P \boldsymbol{v}) = \frac{1}{c} \boldsymbol{v} \cdot (\boldsymbol{J} \times \boldsymbol{B}). \tag{6.254}$$

The current density is determined via the Ohms-law-based eqn. (6.251), and Maxwell's equations govern the time-evolution of the electric and magnetic fields.

With a little algebra, the electric field and current density can be eliminated from these equations, to leave only the magnetic field as the agent of electromagnetic effects. The

[16] The *Wikipedia* page on 'Lorentz Transformation' gives a nice summary of this non-relativistic limit (fetched 2012-04-17).

momentum and energy conservation equations become

$$\frac{\partial \rho \boldsymbol{v}}{\partial t} + \nabla \cdot (\rho \boldsymbol{v} \otimes \boldsymbol{v}) + \nabla P = \frac{1}{4\pi}(\nabla \times \boldsymbol{B}) \times \boldsymbol{B} \tag{6.255}$$

and

$$\frac{\partial \rho \varepsilon}{\partial t} + \nabla \cdot (\rho \varepsilon \boldsymbol{v} + P \boldsymbol{v}) = \frac{1}{4\pi} \boldsymbol{v} \cdot (\nabla \times \boldsymbol{B}) \times \boldsymbol{B}. \tag{6.256}$$

Likewise, Faraday's law (the induction equation, 6.246) is rearranged to read

$$\frac{\partial \boldsymbol{B}}{\partial t} = -\frac{c^2}{4\pi\sigma} \nabla \times (\nabla \times \boldsymbol{B}) + \nabla \times (\boldsymbol{v} \times \boldsymbol{B}) \tag{6.257}$$

(where we've assumed that σ is spatially constant). Using the identity

$$\nabla \times (\nabla \times \boldsymbol{B}) = \nabla(\nabla \cdot \boldsymbol{B}) - \nabla^2 \boldsymbol{B} \tag{6.258}$$

the first term vanishes due to the $\nabla \cdot \boldsymbol{B} = 0$ condition, and so the induction equation further simplifies to

$$\frac{\partial \boldsymbol{B}}{\partial t} = \eta_B \nabla^2 \boldsymbol{B} + \nabla \times (\boldsymbol{v} \times \boldsymbol{B}), \tag{6.259}$$

where

$$\eta_B \equiv \frac{c^2}{4\pi\sigma}, \tag{6.260}$$

is the *magnetic diffusivity*.

6.4 Magnetic Pressure and Magnetic Tension

Let's have a look in more detail at the Lorentz-force term in the MHD momentum equation (6.255). Using the identity

$$\nabla(\boldsymbol{B} \cdot \boldsymbol{B}) = 2\boldsymbol{B} \times (\nabla \times \boldsymbol{B}) + 2(\boldsymbol{B} \cdot \nabla)\boldsymbol{B}, \tag{6.261}$$

we obtain the Lorentz force as

$$\boldsymbol{f} = \frac{1}{4\pi}(\nabla \times \boldsymbol{B}) \times \boldsymbol{B} = -\frac{1}{8\pi}\nabla(\boldsymbol{B} \cdot \boldsymbol{B}) + \frac{1}{4\pi}(\boldsymbol{B} \cdot \nabla)\boldsymbol{B}. \tag{6.262}$$

On the right-hand side, the first term is the gradient of the scalar $P_{\rm mag} \equiv B^2/8\pi$. Recalling that the pressure force is also the gradient of a scalar, we can identify $P_{\rm mag}$ as the *magnetic pressure* (and, indeed, the units of $P_{\rm mag}$ are those of a pressure).

The second term on the right-hand side can be interpreted as the directional derivative of $\boldsymbol{B}$ along field lines. If the field *strength* is changing along a field line, then the resulting force is parallel to the field line; whereas if the field *direction* is changing along the field line, then

the resulting force is perpendicular to the field line. Thus, this term behaves like a tension force acting along field lines.

Suppose we have a situation where both the magnetic pressure and magnetic tension forces greatly exceed any of the other terms in the momentum equation (6.255). Then, in order that this equation be satisfied, the pressure and tension forces must be *almost* equal and opposite. Such a configuration is known as *force free* — a slightly confusing term, because there are certainly magnetic forces present. Perhaps the simplest interpretation is that, in a force-free configuration, the *net* Lorentz force is much much smaller than the individual pressure and tension forces.

A special subset of force-free field configurations are those derivable from a scalar potential; for, if

$$\boldsymbol{B} = \nabla \phi_B \tag{6.263}$$

for some scalar ϕ_B, then $\boldsymbol{J} = \nabla \times \boldsymbol{B} = 0$ and the Lorentz force vanishes exactly. A dipole magnetic field — the sort exhibited by the Sun during solar minimum — is an example of a potential field, with

$$\phi_B \propto \frac{\cos\theta}{r^2}. \tag{6.264}$$

6.5 The Magnetic Reynolds Number

Let's now turn to further inspection of the induction equation (6.259). As in §3.5, let L denote the typical length scale of the system under consideration, and V is the typical flow velocity. Then, the induction equation can be cast as

$$\frac{\partial \boldsymbol{B}}{\partial t} \sim \frac{\eta}{L^2}\boldsymbol{B} + \frac{V}{L}\boldsymbol{B} \sim \frac{\eta}{L^2}\left(1 + R_{\rm m}\right)\boldsymbol{B}, \tag{6.265}$$

where

$$\mathcal{R}_{\rm m} \equiv \frac{LV}{\eta_B} \tag{6.266}$$

is the *magnetic Reynolds number*. Comparing this against eqn. (3.91) for the 'ordinary' Reynolds number, we see that the kinematic viscosity ν has been replaced by the magnetic diffusivity η_B. The magnetic Reynolds number characterizes the relative importance of diffusion versus advection (field transport by fluid flow) in the time evolution of the magnetic field. The following subsections examine these limits in greater detail.

6.5.1 The $\mathcal{R}_{\rm m} \ll 1$ Limit

In the limit $\mathcal{R}_{\rm m} \ll 1$, the first term on the right-hand side of the induction equation (6.259) is dominant, and we may approximate the equation as

$$\frac{\partial \boldsymbol{B}}{\partial t} = \eta_B \nabla^2 \boldsymbol{B}. \tag{6.267}$$

This has the standard form of a diffusion equation, with the magnetic diffusivity setting the speed at which the magnetic field diffuses from regions of high concentration to regions of low concentrations. For magnetic structures with a length scale L, the timescale over which these structures will dissolve via field diffusion into a uniform field is given by

$$\tau \sim \frac{L^2}{\eta_B}. \tag{6.268}$$

Because the conductivity of astrophysical plasmas is typically large, the $\mathcal{R}_{\rm m} ll 1$ limit is rarely encountered in practice. The one possible exception is when the length scale L becomes very small. Such situations can arise when we have field lines of opposite polarity pushed very close to each other; then, the diffusion term in the induction equation can dominate, and a *magnetic reconnection* can occur, in which the magnetic topology changes.

6.5.2 The $\mathcal{R}_{\rm m} \gg 1$ Limit: Ideal MHD

In the opposite limit $\mathcal{R}_{\rm m} \gg 1$, the second term in the induction equation (6.259) dominates, and we have

$$\frac{\partial \boldsymbol{B}}{\partial t} = \nabla \times (\boldsymbol{v} \times \boldsymbol{B}). \tag{6.269}$$

A very important physical result follows in this limiting *ideal magnetohydrodynamics* case. Consider the magnetic flux passing through some surface element $\mathrm{d}\tau$ which moves with the fluid:

$$\Phi = \int_{\mathrm{d}\tau} \boldsymbol{B} \cdot \mathrm{d}\boldsymbol{A}. \tag{6.270}$$

Suppose the surface and the bounding curve move along with the fluid. Then, the rate of change of the flux will be

$$\frac{\mathrm{d}\Phi}{\mathrm{d}t} = \frac{\mathrm{d}}{\mathrm{d}t} \int_{\mathrm{d}\tau} \boldsymbol{B} \cdot \mathrm{d}\boldsymbol{A}. \tag{6.271}$$

We have to be careful when taking the time derivative under the integral sign, because the surface element $\mathrm{d}\tau$ changes as it is advected along with the fluid. In fact, we have to make use of a form of the Reynolds transport theorem (§C)), allowing us to obtain

$$\frac{\mathrm{d}\Phi}{\mathrm{d}t} = \int_{\mathrm{d}\tau} \left[\frac{\partial \boldsymbol{B}}{\partial t} + (\nabla \cdot \boldsymbol{B})\boldsymbol{v} \right] \cdot \mathrm{d}A - \oint_{\mathcal{C}} (\boldsymbol{v} \times \boldsymbol{B}) \cdot \mathrm{d}\boldsymbol{s}, \tag{6.272}$$

where $\mathcal{C}$ is the curve bounding $\mathrm{d}\tau$. The divergence of $\boldsymbol{B}$ vanishes, and the second integral can be transformed into a surface integral via Stokes' theorem, so

$$\frac{\mathrm{d}\Phi}{\mathrm{d}t} = \int_{\mathrm{d}\tau} \left[\frac{\partial \boldsymbol{B}}{\partial t} - \nabla \times (\boldsymbol{v} \times \boldsymbol{B}) \right] \cdot \mathrm{d}\boldsymbol{A}. \tag{6.273}$$

Now we invoke the ideal MHD induction equation (6.269), which tells us that the quantity in square brackets must vanish identically; thus,

$$\frac{\mathrm{d}\Phi}{\mathrm{d}t} = 0, \tag{6.274}$$

which is the famous *frozen-flux condition*. Physically, this means that any blob of plasma threaded by a given magnetic flux must remain threaded by the same flux, no matter what happens to the blob — the field is tied to the plasma, and vice versa. A useful analogy here is stiff wires embedded in jello. As the jello is compressed or stretched, the wires must similarly distort; but the jello is free to slide *along* the wires. (Note that we assume the jello doesn't tear).

6.6 MHD Waves

6.6.1 Wave Equation

Let's now see how a magnetized plasma responds to small perturbations. For simplicity, assume that the background state has uniform density and pressure, uniform magnetic field $\boldsymbol{B} = B_0\,\hat{\boldsymbol{z}}$ in the z-direction, and is at rest. In the ideal MHD limit (see above), the linearized equations are

$$\frac{\partial \rho'}{\partial t} + \rho_0 \nabla \cdot \boldsymbol{v}' = 0, \tag{6.275}$$

$$\frac{\partial \boldsymbol{v}'}{\partial t} + \frac{1}{\rho_0}\nabla P' = \frac{B_0}{4\pi\rho_0}\left(-\nabla B_z' + \frac{\partial \boldsymbol{B}'}{\partial z}\right) \tag{6.276}$$

$$\frac{\partial P'}{\partial t} + \gamma P_0 \nabla \cdot \boldsymbol{v}' = 0, \tag{6.277}$$

$$\frac{\partial \boldsymbol{B}'}{\partial t} = B_0 \nabla \times (\boldsymbol{v}' \times \hat{\boldsymbol{z}}). \tag{6.278}$$

Note that the first term in the parentheses of eqn. (6.276) corresponds to the magnetic pressure force, and the second term to the magnetic tension force.

6.6.2 Dispersion Relation

Motivated by our previous experiences with the linearized fluid equations (cf. §4.4.3), let's assume trial solutions of the form

$$\boldsymbol{Y}(\boldsymbol{r}, t) = \boldsymbol{y} \exp[\mathrm{i}(\boldsymbol{k}\cdot\boldsymbol{r} - \omega t)] \tag{6.279}$$

where

$$\boldsymbol{y} \equiv \begin{pmatrix} \rho'/\rho_0 \\ v_x'/a_{\rm ad} \\ v_y'/a_{\rm ad} \\ v_z'/a_{\rm ad} \\ P'/P_0 \\ B_x'/B_0 \\ B_y'/B_0 \\ B_z'/B_0 \end{pmatrix} \tag{6.280}$$

is the vector of unknowns (scaled by the background values), and $\boldsymbol{y}$ is a constant vector to be determined. Substituting this expression for $\boldsymbol{Y}$ into the linearized MHD equations leads to a set of *algebraic* equations of the form given in eqn. (4.126), where now

$$\boldsymbol{M} = \begin{pmatrix} 0 & a_{\rm ad}k_x & a_{\rm ad}k_y & a_{\rm ad}k_z & 0 & 0 & 0 & 0 \\ 0 & 0 & 0 & 0 & a_{\rm ad}k_x/\gamma & -a_{\rm Alf}^2 k_z/a_{\rm ad} & 0 & a_{\rm Alf}^2 k_x/a_{\rm ad} \\ 0 & 0 & 0 & 0 & a_{\rm ad}k_y/\gamma & 0 & -a_{\rm Alf}^2 k_z/a_{\rm ad} & a_{\rm Alf}^2 k_y/a_{\rm ad} \\ 0 & 0 & 0 & 0 & a_{\rm ad}k_z/\gamma & 0 & 0 & 0 \\ 0 & a_{\rm ad}k_x\gamma & a_{\rm ad}k_y\gamma & a_{\rm ad}k_z\gamma & 0 & 0 & 0 & 0 \\ 0 & -a_{\rm ad}k_z & 0 & 0 & 0 & 0 & 0 & 0 \\ 0 & 0 & -a_{\rm ad}k_z & 0 & 0 & 0 & 0 & 0 \\ 0 & a_{\rm ad}k_x & a_{\rm ad}k_y & 0 & 0 & 0 & 0 & 0 \end{pmatrix}, \tag{6.281}$$

where

$$a_{\rm Alf} = \frac{B_0}{\sqrt{4\pi\rho_0}} \tag{6.282}$$

introduces the *Alfvén speed*, being the square root of the ratio between twice the magnetic pressure and the plasma density (contrast this with the sound speed — adiabatic or isothermal — which scales as the square root of the ratio between the *gas* pressure and the plasma density).

The characteristic equation (4.128) leads to the dispersion relation

$$\omega^2[\omega^4 - |\boldsymbol{k}|^2(a_{\rm ad}^2 + a_{\rm Alf}^2)\omega^2 + k_z^2|\boldsymbol{k}|^2 a_{\rm ad}^2 a_{\rm Alf}^2](k_z^2 a_{\rm Alf}^2 - \omega^2) = 0. \tag{6.283}$$

Defining θ as the angle of $\boldsymbol{k}$ to the vertical, so that

$$\cos\theta = \frac{\boldsymbol{k}\cdot\hat{\boldsymbol{z}}}{|\boldsymbol{k}|}, \tag{6.284}$$

the dispersion relation can also be written

$$\omega^2[\omega^4 - |\boldsymbol{k}|^2(a_{\rm ad}^2 + a_{\rm Alf}^2)\omega^2 + |\boldsymbol{k}|^2\,\cos^2\theta\, a_{\rm ad}^2 a_{\rm Alf}^2](|\boldsymbol{k}|^2\,\cos^2\theta\, a_{\rm Alf}^2 - \omega^2) = 0. \tag{6.285}$$

This equation has six non-trivial roots[17] appearing in three pairs; each pair can be written in the form

$$\omega = \pm a|\boldsymbol{k}|, \tag{6.286}$$

and corresponds to waves propagating parallel (+) or anti-parallel (-) to the wavevector $\boldsymbol{k}$, with a phase velocity a (to be determined) For general θ there are three distinct phase velocities (one per pair), corresponding to three distinct types of waves: Alfvén, slow magnetosonic and fast magnetosonic. Fig. 6.14 plots these phase velocities as a function of θ, for both the $a_{\rm Alf} < a_{\rm ad}$ and $a_{\rm Alf} > a_{\rm ad}$ cases (these correspond to 'weak' and 'strong' fields, respectively as compared to the typical strength of gas-pressure forces).

6.6.3 Alvén Waves

Let's focus first on the Alfvén waves, corresponding to the trivial roots

$$\omega = \pm a_{\rm Alf}\, \cos\theta\, |\boldsymbol{k}| \tag{6.287}$$

of the dispersion relation (6.285). The associated eigenvectors have the form

$$\boldsymbol{y} = A \begin{pmatrix} 0 \\ \pm a_{\rm Alf} k_y \\ \mp a_{\rm Alf} k_x \\ 0 \\ 0 \\ -a_{\rm ad} k_y \\ a_{\rm ad} k_x \\ 0 \end{pmatrix} \tag{6.288}$$

where A is an arbitrary dimensionless constant. Evidently, the pressure and the density perturbations vanish for the Alfvén waves, while the velocity and field perturbations are perpendicular to both the equilibrium field *and* the wavevector:

$$\boldsymbol{v}' \cdot \hat{\boldsymbol{z}} = 0, \qquad \boldsymbol{B}' \cdot \hat{\boldsymbol{z}} = 0, \qquad \boldsymbol{v}' \cdot \boldsymbol{k} = 0, \qquad \boldsymbol{B}' \cdot \boldsymbol{k} = 0. \tag{6.289}$$

Physically, this means that perturbations are limited to the horizontal (x-y) plane, and moreover are perpendicular to the direction of propagation; so, Alfvén waves are *transverse*.

What restoring force is at work in Alfvén waves, pushing displaced fluid elements back to their equilibrium positions? It can't be gas pressure, as the perturbation to P is zero. The perturbation to the magnetic pressure is

$$P'_{\rm mag} = \left[\frac{B^2}{8\pi}\right]' = A^2 a_{\rm ad}^2 (k_x^2 + k_y^2), \tag{6.290}$$

[17] Of the two trivial, $\omega = 0$ roots, one corresponds to a case where ρ' is non-zero but all the other perturbations vanish; and the other corresponds to a Lorentz force-free perturbation to the magnetic field.

where the second equality follows from substituting in the solution vector above. This is *second-order* in the perturbation amplitude A, and so to *first order* in A the magnetic pressure perturbation also vanishes. In fact, magnetic tension — arising from the bending of field lines — serves as the restoring force for Alfvén waves. In the present case, the field lines become bent iff B_x' and/or B_y' vary with z[18]. From inspecting the exponential term in eqn. (6.288) we see that this implies k_z must be non-zero — i.e., Alfvén waves cannot propagate in the purely horizontal (field-perpendicular) direction. This explains why $\omega \neq 0$ in eqn. (6.287) requires that $\cos\theta \neq 0$.

For Alfvén waves propagating in the purely vertical (field-parallel) direction, eqn. (6.288) would seem to imply that the solution vectors become the null vector (because both k_x and k_y vanish). In fact, in this special limiting case there are *two* possible pairs of solutions vectors,

$$\boldsymbol{y} = A \begin{pmatrix} 0 \\ 0 \\ \mp a_{\rm Alf}/a_{\rm ad} \\ 0 \\ 0 \\ 0 \\ 1 \\ 0 \end{pmatrix} \tag{6.291}$$

and

$$\boldsymbol{y} = A \begin{pmatrix} 0 \\ \mp a_{\rm Alf}/a_{\rm ad} \\ 0 \\ 0 \\ 0 \\ 1 \\ 0 \\ 0 \end{pmatrix} \tag{6.292}$$

which correspond to two orthogonal polarizations of the Alfvén wave (in the y and x directions, respectively). The appearance of this double solution comes from the fact that the full dispersion relation (6.285) has a double root in ω^2 when $\cos\theta = \pm 1$, arising from a merger between the Alfvén waves and one of the magnetosonic waves. This merger can clearly be seen in both panels of Fig. 6.14.

6.6.4 Magnetosonic Waves

Let's now look at the magnetosonic waves, which arise as the roots of

$$\omega^4 - |\boldsymbol{k}|^2(a_{\rm ad}^2 + a_{\rm Alf}^2)\omega^2 + k^2\cos^2\theta^2 a_{\rm ad}^2 a_{\rm Alf}^2 = 0 \tag{6.293}$$

[18]Without this z dependence, the perturbed field lines would be tilted with respect to the vertical, but still remain straight lines.

(this is just eqn. 6.285 with the Alfvén roots eliminated). The solutions are

$$\omega = \pm\sqrt{\frac{a_{\rm ad}^2 + a_{\rm Alf}^2 \pm \sqrt{(a_{\rm ad}^2 + a_{\rm Alf}^2)^2 - 4\cos^2\theta a_{\rm ad}^2 a_{\rm Alf}^2}}{2}}\,|\boldsymbol{k}|, \tag{6.294}$$

with the inner plus sign corresponding to the fast magnetosonic waves, and the inner minus sign to the slow magnetosonic waves (as usual, the outer plus/minus signs determine the wave propagation direction). In the limit of vertical propagation ($\cos\theta = \pm 1$), the solutions reduce to

$$\omega = \pm a_{\rm ad}\,|\boldsymbol{k}|, \qquad \omega = \pm a_{\rm Alf}\,|\boldsymbol{k}|; \tag{6.295}$$

the first of these corresponds to pure acoustic waves, and the second to the merged Alfvén waves discussed above. In the opposite limit of horizontal propagation ($\cos\theta = 0$), the solutions reduce to

$$\omega = \pm\sqrt{a_{\rm ad}^2 + a_{\rm Alf}^2}\,k, \qquad \omega = 0, \tag{6.296}$$

so now the fast waves have a phase speed $a = \sqrt{a_{\rm ad}^2 + a_{\rm Alf}^2}$ which is the harmonic mean of the sound speed and Alfvén speed; while the slow waves have vanished. At oblique angles, between vertical and horizontal, the slow magnetosonic waves have a frequency below that of the Alfvén waves, and the fast magnetosonic waves above.

As with the Alfvén waves (cf. eqn. 6.288), the solution vectors for the magnetosonic waves offer insights into their physical character. For vertical propagation, the $\omega = \pm a\,k$ magnetosonic waves have solutions

$$\boldsymbol{y} = A\begin{pmatrix} 1 \\ 0 \\ 0 \\ \pm 1 \\ \gamma \\ 0 \\ 0 \\ 0 \end{pmatrix}. \tag{6.297}$$

these are just longitudinal acoustic waves, with no role played by the magnetic field whatsoever. We've already encountered the solution vectors for the vertical $\omega = \pm a_{\rm Alf}\,k$ magnetosonic waves — recall that these merge with the Alfvén waves to give the two distinct polarizations.

Turning therefore to the horizontal limit, the fast waves with $\omega = \pm\sqrt{a_{\rm ad}^2 + a_{\rm Alf}^2}\,|\boldsymbol{k}|$ have

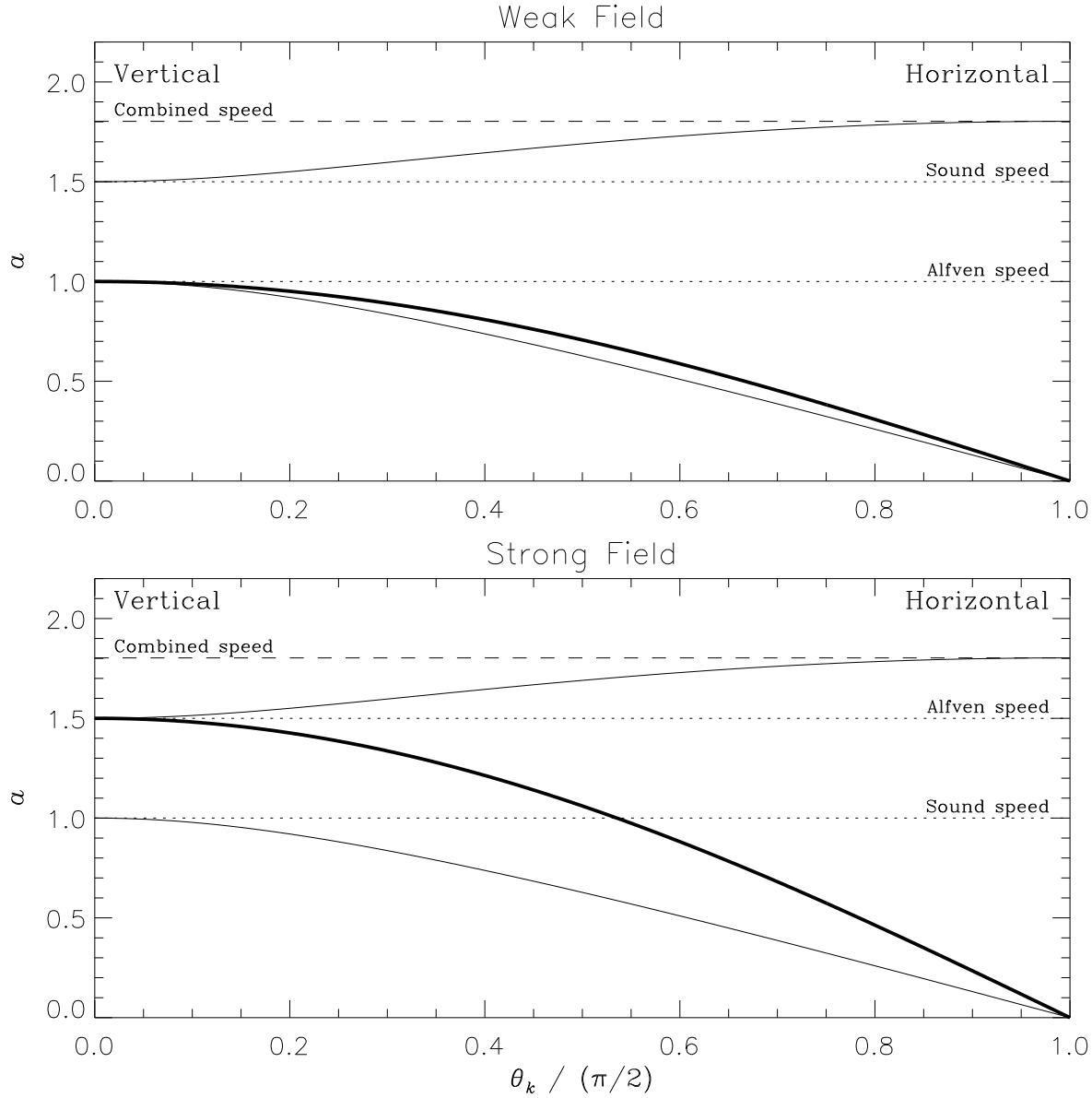

Figure 6.14: Phase velocities c of MHD waves, plotted as a function of propagation angle to the vertical θ, for the weak field ($a_{\rm Alf} < a_{\rm ad}$) and strong field ($a_{\rm Alf} > a_{\rm ad}$) cases. The thick solid line shows the Alfvén waves, while the thin solid lines show the slow (lower) and fast (upper) magnetosonic waves . The horizontal dotted lines show the adiabatic sound speed $a_{\rm ad}$ and Alfvén speed $a_{\rm Alf}$, and the dashed line shows the combined speed $\sqrt{a_{\rm ad}^2 + a_{\rm Alf}^2}$.

solution vectors

$$\boldsymbol{y} = \begin{pmatrix} a_{\rm ad}|\boldsymbol{k}| \\ \pm\sqrt{a_{\rm ad}^2 + a_{\rm Alf}^2}k_x \\ \pm\sqrt{a_{\rm ad}^2 + a_{\rm Alf}^2}k_y \\ 0 \\ \gamma a_{\rm ad}|\boldsymbol{k}| \\ 0 \\ 0 \\ a_{\rm ad}|\boldsymbol{k}| \end{pmatrix}. \tag{6.298}$$

The velocity perturbations are in the direction of propagation, so these are longitudinal waves. Because B'_x and B'_y vanish, the field lines remain straight, and so magnetic tension does not play a role; rather, it's magnetic pressure perturbations (represented by the B'_z term) which work in concert with gas pressure perturbations as the restoring force for the fast magnetosonic waves. Because the restoring force is greater than it would be for pure acoustic waves or for Alfvén waves, the phase velocity of the fast waves exceeds both the acoustic and Alfvén speeds.

Similar reasoning explains why the slow magnetosonic waves have a phase velocity smaller than either the acoustic or Alfvén speeds. For these waves, the gas pressure and magnetic pressure perturbations work in anti-phase, and the ensuing cancellation leads to a smaller restoring force. In the horizontal limit, the cancellation is complete, explaining why the frequencies of these waves tend to zero (cf. Fig. 6.14, eqn. 6.296).

References

[1] Schutz, B., 2009, *A First Course in General Relativity, 2nd edn.* Cambridge University Press

A Vectors, Dyads and Dyadics

Vectors are a familiar concept to any science student, but dyadics are somewhat more arcane — and, potentially, a great source of confusion. This appendix provides a simplified introduction to dyadics, couched in the same geometric terms often used to define vectors.

A.1 Vectors

As a reminder,

A *vector* is a geometrical quantity with a magnitude and a direction.

These notes write vectors using a bold italic font: $\boldsymbol{a}$, $\boldsymbol{b}$, etc. When hand-written, an overbar can be used instead: $\overline{a}$, $\overline{b}$, etc.

Often, we specify a vector relative to an arbitrary (but agreed-upon) set of reference vectors. This allows us to define the vector in terms its components, an ordered list of n scalars (where n is the number of spatial dimensions). Thus, we write

$$\boldsymbol{a} = \sum_{i=1}^{n} a^i \boldsymbol{e}_i, \tag{A.1}$$

where $\{a^i\}$ are the components and $\{\boldsymbol{e}_i\}$ are n unit basis vectors giving the reference directions. Using the Einstein notation, where a twice-repeated index implicitly indicates summation over that index, this expression can also be written as

$$\boldsymbol{a} = a^i \boldsymbol{e}_i. \tag{A.2}$$

A.2 Dyads and Dyadics

In the same spirit as our definition above of vectors,

A *dyad* is a geometrical quantity with a magnitude and two directions.

In these notes we write dyads using a bold sans-serif font: D, E. When hand-written, a double overbar can be used instead: $\overline{\overline{D}}$, $\overline{\overline{E}}$, etc.

Dyads can be constructed from a pair of vectors by taking the outer product $\otimes$ between them:

$$\mathsf{D} = \boldsymbol{a} \otimes \boldsymbol{b} \tag{A.3}$$

Note that the outer product is not commutative; the order of the operands matters, and in general $\boldsymbol{a} \otimes \boldsymbol{b} \neq \boldsymbol{b} \otimes \boldsymbol{a}$. If we specify $\boldsymbol{a}$ and $\boldsymbol{b}$ in terms of their components, then

$$\mathsf{D} = (a^i \boldsymbol{e}_i) \otimes (b^j \boldsymbol{e}_j). \tag{A.4}$$

The outer product doesn't act on scalars, and so we can rewrite this as

$$\boldsymbol{D} = a^i b^j \boldsymbol{e}_i \otimes \boldsymbol{e}_j, \tag{A.5}$$

or even more compactly as

$$\boldsymbol{D} = D^{ij} \boldsymbol{E}_{ij} \tag{A.6}$$

where

$$D^{ij} \equiv a^i b^j, \tag{A.7}$$
$$\boldsymbol{E}_{ij} \equiv \boldsymbol{e}_i \otimes \boldsymbol{e}_j. \tag{A.8}$$

Now let's introduce a related concept:

A *dyadic* is a linear combination of dyads.

From this definition, we can see that $\boldsymbol{D}$ is itself a dyadic, because it is a sum of basis dyads $\{\boldsymbol{E}_{ij}\}$ weighted by the scalars $\{D^{ij}\}$. In fact, all dyads are dyadics — but not all dyadics are dyads. The simplest counterexample is the identity dyadic $\boldsymbol{I}$,

$$\boldsymbol{I} = \boldsymbol{e}_i \otimes \boldsymbol{e}_i = \boldsymbol{E}_{ii}, \tag{A.9}$$

which *cannot* be written as a single outer product between two vectors. The identity dyadic has components

$$I^{ij} = \delta_{ij}, \tag{A.10}$$

where δ_{ij} is the usual Kronecker delta:

$$\delta_{ij} = \begin{cases} 1 & i = j \\ 0 & i \neq j \end{cases}. \tag{A.11}$$

Dyads and dyadics are an old-fashioned approach to tensor analysis, which has been largely superseded by the absolute differential calculus framework introduced by Levi-Civita and Ricci-Curbastro. They are ultimately not as flexible nor useful as absolute differential calculus, but are much easier to grasp and therefore can still be useful in situations such as fluid dynamics, where we don't need the full formalism. To relate the two approaches, note that rank-2 contravariant tensor[19] are dyadics, and vice versa.

[19] A $\binom{2}{0}$ tensor in the notation of the Schutz [1] book — an excellent introduction, by the way, to modern tensor analysis.

A.3 Algebra with Vectors and Dyadics

Both vectors and dyadics obey the rules of linear algebra: we can multiply them by scalars, add them and subtract them, to obtain a different vector/dyadic. A pair of vectors can also be reduced to a scalar via the dot product (also known as the dot product or inner product):

$$\boldsymbol{a} \cdot \boldsymbol{b} = \boldsymbol{b} \cdot \boldsymbol{a} = a^i b^i \tag{A.12}$$

The dot product can also be used to reduce a dyad and a vector to a (different) vector. This works by the fundamental identity

$$(\boldsymbol{a} \otimes \boldsymbol{b}) \cdot \boldsymbol{c} = \boldsymbol{a}(\boldsymbol{b} \cdot \boldsymbol{c}) = b^i c^i \, \boldsymbol{a}. \tag{A.13}$$

We can apply the same machinery to calculate the dot product between a dyadic and a vector, if we first expand the dyadic as a sum over basis dyads:

$$\begin{aligned} \boldsymbol{D} \cdot \boldsymbol{c} &= (D^{ij} \boldsymbol{E}_{ij}) \cdot \boldsymbol{c} && \text{(A.14)} \\ &= D^{ij} (\boldsymbol{e}_i \otimes \boldsymbol{e}_j) \cdot \boldsymbol{c} && \text{(A.15)} \\ &= D^{ij} \boldsymbol{e}_i (\boldsymbol{e}_j \cdot \boldsymbol{c}) && \text{(A.16)} \\ &= D^{ij} c^j \boldsymbol{e}_i. && \text{(A.17)} \end{aligned}$$

From this, we can see that the dot product between the identity dyadic and a vector is the same vector:

$$\boldsymbol{I} \cdot \boldsymbol{c} = I^{ij} c^j \boldsymbol{e}_i = \delta_{ij} c^j \boldsymbol{e}_i = c^i \boldsymbol{e}_i. \tag{A.18}$$

A.4 Calculus with Vectors and Dyadics

A.5 Vector Operators

$$\nabla \cdot (\phi \boldsymbol{I}) = \nabla \phi \tag{A.19}$$

$$\nabla \cdot (\boldsymbol{a} \otimes \boldsymbol{b}) = (\nabla \cdot \boldsymbol{a}) \boldsymbol{b} + (\boldsymbol{a} \cdot \nabla) \boldsymbol{b} \tag{A.20}$$

$$\nabla (\boldsymbol{a} \cdot \boldsymbol{b}) = \boldsymbol{a} \times (\nabla \times \boldsymbol{b}) + \boldsymbol{b} \times (\nabla \times \boldsymbol{a}) + (\boldsymbol{b} \cdot \nabla) \boldsymbol{a} + (\boldsymbol{a} \cdot \nabla) \boldsymbol{b}. \tag{A.21}$$

A.6 The Divergence Theorem

Here, $\mathcal{V}$ denotes an arbitrary volume, and $\partial \mathcal{V}$ the boundary surface of the volume.

$$\int_{\partial \mathcal{V}} \boldsymbol{a} \cdot \mathrm{d}\boldsymbol{A} = \int_{\mathcal{V}} \nabla \cdot \boldsymbol{a} \, \mathrm{d}\tau \tag{A.22}$$

$$\int_{\partial \mathcal{V}} \mathrm{d}\boldsymbol{A} \cdot \boldsymbol{D} = \int_{\mathcal{V}} \nabla \cdot \boldsymbol{D} \, \mathrm{d}\tau \tag{A.23}$$

(Both the vector $\boldsymbol{a}$ and the dyadic $\boldsymbol{D}$ must be continuous functions of position.)

B Worked Examples

B.1 Hubble Flow

Consider spherically symmetric, isothermal outflow of gas, with an initial ($t = 0$) state having homogeneous density and a radial velocity proportional to the distance from the origin — i.e., a *Hubble* flow:

$$\rho(t = 0) = \rho_0, \qquad v_r(t = 0) = H_0 r. \tag{B.1}$$

What is the subsequent ($t > 0$) evolution of this system?

To solve this problem, we'll need to use the fluid equations of mass conservation (1.13) and momentum conservation (1.17). In spherically symmetric geometry, these are

$$\frac{\partial \rho}{\partial t} + \frac{1}{r^2}\frac{\partial}{\partial r}\left(r^2 \rho v_r\right) = 0 \tag{B.2}$$

and

$$\frac{\partial \rho v_r}{\partial t} + \frac{1}{r^2}\frac{\partial}{\partial r}\left(r^2 \rho v_r^2\right) + \frac{\partial P}{\partial r} = 0, \tag{B.3}$$

respectively. Because the flow is isothermal, the pressure and density are related by the equation of state

$$P = a^2 \rho, \tag{B.4}$$

where the isothermal sound speed a is a constant. Hence, the momentum equation can also be written as

$$\frac{\partial \rho v_r}{\partial t} + \frac{1}{r^2}\frac{\partial}{\partial r}\left(r^2 \rho v_r^2\right) + a^2\frac{\partial \rho}{\partial r} = 0, \tag{B.5}$$

Let's now start by *guessing* that the solutions remain homogeneous and Hubble-like,

$$\rho(r, t) = \rho(t), \qquad v_r(r, t) = H(t) r. \tag{B.6}$$

Under these assumptions (which will turn out *a posteriori* to be correct), the mass and momentum conservation equations become

$$\frac{\mathrm{d}\rho}{\mathrm{d}t} + 3H\rho = 0 \tag{B.7}$$

and

$$rH\frac{\mathrm{d}\rho}{\mathrm{d}t} + r\rho\frac{\mathrm{d}H}{\mathrm{d}t} + 4rH^2\rho = 0 \tag{B.8}$$

(note that the a^2 term has vanished, as the density gradient is always zero). Multiplying the first equation by rH and subtracting it from the second, we arrive at an ordinary differential equation for H:

$$r\rho\left(\frac{\mathrm{d}H}{\mathrm{d}t}+H^2\right)=0. \tag{B.9}$$

This is easily solved (in tandem with the boundary condition $H(0)=H_0$, to find

$$H(t)=\frac{H_0}{H_0t+1}. \tag{B.10}$$

The corresponding velocity field is

$$v(r,t)=\frac{H_0r}{H_0t+1}, \tag{B.11}$$

and by substituting this back into eqn. (B.7) we find the density as

$$\rho(r,t)=\frac{\rho_0}{(H_0t+1)^3}. \tag{B.12}$$

These expressions completely describe the $t>0$ evolution of the system — and demonstrate that an initially homogeneous Hubble flow remains homogeneous and Hubble-like.

To finish, let's examine the Hubble flow from the perspective of a fluid element participating in the flow. It's easily shown that the Stokes velocity derivative vanishes,

$$\frac{\mathrm{D}v_r}{\mathrm{D}t}=0, \tag{B.13}$$

meaning that the fluid element experiences no acceleration — it moves with constant velocity. This is because there are no gas-pressure-gradient forces acting on the element. Of course the overall flow doesn't have a constant velocity, in either space or time; but the individual elements comprising it *do*.

B.2 Nozzle Flow

To lay the groundwork for discussing the solar wind (§B.3), consider isothermal flow along a tube of varying cross-sectional area. This problem is essentially 1-dimensional, and so we sometimes refer to it as 'quasi-1D flow' — the 'quasi' qualifier indicating that the geometry isn't quite Cartesian, due to the varying cross section. The fluid equations for mass and momentum conservation then read

$$\frac{\partial\rho}{\partial t}+\frac{1}{A}\frac{\partial}{\partial x}\left(A\rho v\right)=0, \tag{B.14}$$

$$\frac{\partial\rho v}{\partial t}+\frac{1}{A}\frac{\partial}{\partial x}\left(A\rho v^2\right)+\frac{\partial P}{\partial x}=0, \tag{B.15}$$

where x is the spatial coordinate and $A(x)$ is a function describing the cross-sectional area (for the moment, left unspecified).

In a steady state, the time derivatives in these equations vanish. The continuity equation (B.14) can then be trivially integrated to obtain

$$A\rho v = C; \tag{B.16}$$

the constant of integration C gives the amount of fluid flowing per second past any point in the tube. This expression indicates that if the density ρ remains constant, then v varies inversely with A; a constriction in the tube leads to an accelerated flow, and vice versa.

With some algebra, the steady-state momentum equation can likewise be manipulated to the form

$$\left(1 - \frac{a^2}{v^2}\right) v \frac{\mathrm{d}v}{\mathrm{d}x} = \frac{a^2}{A}\frac{\mathrm{d}A}{\mathrm{d}x}. \tag{B.17}$$

Here, a is the isothermal sound speed of the fluid; it appears in this equation because we've eliminated the pressure using the isothermal relation $P = a^2\rho$. If we transform to a new pair of dimensionless variables

$$X = \frac{x}{1\,\mathrm{cm}} \tag{B.18}$$

$$Y = \frac{v}{a}, \tag{B.19}$$

then we arrive at a dimensionless *nozzle equation*

$$\left(1 - \frac{1}{Y^2}\right) Y \frac{\mathrm{d}Y}{\mathrm{d}X} = \frac{1}{A}\frac{\mathrm{d}A}{\mathrm{d}X}. \tag{B.20}$$

This can trivially be integrated to find the solution

$$Y^2 - \ln Y^2 = \ln A^2 + D, \tag{B.21}$$

where D is a constant of integration.

Before we apply this solution to any specific case, let's think a little about the general behavior of the flow along the tube. Assuming for simplicity that Y is positive everywhere[20], we can identify two regimes:

- subsonic flow with $Y < 1$; the velocity gradient $\mathrm{d}Y/\mathrm{d}X$ has the opposite sign to the area gradient $\mathrm{d}A/\mathrm{d}X$, so as the tube narrows ($\mathrm{d}A/\mathrm{d}X < 0$) the flow will accelerate ($\mathrm{d}Y/\mathrm{d}X > 0$).
- supersonic flow with $Y > 1$; the velocity gradient $\mathrm{d}Y/\mathrm{d}X$ has the same sign as the area gradient $\mathrm{d}A/\mathrm{d}X$, so as the tube expands ($\mathrm{d}A/\mathrm{d}X > 0$) the flow will also accelerate ($\mathrm{d}Y/\mathrm{d}X > 0$).

[20] I.e., the flow is in the direction of increasing X.

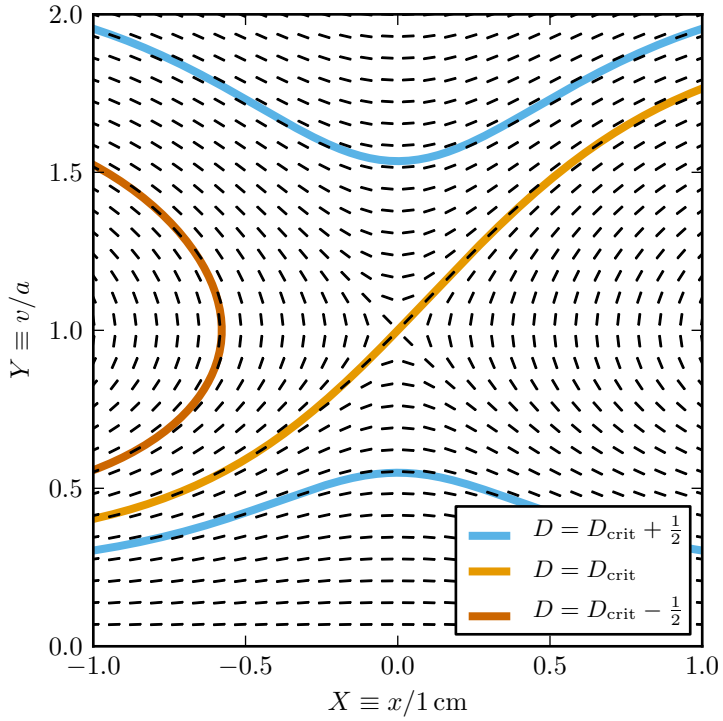

Figure B.1: The flow gradient $\mathrm{d}Y/\mathrm{d}X$ (shown as tick marks) at selected tick points in the (X, Y) plane, for flow through a nozzle with a Gaussian area profile (cf. eqn. B.23). Four different solutions to the nozzle equation are also show, corresponding to three different choices of the integration constant D.

If the tube contains a *nozzle*, where the area function passes through a minimum at some $X = X_{\mathrm{min}}$, then we can imagine these two flow regimes existing back-to-back in such a way that the flow makes a smooth transition from subsonic flow for $X < X_{\mathrm{min}}$ to supersonic for $X > X_{\mathrm{min}}$. However, something special needs to happen at the nozzle throat $X = X_{\mathrm{min}}$. Since $\mathrm{d}A/\mathrm{d}X = 0$ at the throat (by definition) the right-hand side of eqn. (B.20) vanishes, and so therefore must the left-hand side. There are two possible scenarios here:

(i). $\mathrm{d}Y/\mathrm{d}X = 0$ — that is, the throat is an extremum of the flow velocity;

(ii). $Y = 1$ — that is, the throat is a *sonic point* where the flow speed equals the sound speed.

Of these, only scenario (ii) is consistent with a smooth transition from subsonic to supersonic flow. In fact, the throat is the only place the flow can make this transition; at any other point with $\mathrm{d}A/\mathrm{d}X \neq 0$, eqn. (B.20) can't be satisfied with $Y = 1$.

Which of the two scenarios is realized depends on the value of the integration constant D.

Scenario (ii) has $D = D_{\rm crit}$, where the critical value

$$D_{\rm crit} = 1 - \ln A_{\rm throat}^2, \tag{B.22}$$

is found by setting $Y = 1$ in eqn. (B.21); here, $A_{\rm throat}$ is the area at the throat, and hence the minimum area of the tube. Scenario (i) corresponds to $D > D_{\rm crit}$, with larger D corresponding to slower (faster) velocities depending on whether the flow is subsonic (supersonic). As we will see shortly, situations where $D < D_{\rm crit}$ are physically invalid.

To visualize the alternative scenarios, Fig. B.1 plots the flow gradient $\mathrm{d}Y/\mathrm{d}X$ as tick marks at selected points in the (X, Y) plane, for a nozzle with the Gaussian area profile

$$A(X) = 1 - \frac{\mathrm{e}^{-X^2}}{2}. \tag{B.23}$$

(The gradient is calculated at each X, Y using the nozzle equation B.20). Also shown the figure are four solutions to the nozzle equation, corresponding to three different choices of D; these solutions are everywhere tangent to the tick marks. The $D = D_{\rm crit} = 1 - \ln 1/4$ case is the critical solution, and smoothly transitions from subsonic for $X < 0$, to supersonic for $X > 0$. The pair of $D = D_{\rm crit} + \frac{1}{2}$ solutions remain subsonic (supersonic) everywhere, but pass through a velocity maximum (minimum) at the nozzle throat. Finally, the $D = D_{\rm crit} - \frac{1}{2}$ case progressively steepens until $\mathrm{d}Y/\mathrm{d}X \to \infty$ at $X \approx -0.6$; this is unphysical and the solution must therefore be discarded. In fact, this fate befalls all solutions with $D < D_{\rm crit}$, highlighting that the critical case $D = D_{\rm crit}$ is the minimum possible D consistent with physicality.

Looking at Fig. B.1, we can see that there should also be a solution with $D_{\rm crit}$ which smoothly transitions from supersonic for $X < 0$, to subsonic for $X > 0$. This solution is mathematically valid, but if we try to establish such a decelerating flow configuration it rapidly breaks up into a series of shocks; that is, the solution is unstable.

B.3 The Solar Wind

It's straightforward to demonstrate[21] that an isothermal atmosphere in hydrostatic equilibrium (cf. eqn. 1.39) around a spherical gravity source (typically, a star or a planet) will have a finite gas pressure at $r \to \infty$. In the case of the Sun, the finite pressure of the atmosphere (specifically, the corona) at infinity is larger than the pressure of the interstellar medium. Therefore, no static pressure balance between the corona and the ISM is possible, and a wind outflow will necessarily ensue.

In a steady state, the mass and momentum conservation equations for the spherically symmetric solar wind are

$$\frac{1}{r^2}\frac{\partial}{\partial r}\left(r^2 \rho v_r\right) = 0, \tag{B.24}$$

$$\frac{1}{r^2}\frac{\partial}{\partial r}\left(r^2 \rho v_r^2\right) + \frac{\partial P}{\partial r} = -\frac{G\mathrm{M}_\odot}{r^2}\rho. \tag{B.25}$$

[21] Which means this will be a homework question!

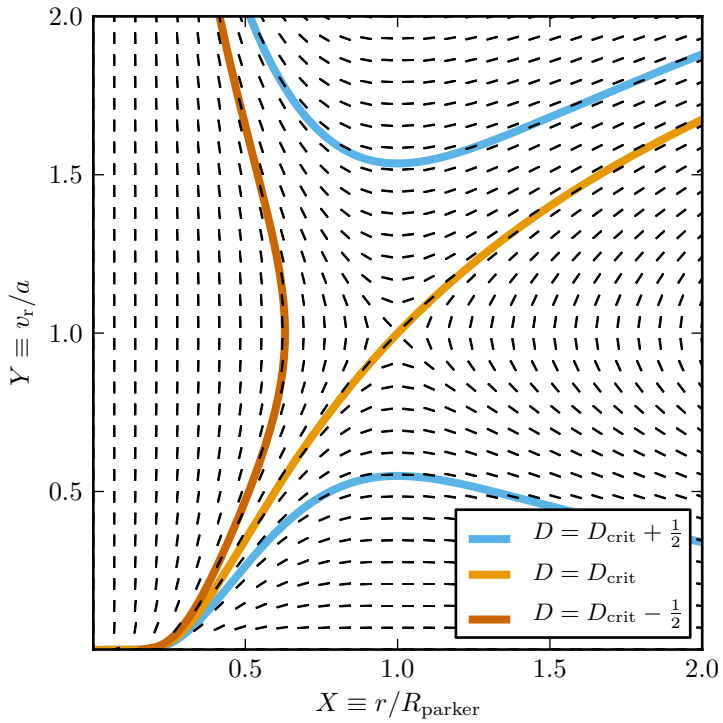

Figure B.2: The flow gradient $\mathrm{d}Y/\mathrm{d}X$ (shown as tick marks) at selected tick points in the (X, Y) plane, for solar wind flow. Four different solutions to the nozzle equation are also shown, corresponding to three different choices of the integration constant D.

(We're assuming that the wind contains negligible mass, so that the gravitational mass at any radius $r > \mathrm{R}_\odot$ is just the solar mass $\mathrm{M}_\odot$). The continuity equation (B.24) is trivially integrated to find

$$r^2 \rho v_r = \frac{\dot{M}}{4\pi}, \tag{B.26}$$

where we've written the constant of integration in terms of the global wind mass-loss rate $\dot{M}$. Using this equation and the isothermal relation $P = a^2\rho$ to eliminate the density and pressure, the momentum equation (B.25) becomes

$$\frac{1}{4\pi r^2}\frac{\partial}{\partial r}\left(v_r \dot{M}\right) + a^2 \frac{\partial}{\partial r}\left(\frac{\dot{M}}{4\pi r^2 v_r}\right) = -\frac{G\mathrm{M}_\odot}{r^2}\frac{\dot{M}}{4\pi r^2 v_r}. \tag{B.27}$$

Let's introduce the dimensionless variables

$$X = \frac{r}{R_{\rm parker}}, \tag{B.28}$$

$$Y = \frac{v}{a}, \tag{B.29}$$

where the so-called *Parker radius* is defined as

$$R_{\text{parker}} = \frac{G\mathrm{M}_\odot}{2a^2}. \tag{B.30}$$

(this is the radius at which the sound speed is equal to the local escape speed). Then, the momentum equation simplifies to

$$\left(1 - \frac{1}{Y^2}\right) Y \frac{\mathrm{d}Y}{\mathrm{d}X} = \frac{2}{X} - \frac{2}{X^2}. \tag{B.31}$$

Written in this form, we can immediately see that the momentum equation is a nozzle-flow equation (cf. B.20), with an area function satisfying

$$\frac{1}{A}\frac{\mathrm{d}A}{\mathrm{d}X} = \frac{2}{X} - \frac{2}{X^2} \tag{B.32}$$

and the nozzle throat at $X = 1$. We can trivially integrate this to obtain

$$\ln A = 2\ln X + \frac{2}{X}, \tag{B.33}$$

where we've set the constant of integration to zero because its value has no effect on solutions. Note that this expression doesn't describe the area of any physical object; it's a virtual area chosen such that quasi-1D flow along a tube with the same area will share the same flow properties as the solar wind.

Substituting this expression into the general solution (B.21) to the nozzle equation, we obtain the result

$$Y^2 - \ln Y^2 = 4\ln X + \frac{4}{X} + D. \tag{B.34}$$

Fig. B.2 plots these solutions in the (X, Y) plane, together with the gradient tick-marks calculated using the nozzle equation (B.32). As with Fig. B.1, solutions corresponding to three values of D are plotted, including the critical value $D_{\text{crit}} = -3$.

B.4 Flow Around A Cylinder

Let's now consider the problem of steady-state incompressible, irrotational flow around an infinite cylinder, as this classic example provides a very important insight into the importance of viscosity. For simplicity, we'll assume

1. the cylinder is aligned along the Cartesian z axis, and has radius R;
2. the flow velocity at $r = R$ is tangential to the surface of the cylinder;
3. the flow velocity at large cylindrical radii is $\boldsymbol{v} = v_\infty \hat{\boldsymbol{x}}$.

Because the flow is irrotational, we can calculate the flow velocity by first solving Laplace's equation for the velocity potential Φ_v (cf. §2.6). The natural coordinate system for this is cylindrical; thus, we need to solve

$$\frac{1}{r}\frac{\partial}{\partial r}\left(r\frac{\partial \Phi_v}{\partial r}\right) + \frac{1}{r^2}\frac{\partial^2 \Phi_v}{\partial \phi^2} + \frac{\partial^2 \Phi_v}{\partial z^2} = 0. \tag{B.35}$$

The boundary conditions (either at the cylinder or at infinity) don't depend on z, so neither will solutions, and the problem reduces to

$$\frac{1}{r}\frac{\partial}{\partial r}\left(r\frac{\partial \Phi_v}{\partial r}\right) + \frac{1}{r^2}\frac{\partial^2 \Phi_v}{\partial \phi^2} = 0. \tag{B.36}$$

This is now the 2-D Laplace equation in polar coordinates, and is solved using separation of variables. General solutions have the form

$$\Phi_v = A_0 + B_0 \ln r + \sum_{n=1}^{\infty} \left(A_n r^n + B_n r^{-n}\right)\left(C_n \cos n\phi + D_n \sin n\phi\right). \tag{B.37}$$

where the A_n, B_n, C_n and D_n are constants of integration, to be determined from the boundary conditions. This expression leads to the velocity components

$$v_r \equiv \frac{\partial \Phi_v}{\partial r} = \frac{B_0}{r} + \sum_{n=1}^{\infty} \left(A_n n r^{n-1} - B_n n r^{-n-1}\right)\left(C_n \cos n\phi + D_n \sin n\phi\right), \tag{B.38}$$

$$v_\phi \equiv \frac{1}{r}\frac{\partial \Phi_v}{\partial \phi} = \sum_{n=1}^{\infty} \left(A_n r^{n-1} + B_n r^{-n-1}\right)\left(-C_n n \sin n\phi + D_n n \cos n\phi\right). \tag{B.39}$$

Let's now figure out what the coefficients should be. We can set $A_0 = 0$ since it will have no effect on the velocity field. At very large radii, the boundary condition $\boldsymbol{v} = v_\infty \hat{\boldsymbol{x}}$ can be written in polar coordinates as

$$v_r = v_\infty \cos\phi, \tag{B.40}$$

$$v_\phi = -v_\infty \sin\phi. \tag{B.41}$$

Comparing these expressions against eqns. (B.38–B.39) in the $r \to \infty$ limit, we see that the coefficients must satisfy

$$A_1 C_1 = v_\infty, \tag{B.42}$$

$$A_n C_n = 0 \quad \text{for all } n \geq 2, \tag{B.43}$$

$$A_n D_n = 0 \quad \text{for all } n. \tag{B.44}$$

Likewise, on the surface of the cylinder the boundary condition that the flow is tangential to the surface requires that $v_r = 0$, and hence

$$B_0 = 0, \tag{B.45}$$

$$A_n n R^{n-1} - B_n n R^{-n-1} = 0 \quad \text{for all } n \geq 1. \tag{B.46}$$

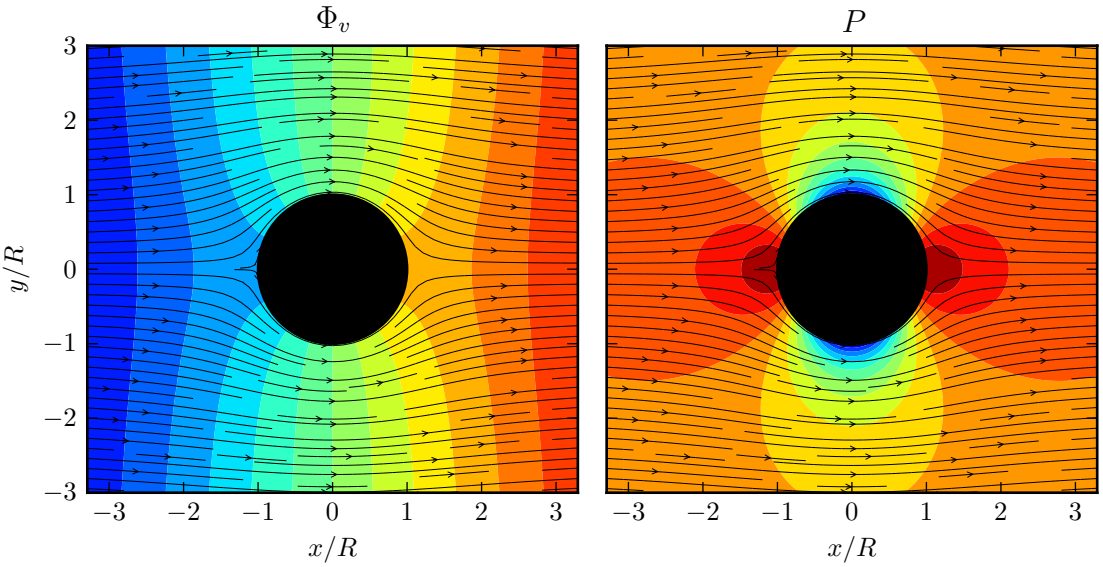

Figure B.3: Steady-state incompressible, irrotational flow around a cylinder. The left-hand panel shows the velocity potential Φ_v, with blue corresponding to low values and red to high values. The right-hand panel shows the pressure, with the same coloring convention. In both panels, the flow streamlines are overplotted.

Combined with the other constraints on the coefficients, we therefore arrive at the specific solution

$$\Phi_v = v_\infty \left(r + \frac{R^2}{r} \right) \cos\phi, \tag{B.47}$$

corresponding to a flow velocity

$$v_r = v_\infty \left(1 - \frac{R^2}{r^2} \right) \cos\phi, \tag{B.48}$$

$$v_\phi = -v_\infty \left(1 + \frac{R^2}{r^2} \right) \sin\phi. \tag{B.49}$$

Figure B.3 illustrates this solution by showing both the velocity potential and the gas pressure, overplotted with streamlines (a streamline is the path followed by a fluid element). The pressure is calculated using Bernoulli's theorem, which states that for an incompressible fluid the stream function

$$F = \frac{v^2}{2} + \frac{P}{\rho} \tag{B.50}$$

is constant along streamlines (this is easily proven by showing that the Stokes derivative of F vanishes). If we assume at large r that the pressure is constant[22], $P = P_\infty$, then

$$F = \frac{v_\infty^2}{2} + \frac{P_\infty}{\rho} \tag{B.51}$$

for all streamlines. Hence, the pressure everywhere is found as

$$P = P_\infty + \frac{\rho}{2}(v_\infty^2 - v^2). \tag{B.52}$$

From this expression, we see that the flow velocity and pressure are anti-correlated: maximum pressure occurs at minimum velocity, and vice versa.

An interesting issue raised by Fig. B.3 is that the velocity potential and pressure are left-right symmetric about $x = 0$. This means that the upstream pressure forces acting on the surface of the cylinder are exactly balanced by the corresponding downstream forces — and so the *net* force on the cylinder is zero. This surprising result, known as *d'Alembert's Paradox*, seems to fly against our intuitive notion that there should be some kind of drag force acting on the cylinder.

In fact, our intuition is correct here; there *is* a drag force on the cylinder, pushing it in the downstream direction, but our analysis lacks the vital ingredient necessary to model this force: *viscosity*. A tentative step toward including viscosity is to replace the tangential flow ($v_r = 0$) boundary condition at the surface of the cylinder with a *no-slip condition*: the fluid velocity relative to the surface is zero, meaning that $v_r = 0$ *and* $v_\phi = 0$. However, this immediately causes problems because the coefficients in the general solution (B.37) must now satisfy the constraints

$$B_0 = 0, \tag{B.53}$$

$$A_n n R^{n-1} - B_n n R^{-n-1} = 0 \quad \text{for all } n \geq 1, \tag{B.54}$$

$$A_n R^{n-1} + B_n R^{-n-1} = 0 \quad \text{for all } n \geq 1. \tag{B.55}$$

The only solution to these is the trivial solution, $A_n = B_n = 0$. What this result tells us that there are no non-trivial solutions to steady-state incompressible, irrotational *viscous* flow around a cylinder!

Fortunately, we *can* find solutions if we relax the assumption of irrotationality. The price to be paid for this is, however, steep: we can no longer use a velocity potential to model the flow, and must instead resort to solving the full incompressible Navier-Stokes equations.

B.5 Viscous Flow Through a Pipe

A simple example of viscosity in action is the flow of an homogeneous, incompressible (but *not* inviscid!) fluid through a uniform pipe — so-called *Hagen-Poiseuille* flow. The problem is easiest handled in cylindrical coordinates aligned with the pipe. We start with the following assumptions:

[22] Note that we don't necessarily have to make this assumption; but it keeps things simple.

1. the flow is steady;
2. the flow is in the z direction everywhere;
3. the flow speed depends only on the radial coordinate r.

With these conditions, the continuity equation and the ϕ component of the momentum equation are trivially satisfied, and we shan't consider them further. The radial component of the momentum equation reduces to

$$\frac{\partial p}{\partial r} = 0, \tag{B.56}$$

meaning that the pressure must be uniform across the tube, and only vary with z. The z component of the momentum equation likewise becomes

$$\frac{\partial p}{\partial z} = \mu \nabla^2 v_z = \frac{\mu}{r} \frac{\partial}{\partial r} \left(r \frac{\partial v_z}{\partial r} \right) \tag{B.57}$$

Integrating twice with respect to r, we thus obtain the velocity solution

$$v_z(r) = \frac{1}{4\mu} \frac{\partial p}{\partial z} r^2 + C_1 \ln r + C_2. \tag{B.58}$$

The constants of integration C_1 and C_2 are determined by the boundary conditions. In order that v_z remain finite as $r \to 0$, $C_1 = 0$. Likewise, if we impose the *no-slip* condition that $v_z \to 0$ as $r \to R$, where R is the pipe radius, then C_2 is such that the solution becomes

$$v_z(r) = \frac{1}{4\mu} \frac{\partial p}{\partial z} (r^2 - R^2) \tag{B.59}$$

From this solution, we see that the flow has a parabolic velocity profile, with the maximum at the center of the pipe; and that it travels from the high-pressure end of the pipe to the low-pressure end. The total mass flow rate can be obtained by integrating over the cross section,

$$\dot{M} = 2\pi \int_0^R \rho v_z r \, \mathrm{d}r = -\frac{\pi}{16\mu} \rho R^4 \frac{\partial p}{\partial z}. \tag{B.60}$$

This result is known as *Poiseuille's formula*, and relates the mass flow rate through a pipe to the pressure drop between the ends. Sometimes this is written in terms of the *kinematic viscosity* $\nu \equiv \mu/\rho$ as

$$\dot{M} = -\frac{\pi}{16\nu} R^4 \frac{\partial p}{\partial z}. \tag{B.61}$$

Poiseuille's formula explains why we have to suck harder on a straw when we drink a more-viscous liquid — to maintain a given flow rate, we must match any increase in ν with a corresponding increase in $|\partial p/\partial z|$ or the straw radius. The formula is useful experimentally, as it gives us a way to measure the viscosity of a fluid by forcing it through a pipe. However, there *are* limits to this technique; if ν is 'suitably' small, resulting in large flow rates, the flow becomes unstable and non-steady, meaning that the assumptions in the derivation here break down.

B.6 Thin Accretion Disk

Accretion disks are very common structures in astrophysics. Typically, a disk forms when material is drawn toward a central gravity source (star, black hole, etc.), but has too much angular momentum to accrete directly. The disk provides a mechanism for the material to slowly shed its angular momentum and eventually fall onto the central source.

Let's consider a disk around a central object of mass M. Quite reasonably, we'll assume that the disk is axisymmetric and that there are no fluid flows parallel to the symmetry axis. The natural coordinate system is cylindrical, aligned with the symmetry axis. The mass and momentum fluid equations are found (after some rather messy algebra, involving vector operators in curvilinear coordinates) as

$$\frac{\partial \rho}{\partial t} + \frac{1}{r}\frac{\partial}{\partial r}(r\rho v_r) = 0, \tag{B.62}$$

$$\frac{\partial \rho v_r}{\partial t} + \frac{1}{r}\frac{\partial}{\partial r}(r\rho v_r^2) - \rho\frac{v_\phi^2}{r} + \frac{\partial P}{\partial r} = [\nabla\cdot\boldsymbol{\sigma}]_r - \rho\frac{\partial \Phi}{\partial r}, \tag{B.63}$$

$$\frac{\partial \rho v_\phi}{\partial t} + \frac{1}{r^2}\frac{\partial}{\partial r}(r^2\rho v_r v_\phi) = [\nabla\cdot\boldsymbol{\sigma}]_\phi \tag{B.64}$$

$$\frac{\partial P}{\partial z} = [\nabla\cdot\boldsymbol{\sigma}]_z - \rho\frac{\partial \Phi}{\partial z}. \tag{B.65}$$

Here, $\boldsymbol{\sigma}$ is the viscous stress tensor, and

$$\Phi \equiv -\frac{GM}{\sqrt{r^2+z^2}} \tag{B.66}$$

is the gravitational potential.

Let's think about steady-state solutions to these equations, where the explicit time derivatives vanish. Generally speaking, the terms involving the viscous stress are small and can be neglected. However, in the azimuthal momentum equation (B.64) in the steady state, the viscous stress term must be retained in order to balance the inertia term on the left hand side. Thus, our steady-state fluid equations read

$$\frac{1}{r}\frac{\partial}{\partial r}(r\rho v_r) = 0, \tag{B.67}$$

$$\frac{1}{r}\frac{\partial}{\partial r}(r\rho v_r^2) - \rho\frac{v_\phi^2}{r} + \frac{\partial P}{\partial r} = -\rho\frac{\partial \Phi}{\partial r}, \tag{B.68}$$

$$\frac{1}{r^2}\frac{\partial}{\partial r}(r^2\rho v_r v_\phi) = [\nabla\cdot\boldsymbol{\sigma}]_\phi \tag{B.69}$$

$$\frac{\partial P}{\partial z} = -\rho\frac{\partial \Phi}{\partial z}. \tag{B.70}$$

Let's now focus on the vertical momentum equation. Substituting in eqn. (B.66), we obtain

$$\frac{\partial P}{\partial z} = -\rho\frac{GM}{(r^2+z^2)^{3/2}}z. \tag{B.71}$$

This, of course, amounts to the requirement that the disk is in vertical hydrostatic equilibrium! In the vicinity of the disk midplane, where $|z| \ll r$, this HSE equation can be approximated as approximated as

$$\frac{\partial P}{\partial z} = -\rho \frac{GM}{r^3} z. \tag{B.72}$$

If we assume an isothermal equation of state, with $P = a^2 \rho$ as usual, then the equation is trivially solved to find

$$P(r, z) = P(r, z = 0) \exp\left(-\frac{z^2}{H^2}\right). \tag{B.73}$$

This is a Gaussian pressure distribution centered on the midplane, with a characteristic scale height

$$H \equiv \sqrt{\frac{r^3 a^2}{GM}}. \tag{B.74}$$

Since the local escape speed at radius r is $v_{\rm esc} = \sqrt{2GM/r^3}$, we see that

$$H = \sqrt{2} \frac{a}{v_{\rm esc}} \tag{B.75}$$

If the material in the disk is cool, then its sound speed (which has the same order-of-magnitude as the particle thermal speed) will be much smaller than the escape speed; hence, we expect the disk to be thin, $H \ll r$.

Let's now focus on the steady-state radial momentum equation (B.68). If the disk is thin, then the pressure term on the left-hand side will be small compared with the gravitational term on the right-hand side. If we moreover assume the inflow/outflow velocity is subsonic ($v_r < a$) then we can also neglect the leading inertia. This leaves us with a balance between gravity and the centrifugal force,

$$\rho \frac{v_\phi^2}{r} = -\rho \frac{GM}{(r^2 + z^2)^{3/2}} r \approx -\rho \frac{GM}{r^2}. \tag{B.76}$$

But this is just the condition for circular orbits following Kepler's laws. So, we see that a thin, steady-state, subsonic disk is necessarily Keplerian. We can also write this as an equation governing the angular velocity:

$$\Omega \equiv \frac{v_\phi}{r} = \sqrt{\frac{GM}{r^3}}, \tag{B.77}$$

and so we see that Ω falls off as $r^{-3/2}$.

As a final step, let's turn to the azimuthal momentum equation (B.69). Substituting an expression for the ϕ component of the viscous stress divergence[23], this equation becomes

$$\frac{1}{r^2} \frac{\partial}{\partial r} (r^2 \rho v_r v_\phi) = \frac{1}{r^2} \frac{\partial}{\partial r} \left[r^3 \mu \frac{\partial}{\partial r} \left(\frac{v_\phi}{r} \right) \right]. \tag{B.78}$$

[23] Found from a costly expedition through a jungle of vector calculus!

Writing the coefficient of viscosity in terms of the kinematic viscosity, and replacing v_ϕ/r with Ω this becomes

$$\frac{1}{r^2}\frac{\partial}{\partial r}(r^3\rho v_r\Omega) = \frac{1}{r^2}\frac{\partial}{\partial r}\left[r^3\rho\nu\frac{\partial\Omega}{\partial r}\right]. \tag{B.79}$$

As a final step, let's integrate in the vertical direction to obtain

$$\frac{1}{r^2}\frac{\partial}{\partial r}(r^3\Sigma\Omega) = \frac{1}{r^2}\frac{\partial}{\partial r}\left[r^3\Sigma\nu\frac{\partial\Omega}{\partial r}\right], \tag{B.80}$$

where we've introduced

$$\Sigma \equiv \int_{-\infty}^{\infty}\rho\,\mathrm{d}z \tag{B.81}$$

as the disk surface density. We can trivially integrate (B.80) in the radial direction, finding

$$r^3\Sigma\Omega v_r = r^3\Sigma\nu\frac{\mathrm{d}\Omega}{\mathrm{d}r} + C, \tag{B.82}$$

To determine the constant of integration C, let's consider what happens in the vicinity of the surface of the accreting object. Because the no-slip condition applies at this surface, there must exist a boundary layer where the angular velocity of the disk drops below the Keplerian rate given by eqn. (B.77). At the top of this boundary layer, the turn-over in the angular velocity profile means that $\mathrm{d}\Omega/\mathrm{d}r = 0$; hence,

$$C = R_\mathrm{b}^3(\Sigma\Omega v_r)_{r=R_\mathrm{b}} \approx R_\mathrm{b}^3(\Sigma v_r)_{r=R_\mathrm{b}}\sqrt{\frac{GM}{R_\mathrm{b}^3}}, \tag{B.83}$$

where the second equality follows from applying eqn. (B.77) at the top of the boundary layer $r = R_\mathrm{b}$. Assuming the boundary layer is thin, we can approximate R_b with the surface radius R of the accreting object, and so

$$C \approx R(\Sigma v_r)_{r=R}\sqrt{\frac{GM}{R^3}}. \tag{B.84}$$

Further simplifications come from integrating the steady continuity equation (B.67) in vertical and radial directions, giving

$$r\Sigma v_r = -\frac{\dot{M}}{2\pi} \tag{B.85}$$

where $\dot{M}$ is the mass accretion rate, appearing as another constant of integration[24]. Hence,

$$(\Sigma v_r)_{r=R} = \frac{\dot{M}}{2\pi R}. \tag{B.86}$$

[24]Note that $\dot{M}$ is positive when v_r is negative, and vice versa.

Likewise, from eqn (B.77) it follows that

$$\frac{\mathrm{d}\Omega}{\mathrm{d}r} = -\frac{3}{2}\sqrt{\frac{GM}{r^5}}, \tag{B.87}$$

and so eqn. (B.82) becomes

$$-r^2\frac{\dot{M}}{2\pi}\sqrt{\frac{GM}{r^3}} = -\frac{3}{2}r^2\Sigma\nu\sqrt{\frac{GM}{r^3}} - R^2\frac{\dot{M}}{2\pi}\sqrt{\frac{GM}{R^3}}. \tag{B.88}$$

We can solve this for the surface density, finding

$$\Sigma = \frac{\dot{M}}{3\pi\nu}\left(1 - \sqrt{\frac{R}{r}}\right). \tag{B.89}$$

The radial velocity trivially follows as

$$v_r = -\frac{3\nu}{2r}\left(1 - \sqrt{\frac{R}{r}}\right)^{-1}. \tag{B.90}$$

Note that v_r diverges as we approach the stellar surface — this indicates that the assumption of small (sub-sonic) inflow velocity necessarily breaks down as we approach the boundary layer.

Since the inflow velocity is independent of $\dot{M}$, it would seem that dumping more mass into the accretion disk will raise the surface density and hence accretion rate, but will otherwise leave things unchanged. So, it would seem that we can have achieve rates as high as we like, right? In fact, toward higher accretion rates the viscous dissipation term in the energy equation becomes large, and (unless efficient radiative cooling kicks in) the disk will heat up in response. The energy dissipated per unit surface area of the disk is given by

$$D(r) = \int_{-\infty}^{\infty} \Phi\,\mathrm{d}z, \tag{B.91}$$

where Φ is the dissipation rate per unit volume introduced in eqn. (3.86). Assuming that $v_\phi \gg v_r$, this rate is given by

$$\Phi = \rho\nu r^2\left(\frac{\mathrm{d}\Omega}{\mathrm{d}r}\right) = \frac{9}{4}\rho\nu\frac{GM}{r^3}. \tag{B.92}$$

Hence,

$$D(r) = \frac{9}{4}\Sigma\nu\frac{GM}{r^3} = \frac{3GM\dot{M}}{4\pi r^3}\left(1 - \sqrt{\frac{R}{r}}\right). \tag{B.93}$$

When the disk is in thermal equilibrium, this dissipation rate must match the rate at which the disk radiates energy away. Assuming the disk radiates from its upper and lower surfaces

as a black-body, we can determine the local surface temperature T_s by applying the Stefan-Boltzmann law:

$$2\sigma_{SB}T_s^4 = \frac{3GM\dot{M}}{4\pi r^3}\left(1-\sqrt{\frac{R}{r}}\right), \tag{B.94}$$

where σ_{SB} is Stefan's constant. Interestingly, this expression is independent of the kinematic viscosity (which is typically a very uncertain parameter), depending only on the product $M\dot{M}$. At large radii $r \gg R$, the surface temperature follows the characteristic scaling $T_s \sim r^{-3/4}$ — the disk becomes cooler and dimmer the further out we look.

If we integrate $D(r)$ over the whole disk, then we can arrive at an expression for the total luminosity radiated by the disk:

$$L = \int_R^\infty D(r) 2\pi r \, \mathrm{d}r \tag{B.95}$$

$$= \frac{3GM\dot{M}}{2}\int_R^\infty \left(1-\sqrt{R}r\right) r^{-2}\,\mathrm{d}r \tag{B.96}$$

$$= \frac{GM\dot{M}}{2R}. \tag{B.97}$$

This is half of the luminosity $GM\dot{M}/R$ released by the accretion; the other half remains in the orbital kinetic energy of the accreting material. Sound familiar? Indeed, it does — this is nothing other than the virial theorem!

B.7 Supersonic Colliding Flows

A oft-encountered situation in astrophysics is the collision between two highly-supersonic flows. Let's use the Rankine-Hugoniot relations to build up a picture of the resulting flow structure. For simplicity, we assume that the colliding flows have equal and opposite momenta, so that

$$\rho_L v_L = -\rho_R v_R \tag{B.98}$$

where the subscript L refers to the flow coming in from the left and traveling right, and the subscript R refers to the flow coming in from the right and traveling left.

This configuration can't satisfy the RH relations (5.224–5.226), no matter what the choice S. The reason is that the collision region contains jumps in more than one of the multiple characteristic variables w_i. Let's suppose that in fact there are jumps in all three characteristic variables, meaning that there are two intermediate states (denoted IL and IR) between the left and right flow states. Fig. B.4 sketches this configuration. The IL and IR states are shown as having a finite width; even if this isn't correct at some initial time, it becomes true at some later time, as we shall see.

We now apply the RH relations across each of the boundaries between adjacent flow states. First consider the middle boundary, between the IL and IR intermediary states. Because

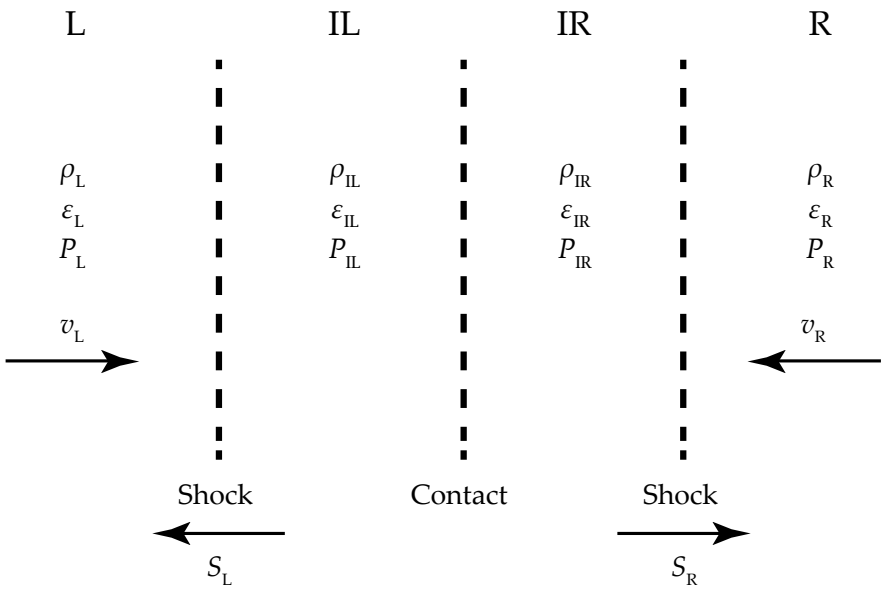

Figure B.4: Schematic of two colliding flows, showing the L(eft) and R(ight) states and the IL and IR intermediate states.

of the matched momentum condition (B.98), a membrane placed on this boundary would remain at rest indefinitely. Thus, the fluid on either side of the boundary must be at rest,

$$v_{\rm IL} = v_{\rm IR} = 0, \tag{B.99}$$

and we can identify the middle boundary as a contact discontinuity, with $P_{\rm IL} = P_{\rm IR}$ (but, in general, $\rho_{\rm L} \neq \rho_{\rm R}$).

Now let's focus on the left-hand boundary, between the L and IL states. Because the flow speed in the L state is highly supersonic, we can assume that the boundary is a strong shock, such that we can neglect the gas pressure in the L state. The RH relations then become

$$S_{\rm L}(\rho_{\rm IL} - \rho_{\rm L}) = -\rho_{\rm L} v_{\rm L} \tag{B.100}$$

$$S_{\rm L}(-\rho_{\rm L} v_{\rm L}) = (P_{\rm IL}) - (\rho_{\rm L} v_{\rm L}^2) \tag{B.101}$$

$$S_{\rm L}\left(\rho_{\rm IL}\varepsilon_{\rm IL} - \frac{1}{2}\rho_{\rm L} v_{\rm L}^2\right) = (\rho_{\rm IL}\varepsilon_{\rm IL} v_{\rm IL} + P_{\rm IL} v_{\rm IL}) - \frac{1}{2}\rho_{\rm L} v_{\rm L}^3, \tag{B.102}$$

where $S_{\rm L}$ is the speed of the shock. Together with the definition of the total energy in the IL state (with $\gamma = 5/3$),

$$\varepsilon_{\rm IL} = \frac{v_{\rm IL}}{2} + \frac{3P_{\rm IL}}{2\rho_{\rm IL}}, \tag{B.103}$$

and the fact that $v_{\rm IL} = 0$ (from above), these algebraic equations can be solved to find

$$\rho_{\rm IL} = 4\rho_{\rm L}, \tag{B.104}$$

$$P_{\rm IL} = \frac{4}{3}\rho_{\rm L} v_{\rm L}^2, \tag{B.105}$$

$$\varepsilon_{\rm IL} = \frac{1}{2} v_{\rm L}^2, \tag{B.106}$$

$$S_{\rm L} = -\frac{1}{3} v_{\rm L}. \tag{B.107}$$

The factor-four jump in density, from the L state to the IL state, is (unsurprisingly) the same as found for strong shocks in §5.4. Since $v_{\rm L}$ is assumed positive, we can see that the shock speed is negative — that is, the shock propagates upstream into the L state.

A similar analysis can be applied to the boundary between the IR and R states, to find

$$\rho_{\rm IR} = 4\rho_{\rm R}, \tag{B.108}$$

$$P_{\rm IR} = \frac{4}{3}\rho_{\rm R} v_{\rm R}^2, \tag{B.109}$$

$$\varepsilon_{\rm IR} = \frac{1}{2} v_{\rm R}^2, \tag{B.110}$$

$$S_{\rm R} = -\frac{1}{3} v_{\rm R}. \tag{B.111}$$

Because $v_{\rm R}$ is assumed negative, the shock speed $S_{\rm R}$ is positive and the shock propagates upstream into the R state.

Let's now take a step back and think about the physical meaning of the collision region we've found. The intermediate IL and IR states are in pressure balance with each other ($P_{\rm IR} = P_{\rm IL}$), and contain stationary fluid that originated from the L and R flow states, respectively. As time passes, the sizes of the intermediate states grow as the shocks separating them from the incoming flows propagate upstream. In effect, we have a pile-up between the two opposing fluid streams.

The assumption (B.98) of balanced momenta was made to simplify the analysis, by forcing the contact discontinuity between the two shocks to be stationary. The foregoing analysis can be generalized to any frame of reference, however, just by applying a Galilean transformation to the velocities. In particular, suppose we transform to a frame in which the R state is at rest. Then, denoting this new frame with an overbar, the speeds of the shocks are

$$\widetilde{S}_{\rm L} = -\frac{1}{3} v_{\rm L} - v_{\rm R} = \frac{\mathcal{R} - \frac{1}{3}}{\mathcal{R} + 1} \widetilde{v}_{\rm L}, \tag{B.112}$$

$$\widetilde{S}_{\rm R} = -\frac{1}{3} v_{\rm R} - v_{\rm R} = \frac{\frac{4}{3}\mathcal{R}}{\mathcal{R} + 1} \widetilde{v}_{\rm L}, \tag{B.113}$$

where

$$\mathcal{R} \equiv \frac{\rho_{\rm L}}{\rho_{\rm R}} \tag{B.114}$$

is the density contrast between the left and right states. Likewise, the speed of the contact discontinuity is

$$\widetilde{S}_{\rm C} = -v_{\rm R} = \frac{\mathcal{R}}{\mathcal{R}+1}\widetilde{v}_{\rm L}. \tag{B.115}$$

These expressions describe what happens when a flow with velocity $\widetilde{v}_{\rm L}$ collides with fluid at rest. Two shocks arise: the *forward* shock moving with velocity $\widetilde{S}_{\rm R}$ (always positive), and the *reverse* shock moving with velocity $S_{\rm L}$ (positive if $\mathcal{R} > 1/3$, negative otherwise). Between these two shocks is a contact discontinuity, which separates the stationary material swept up by the forward shock (on the right-hand side) from the material piled up by the reverse shock (on the left-hand side).

B.8 The Jeans Instability

We all know that stars are formed from the collapse of giant molecular clouds (GMCs) in the interstellar medium. But what precipitates this collapse? It turns out that when we incorporate the force of self gravity in the linearized equations describing acoustic waves, a new kind of instability appears which can precipitate collapse in a sufficiently-massive cloud. This instability is the *Jeans Instability*.

To derive a criterion for the Jean's instability, let's re-write eqns. (4.111–4.113), describing perturbations to a static, uniform ideal gas, with the requisite self-gravity term:

$$\frac{\partial \rho'}{\partial t} + \rho_0 \nabla \cdot \boldsymbol{v}' = 0, \tag{B.116}$$

$$\frac{\partial \boldsymbol{v}'}{\partial t} + \frac{1}{\rho_0}\nabla P' = -\nabla \Phi', \tag{B.117}$$

$$\frac{\partial P'}{\partial t} + \gamma P_0 \nabla \cdot \boldsymbol{v}' = 0, \tag{B.118}$$

where the perturbation to the gravitational potential satisfies Poisson's equation

$$\nabla^2 \phi' = 4\pi G \rho'. \tag{B.119}$$

As with our previous analyses of waves and instabilities, we proceed by assuming solutions with an exponential space/time dependence. Thus, we write

$$\boldsymbol{Y}(\boldsymbol{r}, t) = \boldsymbol{y} \exp[\mathrm{i}(\boldsymbol{k}\cdot\boldsymbol{r} - \omega t)] \tag{B.120}$$

where

$$\boldsymbol{Y} \equiv \begin{pmatrix} \rho'/\rho_0 \\ v_x'/a_{\rm ad} \\ v_y'/a_{\rm ad} \\ v_z'/a_{\rm ad} \\ P'/P_0 \\ \phi'/a_{\rm ad}^2 \end{pmatrix} \tag{B.121}$$

is the vector of unknowns, and $\boldsymbol{y}$ is as usual a constant vector to be determined. Substituting this expression for $\boldsymbol{Y}$ into the linearized equations leads to the set of algebraic equations for $\boldsymbol{y}$,

$$\boldsymbol{M}\boldsymbol{y} = \omega \boldsymbol{B}\boldsymbol{y} \tag{B.122}$$

where

$$\boldsymbol{M} = \begin{pmatrix} 0 & a_{\rm ad}k_x & a_{\rm ad}k_y & a_{\rm ad}k_z & 0 & 0 \\ 0 & 0 & 0 & 0 & a_{\rm ad}k_x/\gamma & a_{\rm ad}k_x \\ 0 & 0 & 0 & 0 & a_{\rm ad}k_y/\gamma & a_{\rm ad}k_y \\ 0 & 0 & 0 & 0 & a_{\rm ad}k_z/\gamma & a_{\rm ad}k_z \\ 0 & a_{\rm ad}k_x\gamma & a_{\rm ad}k_y\gamma & a_{\rm ad}k_z\gamma & 0 & 0 \\ 4\pi G\rho_0 & 0 & 0 & 0 & 0 & a_{\rm ad}^2|\boldsymbol{k}|^2 \end{pmatrix}, \tag{B.123}$$

and

$$\boldsymbol{B} = \begin{pmatrix} 1 & 0 & 0 & 0 & 0 \\ 0 & 1 & 0 & 0 & 0 \\ 0 & 0 & 1 & 0 & 0 \\ 0 & 0 & 0 & 0 & 0 \\ 0 & 0 & 0 & 1 & 0 \\ 0 & 0 & 0 & 0 & 0 \end{pmatrix}. \tag{B.124}$$

Comparing eqn. (B.122) against (4.126), the appearance of the matrix $\boldsymbol{B}$ in the former is because Poisson's equation doesn't include an explicit time derivative. Equations having the form of eqn. (B.122) are known as *generalized* eigenvalue problems, as distinct from ordinary eigenvalue problems which have $\boldsymbol{B} = \boldsymbol{I}$. The characteristic equation governing the frequencies now becomes

$$\det(\boldsymbol{M} - \omega\boldsymbol{B}) = 0, \tag{B.125}$$

which (as usual, with help from *Mathematica*) leads to the dispersion relation

$$\omega^3 \left(\omega^2 - a_{\rm ad}^2|\boldsymbol{k}|^2 + 4\pi G\rho_0\right) = 0. \tag{B.126}$$

Throwing away the trivial solutions, this becomes

$$\omega^2 - a_{\rm ad}^2|\boldsymbol{k}|^2 + 4\pi G\rho_0 = 0. \tag{B.127}$$

Inspecting the dispersion relation, we can see that if we could magically turn the force of gravity off — by setting $G = 0$, for instance — then we would obtain the same relation

$$\omega = \pm a_{\rm ad}|\boldsymbol{k}| \tag{B.128}$$

as found for ordinary acoustic waves in a uniform medium (see eqn. 4.118). This isn't surprising; if we remove the self-gravity terms, our analysis here is identical to that in §4.4. However, in the opposite limit — where the gravity term dominates the gas pressure term

in the momentum equation (B.117) — we find equation predicts a very different sort of behavior; ω^2 becomes negative, indicating an imaginary ω and thus solutions which grow or decay exponentially with time. This is the Jeans instability. To get a physical idea of how the instability works, imagine we compress a region of a uniform medium. The excess pressure generated by this compression will try to reverse the compression and restore the original state. However, if we sweep up sufficient mass in the compression, the gravitational field generated by this mass enhancement will overcome the pressure force and cause the compression to amplify itself. The result is a self-sustaining gravitational collapse.

Combining the condition for the instability, $\omega^2 < 0$, with the dispersion relation (B.127) leads to the inequality

$$|\boldsymbol{k}|^2 < k_{\mathrm{J}}^2 \equiv \frac{4\pi G\rho_0}{a_{\mathrm{ad}}^2} \tag{B.129}$$

where we have introduced a 'Jeans wavenumber' k_{J}. We can also write this in terms of a length scale for perturbations: the instability will kick in for perturbations with a scale larger than the characteristic Jeans length

$$\lambda_{\mathrm{J}} \equiv \frac{2\pi}{k_{\mathrm{J}}} = \sqrt{\frac{\pi a_{\mathrm{ad}}^2}{G\rho_0}}. \tag{B.130}$$

Associated with the Jeans length is the mass of a sphere with density ρ_0 and radius λ_{J}: the Jeans mass,

$$M_{\mathrm{J}} = \frac{4\pi}{3}\lambda_{\mathrm{J}}^3\rho_0, \tag{B.131}$$

representing the typical amount of mass we need in a system (e.g., a molecular cloud) for the Jeans instability to kick in.

Assuming a density of ~ 100 hydrogen atoms per cubic centimeter, at a temperature of 100 K, the Jeans length works out as around 20 pc, and the Jeans mass to around 84,000 $\mathrm{M}_\odot$. These values fall squarely into the size and mass range of giant molecular clouds, and hence it is in GMCs that we see the Jeans instability in action. Of course, the results of the instability — stars — have a mass much smaller than the Jeans mass; this is because *fragmentation* occurs during the collapse, allowing smaller, denser regions to form and (with their reduced Jeans lengths, due to their higher densities) continue collapsing.

B.9 The Taylor-Sedov Blast Wave

The *Taylor-Sedov Blast Wave* is a model for what happens when we dump a very large amount of energy E_0 into a vanishingly small volume within an initially homogeneous, static medium having density ρ_0. The resulting overpressure at the energy deposition point (henceforth assumed to be at the origin) causes a spherical shock to expand outwards, sweeping up the ambient material as it goes; this shock is known as a blast wave.

To get an idea on how the properties of the blast wave evolve with time, let us denote the shock radius at time t by $R(t)$. Then, the volume of ambient material swept up will be $4\pi R^3/3$, and the mass of swept-up material scales as

$$M \sim R^3 \rho_0 \tag{B.132}$$

(henceforth, we're going to neglect numerical factors such as $4\pi/3$). The average speed of the shock is likewise given by

$$V \sim \frac{R}{t}. \tag{B.133}$$

Combining these expressions, the total kinetic energy of the swept-up material can be estimated as

$$E_{\rm kin} \sim MV^2 \sim \rho_0 R^5 t^{-2}. \tag{B.134}$$

We can likewise estimate the thermal energy of the swept-up material as

$$E_{\rm thm} \sim R^3 P, \tag{B.135}$$

where P is its pressure (recall that pressure is a measure of internal energy per unit volume). To determine this pressure let's assume that the shock is strong; the pressure downstream of the shock is then given (cf. eqn. 5.240) by

$$P \sim \rho_0 V^2 \sim \rho_0 R^2 t^{-2} \tag{B.136}$$

leading to a thermal energy

$$E_{\rm thm} \sim \rho_0 R^5 t^{-2}. \tag{B.137}$$

Clearly, the kinetic and thermal energies share the same scaling with R and t, as does the total energy

$$E = E_{\rm kin} + E_{\rm thm} \sim \rho_0 R^5 t^{-2}. \tag{B.138}$$

Conservation of energy requires that E be fixed and equal to the initial energy E_0; this then means that the shock radius necessarily scales as

$$R \sim \left(\frac{E_0 t^2}{\rho_0}\right)^{1/5}. \tag{B.139}$$

C The Reynolds Transport Theorem

The Reynolds Transport Theorem (RTT) is a mathematical device allowing us to calculate the time derivative of volume integrals whose bounds themselves are changing with time.

Let $\boldsymbol{a}$ denote any arbitrary vector field. For the volume integral of $\boldsymbol{a}$ over a volume $\mathcal{V}$ which moves with the fluid, the theorem states that

$$\frac{\mathrm{D}}{\mathrm{D}t}\int_{\mathcal{V}} \boldsymbol{a}\,\mathrm{d}\tau = \int_{\mathcal{V}} \frac{\partial \boldsymbol{a}}{\partial t}\,\mathrm{d}\tau + \oint_{\partial\mathcal{V}} \boldsymbol{a}\,\boldsymbol{v}\cdot\mathrm{d}\boldsymbol{A}, \tag{C.1}$$

where $\partial\mathcal{V}$ is the closed surface bounding the volume.

A similar expression exists for integrals over a surface which moves with the fluid — although strictly speaking this expression is not the RTT but an instance of the Leibniz integral rule. Denoting the (not necessarily closed) surface as $\partial\mathcal{V}$, we have

$$\frac{\mathrm{D}}{\mathrm{D}t}\int_{\partial\mathcal{V}} \boldsymbol{a}\cdot\mathrm{d}\boldsymbol{A} = \int_{\partial\mathcal{V}} \left[\frac{\partial \boldsymbol{a}}{\partial t} + \boldsymbol{v}\nabla\cdot\boldsymbol{a}\right]\cdot\mathrm{d}\boldsymbol{A} - \oint_{\mathcal{C}} (\boldsymbol{v}\times\boldsymbol{a})\cdot\mathrm{d}\boldsymbol{s}, \tag{C.2}$$

where $\mathcal{C}$ is the closed curve bounding $\mathrm{d}\tau$.